UCRL-17520

cy. 2

CHEMICAL BIODYNAMICS
Annual Report 1966

Lawrence Radiation Laboratory
University of California – Berkeley

DISCLAIMER

UCRL-17520
UC-4 Chemistry
TID-4500 (50th Ed.)

UNIVERSITY OF CALIFORNIA

Lawrence Radiation Laboratory
Berkeley, California

AEC Contract No. W-7405-eng-48

CHEMICAL BIODYNAMICS ANNUAL REPORT, 1966

M. Calvin, Director, Laboratory of Chemical Biodynamics

May 1, 1967

Work done under auspices of the
U. S. Atomic Energy Commission

Printed in the United States of America
Available from
Clearinghouse for Federal Scientific and Technical Information
National Bureau of Standards, U.S. Department of Commerce
Springfield, Virginia 22151
Price: Printed Copy $3.00; Microfiche $0.65

CHEMICAL BIODYNAMICS ANNUAL REPORT, 1966

Contents

*Preceding Reports: UCRL-16806, UCRL-11948.

FOREWORD

Most of the work of the Chemical Biodynamics Group stems from two primary concerns: First, the development of radioactive isotopes and their application principally to chemical and biological systems, and, second, the interaction of biological and chemical systems with radiation. In this annual report we are continuing our custom of selecting a few of our activities for description in order to indicate the scope of the Group's productivity. Many of the particular projects involve the interaction of radiation with both chemical and biological systems as well as the use of the tracer method to define the nature of those interactions.

Our studies in photosynthesis and radiation chemistry have continued on an expanding frontier that includes the metabolic behavior, the physical-chemical structure, and the energy conversion process, a few aspects of which are described in this report. It is perhaps worth mentioning specifically that the radiation chemistry and the fundamental problems of information transfer in biology have led us into the problems of chemical evolution as well as into research on brain mechanisms and learning.

As our penetration into the molecular bases for some of these biological phenomena has increased it has become more obvious that a critical feature of our understanding, and hence manipulation, of the phenomena is the intimate knowledge of the macromolecular geometries and their changes in solution, i.e., in the biological environment. The development and use of new methods of defining these structures and their dynamics are now becoming major activities.

Melvin Calvin, Director
Chemical Biodynamics Group
Lawrence Radiation Laboratory

CHEMICAL BIODYNAMICS ANNUAL REPORT, 1966

Melvin Calvin, Director

Lawrence Radiation Laboratory
University of California
Berkeley, California

May 1, 1967

1. PARAMAGNETIC HYPERFINE STRUCTURE AND RELAXATION EFFECTS IN MÖSSBAUER SPECTRA: ^{57}Fe IN FERRICHROME A†

H. H. Wickman, M. P. Klein, and D. A. Shirley

The Mössbauer effect of ^{57}Fe in the metalloprotein ferrichrome A (FA) has been investigated at temperatures between 0.98 and 300°K; in some cases the absorber was placed in an external field of 18 kOe, oriented perpendicular to the propagation direction. The polycrystalline paramagnetic sample exhibited temperature-, field-, and concentration-dependent magnetic hyperfine structure. At 0.08°K in zero field, a well-resolved six-line spectrum was observed. As the temperature was raised, the pattern coalesced until at 300° K only a single broad non-Lorentzian line was visible. The effect of an applied field was, at all temperatures, to noticeably sharpen the hfs pattern; and at 77°K or below eight lines were easily resolved. Changes of the spectra with temperature and field are attributed to electronic relaxation, and a model is used to calculate relaxation spectra. The model employs the modified Block equations as rate equations to describe fluctuations of an effective hyperfine field. The iron-iron separation was increased by dilution of some of the samples in ethyl alcohol. As is well known from ESR work, spin-spin interactions decrease on dilution: a sharpening of the spectrum resulted. The importance of using solutions in studying Mössbauer spectra of biologically interesting Fe^{3+} compounds is demonstrated. Some of the consequences of paramagnetic hyperfine interactions for Mössbauer spectroscopy are discussed. Differences between the effective hyperfine field and the interactions $\mathbf{A}\mathbf{I}\cdot\mathbf{S}$ are noted, as are certain analogies between Mössbauer and optical spectroscopy, under the $\mathbf{A}\mathbf{I}\cdot\mathbf{S}$ interaction. From previous ESR work the electronic spin Hamiltonian for FA was found to be of the form $D[S_z^2 - \frac{1}{3}S(S+1)] + E[S_z^2 - S_y^2]$. Rather complex hyperfine spectra are predicted for Fe^{3+} with this spin Hamiltonian, and representative spectra are illustrated. It is shown that these spectra, expected in the absence of spin-spin interaction, would be sufficient to determine the ratio E/D of the spin-Hamiltonian parameters; this illustrates the complementary nature of ESR and Mössbauer spectra of the same system.

† Abstract of paper published in Phys. Rev. 152, 345 (1966).

2. CHEMICAL BONDING INFORMATION FROM PHOTOELECTRON SPECTROSCOPY †

C. S. Fadley, S. B. M. Hagström, J. M. Hollander, M. P. Klein, and D. A. Shirley

Introduction

A major source of our information about atoms, molecules, and solids is the study of spectra, whether they be of emitted or absorbed electromagnetic radiation or of particles such as electrons. After new spectroscopic techniques have been introduced they have generally been refined to the point of being sensitive to the chemical environment of a given atom. In this way a good deal of information has been obtained about the nature of chemical bonding.

In recent years, a new spectroscopic tool has been added to the repertoire, photoelectron spectroscopy.[1] This technique also has been shown to be sensitive to chemical effects, and considerable work has already been done on investigations pioneered by K. Siegbahn and co-workers in Uppsala.[2] The principle of the technique is to deduce the binding energies of the inner core electrons of an atom from very accurate measurements of x-ray-produced photoelectron spectra. The precision of these measurements is sufficient to allow detection of shifts of the order of 1 eV in these binding energies. Since shifts due to changes in the chemical environment have been found to be several eV in some cases,[2] they are easily detected. The versatility of the method arises from the fact that the core levels of virtually all atoms can be investigated. By contrast, most other spectroscopic methods are restricted to particular types of quantum mechanical systems or are governed by more restrictive selection rules. For example, nuclear magnetic resonance requires a reasonably abundant isotope with a nuclear magnetic moment, and for work at highest resolution a nuclear spin of 1/2 is requisite. The Mössbauer effect, although exquisitely sensitive, is restricted to nuclei with an appropriate γ-ray transition. Unfortunately, no such nuclei are available for $Z < 19$ nor are they uniformly distributed over the periodic table. The photoelectron method has an additional advantage for the interpretation of results. That is, the core level shifts can be related directly to the principal forces operating in atoms, molecules and solids--namely, those due to the Coulomb and exchange interactions.

In this paper we report some observations on the chemical shifts of core electron binding energies in iodine and europium compounds and indicate that these shifts may be explained in terms of two approximate theoretical models. Finally, we discuss briefly a few of the potential applications of this spectroscopic method to problems in coordination chemistry, biochemistry, and solid-state physics.

Because previous chemical shift measurements have been made on the relatively light elements carbon, nitrogen, sulfur, and chlorine,[2] a study of the chemical shifts for heavier atoms is of interest. In addition, the transition elements and rare earths possess unfilled inner d and f shells respectively. Electrons in these inner shells can participate in chemical bonding, in contrast with other elements in which it is predominantly outer valence shell electrons that serve this role. The selection of iodine ($Z = 53$) and europium ($Z = 63$) for investigation permits a comparison of these two classes of elements, as the neutral atom valence electron configurations are $5s^2 5p^5$ and $4f^7 6s^2$, respectively. Chemical shifts were studied in iodine for nine core levels (out of a possible 13). The four iodine compounds selected for study span a range of 8 in oxidation number. Three core levels were studied in europium in both divalent and trivalent compounds.

Experimental Procedure

The experimental technique involves expelling an electron from some inner level, i, with x radiation of energy well above the photoelectric threshold. Neglecting contact potential effects, the x-ray energy $h\nu$ is divided according to

$$h\nu = E_b(i, \underline{\chi}) + E_{kin}, \qquad (1)$$

where $E_b(i, \underline{\chi})$ is the binding energy of the ith level of an atom in compound $\underline{\chi}$ and E_{kin} is the photoelectron kinetic energy. Since x-ray energies are known to high accuracy, only the kinetic energy need be measured to obtain a binding energy. For this purpose a double-focusing magnetic spectrometer was used.[3] The energy resolution of this spectrometer was adjusted to be 0.06% full width at half maximum, thereby yielding instrumental line widths of 0.6 to 4.8 eV over the kinetic energy range of interest (1 to 8 keV). As the natural line widths are also a few eV, it is easily possible to detect shifts in binding energy of the order of 7 eV with such a spectrometer.

The apparatus used in this investigation

† Science (in press).

is shown schematically in Fig. 2-1. Radiation from the x-ray tube, filtered slightly with aluminum foil, impinges upon a thin rectangular (10×13 mm) powdered sample of the compound under study. Photoelectrons emitted from the sample pass through a narrow slit (0.5×10 mm) into the spectrometer. For a given current in the spectrometer coils, electrons of a narrow energy range are brought to a focus at the entrance to the Geiger counter. The current is scanned in a stepwise fashion over the region of interest and the resulting pulses from the Geiger counter are stored in a multiscaler (multichannel analyzer). Multiple scans were made in order to average out variations in x-ray flux. Although the radiation from an x-ray tube is not monochromatic, the characteristic x-ray lines interact with the core electron levels to give photoelectron peaks that are easily distinguishable above the background.

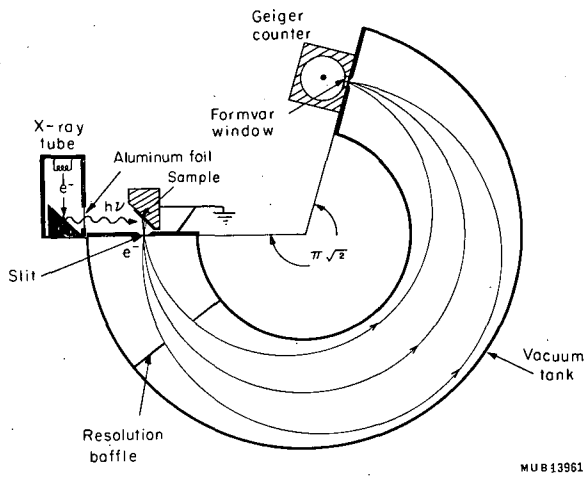

Fig. 2-1. Schematic illustration of the experimental apparatus.

energy. This observation agrees well with theory, as we discuss below. It is thus possible to speak of an average core shift between compounds. These shifts, relative to KI, are: KIBA, 0.0 eV; KIO_3, 5.3 eV; and KIO_4, 6.3 eV. The shifts are all in the direction predicted by a simple shielding model--that is, electrons are bound more tightly in compounds of higher oxidation number. Thus the shift is approximately 0.8 eV per unit change in oxidation number.

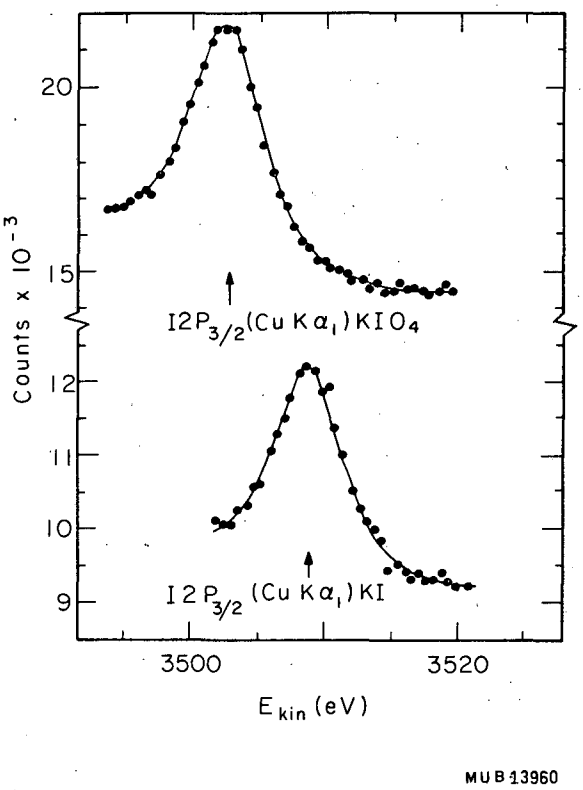

Fig. 2-2. Photoelectron peaks from KI and KIO_4.

Results

Typical photoelectron peaks are shown in Fig. 2-2. The notation $I2p_{3/2}$ ($CuK\alpha_1$) KI indicates a peak due to photoelectrons expelled from the $2p_{3/2}$ level of iodine in KI by the $K\alpha_1$ x-ray line of Cu. A chemical shift of about 6 eV is apparent between the peaks from KI and KIO_4. In iodine such shifts were measured for nine levels from $2S_{1/2}$ ($E_b \approx$ 5191 eV) to $4d_{5/2}$ ($E_b \approx$ 54 eV). The compounds studied were KI (-1 oxidation number), KIO_3 (+5), KIO_4 (+7), and the potassium salt of p-iodobenzoic acid--[KIBA] (?). The shifts are essentially the same for all measured levels in spite of the hundredfold change in binding

Similar shifts were measured for the $3d_{3/2}$ ($E_b \approx$ 1158 eV), $3d_{5/2}$ ($E_b \approx$ 1128 eV), and $4p_{3/2}$ ($E_b \approx$ 258 eV) levels in europium. The compounds studied were $EuAl_2$ (+2), EuO (+2), and Eu_2O_3 (+3). The shifts in this case were again very nearly the same for the three levels, and the binding energies for the two +2 compounds agreed to within experimental error (± 0.5 eV). The average shift in Eu for this unit change in oxidation number is 9.6 eV, and it is again in the direction predicted by the simple shielding model. Note that this is 12 times the corresponding figure for iodine.

Figure 2-3 gives an illustration of the rather striking chemical shift which results from the oxidation of europium metal. Spectrum 3a was obtained from $EuAl_2$, which apparently had oxidized slightly to the +3 state on the surface. The peak arising from electrons in +2 ions is still clearly visible, however. Spectra 3b and 3c were obtained from a piece of europium metal which was initially polished in air to give a shiny surface. This surface oxidized immediately to a mixture of the +2 state (EuO) and the +3 state (Eu_2O_3), as can be seen by comparing Spectra 3a and 3b. Upon prolonged exposure to air, the same sample oxidized completely to the +3 state (Eu_2O_3), as can be seen by comparing Spectra 3c and 3d. The spectral intensity does not decrease to background level on the left side of the peaks, principally because of the close proximity of the peak arising from the $K\alpha_2$ x-ray line, which is 20 eV lower in energy than $k\alpha_1$ for copper. The interpretation in terms of chemical reaction is nevertheless straightforward.

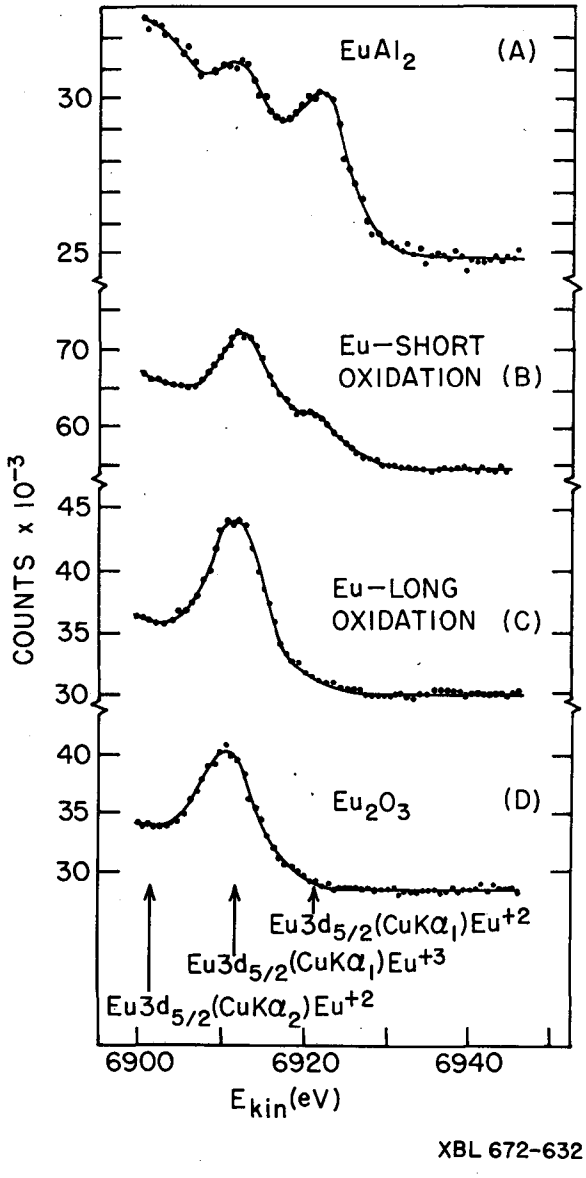

Fig. 2-3. Photoelectron peaks from various europium compounds.

Theory and Interpretation

In order to extract useful information about chemical bonding from chemical shift data, some theoretical model must be considered. We present here two such models. Both are partly classical (and therefore approximate), but the first gives some essential insights into the nature of core electron chemical shifts as well as semiquantitative estimates of their magnitude, and the second should be able to predict such shifts with reasonably good accuracy for solids with long-range order. A detailed description of these models will soon be published elsewhere,[4] so we indicate here only their salient features and the results of their application to our iodine and europium data.

The first model is constructed by assuming that all electronic charge participating in chemical bonding is removed from the valence shell (a quantum state) and subsequently becomes a spherical shell of charge of some radius r centered on the atom of interest (a classical state). The radius r will be larger than the average radius of the valence shell, as the sphere must somehow approximate the molecular electron orbitals that exist between the central atom and its nearest neighbors. The net energy shift of a core level upon forming a chemical bond can thus be calculated in two steps, the first representing the decrease in shielding when valence electrons are removed to infinity, the second representing the repulsive potential of the spherical shell of charge outside the core electrons. The first quantity can be calculated with existing free-ion (atom) computer programs, and for this calculation we have used such a program written by Roothaan and Bagus.[5] The second quantity is obtained from elementary electrostatics. This model was applied to our europium data as a qualitative check of its validity. We assume to a first approximation that only the 4f subshell of europium is altered in going from $EuAl_2$ to Eu_2O_3. It is known that the 4f configurations in these compounds are $4f^7$ and $4f^6$, respectively.[6,7] From our calculations, the free-ion shift between Eu^{+2} ($4f^7$) and Eu^{+3} ($4f^6$) is approximately 20 eV. Thus a 10-eV repulsive correction is required to give the experimental value we have observed. This corresponds to a

spherical shell radius of approximately 1.3 Å, which is approximately half the Eu-O interatomic distance in Eu_2O_3. The model thus correctly predicts that the bonding charge is located at a position intermediate between the Eu and O atoms.

The second model is a generalized and slightly modified version of one used previously to predict valence electron binding energies in the alkali halides.[8] Suppose we are interested in the binding energy of the ith core level of atom A in the solid compound $\underline{X}$ ($E_b(i, \underline{X})$. Atom A is assumed to possess some net charge Z_x, and all other atoms in the compound are given net charges also, the only restriction being overall electroneutrality. For strictly ionic solids all charges are assumed to be integral numbers, but for solids with some covalent character the charges can be used as variable parameters. The binding energy can now be calculated by means of the following energy cycle: The first step is to remove A from the lattice to form the free ion $A^{Z}x$. The energy required is denoted by E_1. Next an electron is removed from the ith level of this ion. The energy required is the binding energy of an ith-level electron in a free ion of charge Z_x [$E_b(i, Z_x)$]. Then the ion $A^{Z}x^{+1}$ is inserted back into the lattice. The energy is denoted E_2. Since the net result of this cycle is the same as that of a photoelectric process (subtracting any kinetic energy), the experimental binding energy in the solid should be given by $E_1 + E_b(i, Z_x) + E_2$. To obtain the chemical shift in binding energy between two compounds $\underline{X}$ and $\underline{Y}$, we simply take a difference and find

$$\Delta E_b(i, \underline{X}\text{-}\underline{Y}) = E_b(i, \underline{X}) - E_b(i, \underline{Y}) = E_b(i, Z_x) - E_b(i, Z_y) + (E_1+E_2)_x - (E_1+E_2)_y. \quad (2)$$

The necessary free-ion binding energies can be calculated with the aforementioned computer program. The sums, E_1+E_2, represent the classical Coulomb interaction energy of an electron in the ion of interest with all the other ions in the lattice, which are treated as point charges. This is true provided we neglect lattice distortion and electron-cloud polarization during the photoelectric process. This classical Coulomb energy is related to the Madelung constant of the solid, and for certain simple lattice structures can be derived from this constant. For solids of more complex structure this "Madelung energy" is more complicated to evaluate, although by no means impossible. As a rough estimate of its magnitude the Madelung energy for alkali halides ranges from 5 to 10 eV. This is to be compared with free-ion core shifts upon removing a valence electron, which are roughly 10 eV for iodine and 20 eV for europium.

We also note that because the photoelectrons of interest are expelled from a shallow region near the surface, the full Madelung energy may not be required in Eq. 2. Further experimental investigation is needed to evaluate this surface correction accurately, however.

A consideration of Eq. 2 explains why all the core levels in iodine and those measured in europium are shifted by very nearly the same amount. Note that the Madelung energies do not vary with i, so that any differences in the shifts of various core levels must be due solely to the free-ion terms in Eq. 2. Table 2-I gives the results of our free-ion calculations on iodine, and it is apparent that over a broad charge range all core levels shift by the same amount to within ±2%. Similar calculations indicate the same pattern for europium, but to a lesser degree, as the 4f shell penetrates much more deeply into the atom than the 5p shell. In fact, free-ion calculations on europium indicate up to a 50% variation in shifts between inner and outer core levels. This points out a potentiality of the photoelectron spectroscopic method, in that it may be possible to determine which electrons enter into chemical bonding by means of the relative shifts of various core electron binding energies.

Calculations of the Madelung energy were made for the three inorganic iodine compounds in such a way that the chemical shifts relative to KI were obtained as a function of the charge on the iodine atom in KIO_3 and KIO_4. By simply matching the observed shifts to the appropriate charge values, it is thus possible to estimate, for both compounds, the iodine charge and a corresponding fractional ionic character of the I-O bond. These are shown in Table 2-II, along with analogous results obtained from Mössbauer measurements.[9] The use of 75% of the full Madelung values represents a surface correction corresponding to a photoelectron-producing layer approximately as thick as the length required for convergence of a Madelung sum over lattice sites.

The agreement between the two sets of values is satisfactory in the sense that Madelung corrections in the allowable range can bring our derived values into agreement with the Mössbauer results. With more accurate calculations of the Madelung energy and more sophisticated data treatment involving all the atoms in the compounds under consideration, it should be possible to obtain values of charge and ionic character with much better accuracy. We also note that our results have been obtained without any detailed assumptions as to the bonding orbitals involved in each compound, whereas the Mössbauer results rely heavily on such assumptions. There is thus a possibility in the photoelectron spectroscopic

Table 2-I. Calculated binding energy shifts arising from removal of a 5p electron from various free-ion configurations of iodine. Since the calculations were nonrelativistic, levels are not distinguished by the quantum number j, and the notation 2p, for example, represents both $2p_{1/2}$ and $2p_{3/2}$.

$I^{-1}\ 5s^2 5p^6$	$I^{0}\ 5s^2 5p^5$	$I^{+1}\ 5s^2 5p^4$	$I^{+2}\ 5s^2 5p^3$	$I^{+3}\ 5s^2 5p^2$	$I^{+4}\ 5s^2 5p^1$
Level i	ΔE_b(i,0-[-1]) (eV)	ΔE_b(i, 1-0) (eV)	ΔE_b(i, 2-1) (eV)	ΔE_b(9, 3-2) (eV)	ΔE_b(i, 4-3) (eV)
2s	8.80	9.90	10.93	12.23	13.14
2p	8.79	9.87	10.93	12.19	13.16
3s	8.83	9.89	10.91	12.15	13.04
3p	8.79	9.87	10.89	12.12	13.01
3d	8.78	9.87	10.89	12.15	13.06
4s	8.85	9.87	10.82	11.97	12.78
4p	8.84	9.86	10.79	11.92	12.73
4d	8.84	9.85	10.78	11.92	12.72
5s	8.10	8.65	9.22	9.77	10.21
5p	8.39	9.37	10.73	9.44	9.90

Table 2-II. Comparison of our results for iodine charge and fractional ionic character in KIO_3 and KIO_4, with those obtained from Mössbauer measurements (Ref. 9). Those denoted "3/4 Madelung" represent a possible surface correction to our results.

Compound	I-O bond fractional ionic character	Charge on iodine
Photoelectron spectroscopy:		
Full Madelung⁻		
KIO_3	0.67	2.99
KIO_4	0.48	2.86
3/4 Madelung⁻		
KIO_3	0.35	1.10
KIO_4	0.46	2.71
Mossbauer:		
KIO_3	0.31	0.83
KIO_4	0.31	1.44

technique of inferring the orbital makeup directly, instead of assuming it in order to calculate some other property.

The fact that the shift per unit change in oxidation number is 12 times as large in europium as in iodine can be qualitatively understood. As has been stated, the free-ion shift for a given change in charge is about twice as large for europium. Also, the actual charge that is being moved into bonding orbitals is much greater between Eu^{+2} and Eu^{+3} than it is between, e.g., I^{-1} and I^0. As we have mentioned, one 4f electron is transferred between $EuAl_2$ and Eu_2O_3 ($4f^7$ to $4f^6$). However, the results of Table 2-II indicate that for a

similar unit change in the oxidation number of iodine less than 0.5 electron is transferred.

Our experimental results for the potassium salt of p-iodobenzoic acid are presented largely to indicate the feasibility of making measurements on heavy atoms as constituents in organic compounds. Since iodine is bonded only to carbon in this molecule and the two atoms have equal electronegativities, it is not surprising that the binding energies are close to those of KI rather than to those of KIO_3 or KIO_4.

Further Applications of the Technique

The theoretical interpretation of the chemical shifts reported here and the observations of the chemical shifts in carbon, nitrogen, sulfur, and chlorine reported by the Uppsala group provide a firm basis for anticipating a wide range of applications of this spectroscopic method. We illustrate this potential by describing three problems of current interest in this Laboratory.

A number of investigators are focusing attention on a class of non-heme iron proteins, called Ferredoxins,[10] which act as electron transport proteins in both photosynthesis and bacterial metabolism. The common characteristic of these proteins is their content of from two to seven iron atoms together with four sulfur atoms per iron. The photoelectron spectra will be examined in order to measure the nature and diversity of the iron and sulfur atoms contained in these proteins both before and after reduction.

It is also planned to study the coordination chemistry of metal porphyrins by examining the photoelectron spectra of the central metal ion and the nitrogen ligands. Comparison and interpretation of the spectra in the presence of and absence of the metal ion should permit a determination of the fractional contribution to the bonds of each of the constituents of the complex. In fact, the valence electronic levels have already been examined by low energy photoelectron spectroscopy in a closely related compound, copper phthalocyanine.[11]

The fractional charge or degree of ionization of impurity atoms in elemental semiconductors, as well as the relative charges on the atoms in compound semiconductors of the III-V and II-VI types, could also be investigated.

Summary

The technique of photoelectron spectroscopy has already been shown to be sensitive to changes in the chemical environment of a given atom. We have used this technique to measure shifts in the core electron binding energies of iodine and europium. We have found shifts of 0.8 eV and 9.6 eV respectively for a unit change in oxidation number.

Two theoretical models are proposed for the interpretation of these shifts and are applied to the analysis of our experimental results. The first consists of a charged shell approximation for the molecular orbitals. The second uses an energy cycle to divide the binding energy into a free-ion term and a lattice interaction (Madelung) term. All our observations can be understood in terms of one or the other of these models, and in particular, we can estimate the iodine charge in the compounds KIO_3 and KIO_4. The results agree reasonably well with those obtained from Mössbauer measurements.

The application of photoelectron spectroscopy to a wide range of problems in physics, chemistry, and biology seems feasible.

References

1. S. Hagström, C. Nordling, and K. Siegbahn, Table of Electron Binding Energies, in Alpha-, Beta-, and Gamma-Ray Spectroscopy, K. Siegbahn, Ed. (North Holland Publishing Co., Amsterdam, 1965).
2. S. Hagström, C. Nordling, and K. Siegbahn, Z. Physik 178, 433 (1964); A Fahlman, R. Carlsson, and K. Siegbahn, Arkiv. Kemi 25, 301 (1966); G. Axelson et al., Nature 213 [No. 5071], 70 (1967).
3. K. Siegbahn, C. Nordling, and J. M. Hollander, UCRL-10023, 1962.
4. C. S. Fadley, S. V. Hagström, D. A. Shirley, and M. P. Klein, Chemical Effects on Core Electron Binding Energies in Iodine and Europium, UCRL-17005, July 1966 (to be submitted to J. Chem. Phys.).
5. C. C. J. Roothaan and P. Bagus, Methods in Computational Physics (Academic Press, New York, 1963), Vol. 2.
6. V. Jaccarino, B. F. Matthias, M. Peter, H. Luhl, and J. H. Wernick, Phys. Rev. Letters 5, 251 (1960).
7. A. L. Borovik-Romanov and N. M. Kreiss, Soviet Physics JETP 2, 657 (1956).
8. N. F. Mott and R. W. Gurney,

Electronic Processes in Ionic Crystals (Clarendon Press, Oxford, 1948), p. 80.
9. D. W. Hafemeister, G. de Pasquali, and H. de Waard, Phys. Rev. 135, B1089 (1964).
10. D. I. Arnon, Science 149, 1460 (1965); also in Non-Heme Iron Proteins: Role in Energy Conversion, A. San Pietro, Ed. (Antioch Press, Yellow Springs, Ohio, 1965).
11. B. H. Schechtman and W. E. Spicer, Bull Am. Phys. Soc. 11, 899 (1966).

3. FOURIER TRANSFORM NUCLEAR MAGNETIC RESONANCE SPECTROSCOPY

Melvin P. Klein and Donald E. Phelps

The application of the Fourier transform technique to optical and infrared spectroscopy has been known for nearly fifty years,[1] but has only recently been used for high-resolution nuclear magnetic resonance.[2] The conventional method of producing a nuclear magnetic resonance spectrum employs a scan by either magnetic field or radio frequency through the region of interest. The rate of scanning is decided by the requisite resolution. Lines which are separated by 1 Hz must be scanned at only a fraction of 1 Hz.[2] When this maximum scanning rate is exceeded, the spectrum is distorted. Also to be considered is that during a frequency or field scan only a single point is being observed at any instant. Thus time is not being used with optimal efficiency, a factor which enters into the ultimate sensitivity of NMR spectroscopy.

It has been shown that the free-induction decay following a short, intense radio-frequency pulse is the Fourier transform of the conventional spectrum.[3] The most compelling reason to resort to this technique is that the entire spectrum is generated for each radio-frequency pulse, with a consequent increase in the efficiency of time usage. The pulses may be repeated at intervals of several seconds.

The accompanying figures dramatically illustrate the time which may be saved by employing the transform technique. Figure 3-1 shows a field-swept spectrum of the ^{31}P NMR of $P(OCH_3)_3$ taken during the sweep times noted on the traces. It is apparent that at least 100 seconds must be spent to obtain a fully resolved undistorted spectrum. Figure 3-2 illustrates the impulse response (above) and the spectrum derived therefrom by a Fourier transformation (below). The time scale for the impulse response was 1.25 sec, demonstrating that much less time--by about a factor of one hundred--is required for this method. The Fourier transformation of the impulse response is performed either by a digital computer or by conventional spectrum analyzers. The former is more accurate, and capable of producing better spectra; the latter method is useful because it may be performed in the NMR laboratory, giving results immediately.

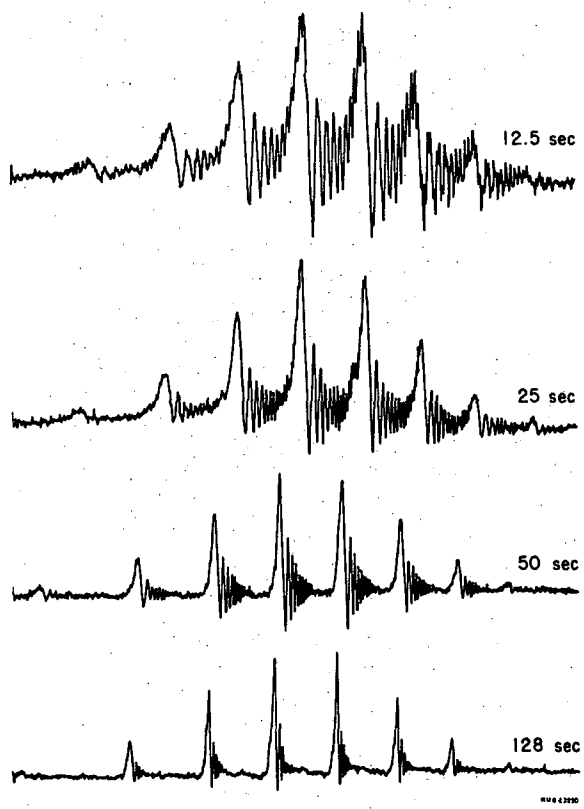

Fig. 3-1. Conventional field-swept NMR spectra of ^{31}P in $P(OCH_3)_3$. The time per sweep is indicated beside each spectrum. The degradation of the spectrum with decreasing sweep times is illustrated.

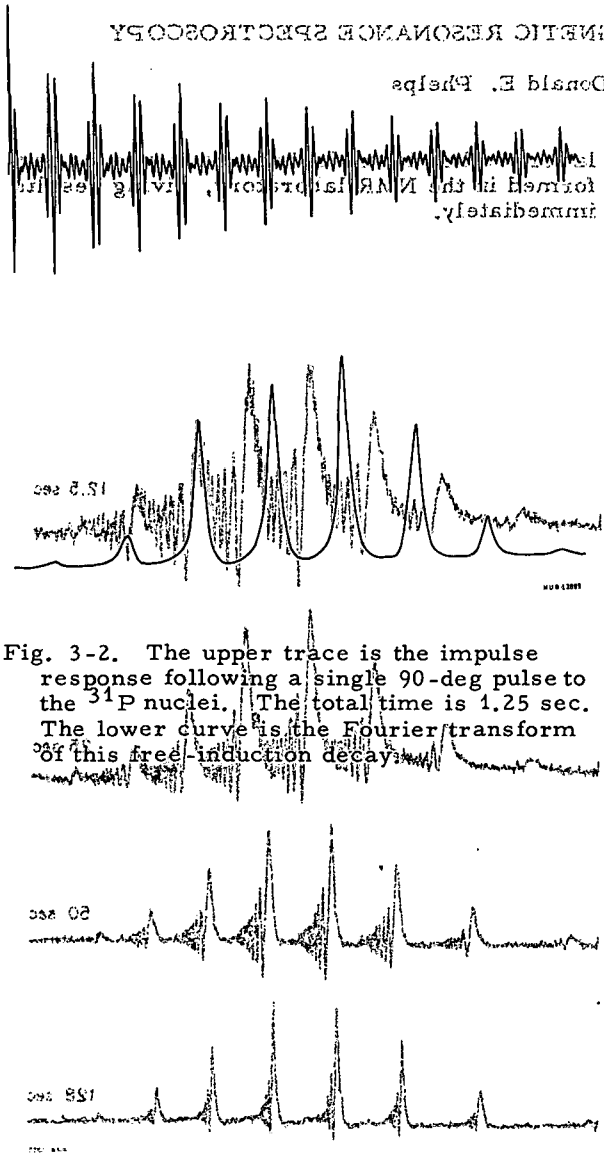

Fig. 3-2. The upper trace is the impulse response following a single 90-deg pulse to the ^{31}P nuclei. The total time is 1.25 sec. The lower curve is the Fourier transform of this free-induction decay.

The great saving in time means that the ultimate sensitivity of NMR experiments may be extended by an order of magnitude when averaging techniques are used.[4] This will permit the observation of NMR spectra of biologically significant molecules which have previously eluded observation or have yielded spectra with an inadequate signal-to-noise ratio.

References

1. Rubens and Wood, Phil Mag. 21, 249 (1911).
2. R. R. Ernst and W. A. Anderson, Rev. Sci. Instr. 37, 93 (1966).
3. I. J. Low and R. E. Norberg, Phys. Rev. 107, 46 (1957).
4. M. P. Klein and G. W. Barton, Rev. Sci. Instr. 34, 754 (1963).

4. PRODUCT INVENTORY IN THE RADIOLYSIS OF CRYSTALLINE CHOLINE CHLORIDE

Margaret Ackerman and Richard M. Lemmon

Introduction

The earliest report of the unique radiation sensitivity of crystalline choline chloride indicated that the identified radiolysis products, trimethylamine and acetaldehyde, accounted for essentially all the decomposed choline.[1] However, that indication was provided principally by paper chromatographic studies of nonvolatile products. The present study, which includes quantitative measurements of all detectable products, was undertaken in the hope that a full product inventory would shed further light on this unique radiolysis mechanism.

Experimental Section

Sample Preparation and Irradiation

The unlabeled choline chloride used was the Eastman Organic Chemicals "white label" product. The ^{14}C-methyl-labeled compound was prepared by reacting $^{14}CH_3I$ with dimethylaminoethanol; the resultant iodide was converted to chloride by treatment with Ag_2O followed by HCl. The labeled chloride was recrystallized from ethanol-ether.

Fourteen-mm o. d. Pyrex tubes fitted with a break seal were each charged with 133 mg of choline chloride dissolved in 0.5 ml of methanol. After the bulk of the methanol was evaporated under a stream of dry nitrogen, the tubes were placed in an ice-salt bath and connected to a vacuum line. The samples were evacuated very slowly and pumping was continued for approximately 24 hr while the cooling bath was allowed to warm to room temperature. The samples were then heated to 100° for 30 min, and the tubes sealed. By means of a 3000-curie ^{60}Co source, the samples were given a total dose of from 28 to 192 Mrads at a rate of 11.6×10^5 rads/hr. In order to look for a dose-rate effect, in one experiment the dose rate was increased to 116×10^5 rads/hr.

Determination of Hydrogen, Methane, and Acetaldehyde

The irradiated samples were connected to a vacuum system of known volume fitted with a Zimmerli pressure gauge and two traps. The first trap served both as a collector of volatile products and as a reservoir for the ethanol used to dissolve the crystalline sample. The second trap was packed with a 4A molecular sieve (Linde). Preliminary work with this sieve (200 to 500 mg) had shown that a 1-ml sample of methane injected into the system with a gas-tight syringe was totally absorbed at -196°, and was not released even after evacuation of the trap to a pressure of 10 μ for 20 min. (Carbon monoxide is known to be even more strongly bonded to the molecular sieve.) However, subsequent heating to 150° for a few minutes gave 100% recovery of the methane from the sieve.

After 250 μl of ethanol solvent was frozen in the first trap, the entire system was thoroughly evacuated. The sieve trap and the Zimmerli gauge were closed and the sample tube opened after it had been cooled with liquid N_2 (to prevent any sudden release of gaseous products that might carry some solid sample out of the tube), and then allowed to come to room temperature. The volatile products were distilled into the first trap, which was held at -196°. The sieve trap was cooled to -196°, opened, and 20 min allowed for the transfer of volatile compounds from the first trap to the sieve (only CH_4 was subsequently seen on the gas chromatograph). Following this transfer, the Zimmerli gauge was opened and the pressure of H_2 read. The H_2 was then pumped off, the sieve trap closed, and the contents of the first trap distilled into the sample tube in order to dissolve the crystalline sample. After the sample was in solution, all the volatile material was again distilled into the first trap. The transfer of methane into the sieve trap and the determination of H_2 pressure was repeated (no further H_2 was observed).

The sieve trap was connected to the injection port of a Varian Aerograph Model A-350 gas liquid chromatograph. After the trap was heated to 200°, the contents were injected onto a 4-ft, 0.25-in. 5A molecular sieve column maintained at 80°; He flow rate (F) 30 ml/min. (Only CH_4, retention time [t_R] 16 min, was detected.) The first trap was packed in dry ice, transferred to a dry box, and opened. The contents were drawn into a syringe which had been cooled in dry ice, then quickly injected into the A-350 and chromatographed on a 20-ft, 0.25-in. column of 30% "UCON Polar" on acid- and dimethylchlorosilane-treated 45/60 mesh Chromosorb W (He F 30 ml/min, temp. 70°). This column showed, in addition to the expected acetaldehyde (t_R 32 min) and ethanol solvent

(t_R 70 min), a trace of CH_3Cl (t_R 20 min) and three unidentified compounds with retention times of 88, 110, and 140 min. No other peaks were detectable, even when the column temperature was raised to 170° and the chromatogram allowed to run for another hour. This eliminates, as detectable products, such possibilities as ethylene glycol, ethylene chlorohydrin, methylaminoethanol, and dimethylaminoethanol. In order to identify the observed peaks, several 0.5-g crystalline choline chloride samples were irradiated (30 M rads). The volatile products from these samples were pumped into a trap suitable for injection and separated by chromatography on the same "UCON Polar" column, as above. Samples processed in this manner contained only two of the unknown compounds, and it was necessary to process a sample with ethanol as a solvent to obtain the third. Following purification by gas chromatography, the mass spectrum of each of the unknown compounds was determined on a Consolidated Electrodynamics Corporation Model 21-130 mass spectrometer. Comparison of these spectra with published spectra and spectra of known compounds obtained on our instrument enabled us to identify the first unknown compound (t_R 88 min, appearing only when ethanol was used as a solvent) as the addition product of ethanol and acetaldehyde, acetal. The other two unknown compounds were also products of acetaldehyde, crotonaldehyde (t_R 110 min), and paraldehyde (t_R 140 min).

Since the pressure of H_2 in a known volume was read, the quantity could be directly calculated. The quantity of the other components was determined by comparison of their gas chromatographic peak areas with the peak areas obtained when known quantities were chromatographed.

Methyl Chloride as a Radiolysis Product

During the course of earlier work on the radiolysis of choline chloride, traces of methyl chloride had been observed (but not reported) on gas chromatograms used to purify deuterated acetaldehyde and trimethylamine products.[2] In the present study, at a total dose of 30 Mrads, only barely detectable amounts of methyl chloride were formed. In the earlier work, higher total doses at higher dose rates were usually employed. Suspecting that either or both of these factors could be responsible for the production of methyl chloride we prepared four 0.5-g samples of crystalline choline chloride. Sample 1 received 30 Mrads at 11.6×10^5 rads/hr (the same dose rate, and approximately the same total dose as given to all other samples in the present work). Sample 2 received 30 Mrads at 116×10^5 rads/hr. Sample 3 received 192 Mrads at 116×10^5 rads/hr (the dose rate and total dose used in the previous work[2]). Sample 4 received 192 Mrads at 11.6×10^5 rads/hr. The volatile products from all samples were chromatographed on "UCON Polar," as previously described. Only Samples 3 and 4, those receiving a total dose of 192 Mrads, contained a detectable amount (about 0.2% of the decomposed choline) of methyl chloride.

Determination of Trimethylamine and Polymer

Current and past work have shown that the trimethylamine produced in the radiolysis appears as the hydrochloride salt. No detectable amounts of trimethylamine had ever been observed until base was added to an irradiated sample. Past work had also indicated that no other aminos were being formed in appreciable quantity, since radioautographs of paper chromatograms of irradiated methyl-^{14}C-labeled choline chloride revealed only two active spots; one was undecomposed choline chloride and the other was trimethylamine hydrochloride. In order to confirm this observation by gas chromatography, a 1-g sample of irradiated choline chloride was transferred to a tube fitted with a side arm bearing a serum cap. The tube was connected to a vacuum line containing a trap suitable for direct injection into the A-350 chromatograph. The system was thoroughly evacuated. Then, sufficient alcoholic KOH to dissolve the sample was added by syringe through the serum cap. The evolved gas and a small amount of the methanol solvent were transferred to the trap and chromatographed on a 10-ft, 0.25-in. column of 15% THEED 5% TEP on 60/80 Chromosorb W (temp. 65°, He F 40 ml/min)--a column that will cleanly separate NH_3, methylamine, dimethylamine, and trimethylamine. Only trimethylamine (t_R 2.7 min) was observed on this chromatogram.

Paper (rather than gas) chromatography was chosen as the means of determining the amount of trimethylamine formed, because the amount of undecomposed choline chloride and the amount of polymer formed could be determined simultaneously. Consequently, two 100-mg samples of the methyl-^{14}C-labeled compound, containing a total activity of 9.2×10^4 dpm, were prepared and irradiated (30 Mrads). The samples were stored 422 days, then the tube was opened and the crystals dissolved in 1 ml of methanol. An aliquot (10 µl) was withdrawn from each sample and chromatographed (one direction) on Whatman No. 1 paper with n-butanol:water:12 N HCl (4:1:1) used as a developing solvent. Radioautographs of these chromatograms were used to locate the radioactive spots so that the amount of activity could be measured by a Geiger tube.

Trimethylamine hydrochloride and undecomposed choline chloride were the only detectable radioactive spots. Polymeric material, which had been observed previously on the origin of chromatograms from samples given 192 Mrads, was not produced in detectable amounts by the 30 Mrad dose given these samples (under conditions when as little as 1% could have been observed). The percentages of trimethylamine hydrochloride are essentially equivalent to the percentages of choline decomposed.

Search for Cl_2 as a Possible Radiolysis Product

The search for Cl_2 was made by chromatographing all the volatile products from the irradiated crystals; the crystals were dissolved in absolute ethanol and the volatiles (including EtOH) vacuum-line transferred into a trap from which they could be directly injected into a gas chromatograph (Varian Aerograph Model A-350, 5-ft., 0.25-in. column of "Poropak Q", (temp. 50°, He flow rate 40 ml/min). Under these conditions the t_R for Cl_2 is 2.3 min.

Results and Discussion

The quantitative data on the radiolysis products are presented in Table I and may be summarized as follows:

(1) Experiment 1-3 show that H_2 and CH_4 are only very minor products at doses of about 30 Mrads and post-irradiation storage times of 15 to 232 days. The average percent of decomposed choline appearing as H_2 is 2.7%. This corresponds to a $G(H_2)$ from choline chloride of 1.1. The corresponding average figure for $G(CH_4)$ is 0.9. These are representative G values for the production of H_2 and CH_4 from, for example, saturated hydrocarbons.[3] Since the radiolysis of crystalline choline chloride has been observed with G(-M) values as high as 55,000,[4] it is reasonable to conclude that the H_2 and CH_4 come from ordinary, random, radiolytic processes that are unrelated to the unique, chain-decomposition mechanism.

(2) Experiments 4 and 5 demonstrate that CH_3Cl is also a very minor product. We were unable to detect this compound in 30 Mrad irradiations. At 192 Mrads we did find detectable CH_3Cl--about 0.2 percent of the total decomposition products, and independent of the dose rate. The corresponding $G(CH_3Cl)$ is 0.06.

(3) Experiments 6 and 7 show that there is very little polymer formed at 30 Mrads. We know from previous unpublished observations that extensive radiation decomposition leads to more polymer; here, however, at about 30% decomposition, the polymer formation is negligible. What this polymer may be is suggested by the appearance of contronaldehyde and paraldehyde (see footnotes d, e, and j). It is well known that aldehydes tend to polymerize on irradiation.[5]

(4) Experiment 7 relates the appearance of acetaldehyde (determined by gas chromatography to that of trimethylamine (determined by paper chromatography). An exact duplicate of this experiment was performed and led to almost identical results; that experiment, in the interests of space saving, is not recorded in the table. This work further indicates that acetaldehyde and trimethylamine account for nearly all the choline's radiation decomposition. The 96.5% value for acetaldehyde (last column) is a minimal figure; small mechanical losses are expected during transfer operations.

(5) Experiment 8 was a direct search for molecular chlorine as a possible radiolysis product. (Again, a separate experiment, with very similar results, was performed.) This search was made because of the possibility that Cl atoms could be involved in the radiolysis mechanism. If so, one might expect a significant yield of their dimer, molecular chlorine. However, the results of this work indicate that if any Cl_2 is formed it is less than 1% of the decomposed choline (we are unable to set a smaller upper limit because water and Cl_2 have the same retention time on our "Poropak" columns).

The present work clearly indicates that the decomposition mechanism is very clean. The chain mechanism leads very specifically to a scission of the choline cation between the nitrogen atom and the adjacent methylene carbon, leading to the production of trimethylamine and acetaldehyde. For doses up to about 3×10^7 rads, and approximately 30% choline decomposition, all other products comprise, at most, only 3% of the total radiolysis yield,

Summary

A quantitative study was made of all detectable products that appear when the extraordinarily radiation-sensitive organic crystal, choline chloride, was exposed to γ radiation. Besides the known major products, trimethylamine and acetaldehyde, only trace amounts of other products (H_2, CH_4, CH_3Cl, Cl_2, crotonaldehyde, and paraldehyde) are detectable. The total yield of these trace products is not more than 3% of the decomposed crystal. These results emphasize the very specific nature of the radiolysis mechanism.

Table 4-I. Products appearing in the γ-radiolysis of crystalline choline chloride.

Expt. No.	Dose (Mrads) (at 11.6×10^5 rads/hr)	Time of storage at 25° (days[a])	Choline decomposed (mmoles)	Product formation		
				cpd.	mmoles	% decomposed choline
1	37.2	143	0.372[b]	H_2	0.014	3.8
				CH_4	0.008	2.1
				CH_3CHO	0.351[d]	94.4
2	34.9	232	0.358[c]	H_2	0.008	2.2
3	28.2	15	0.311[b]	H_2	0.007	2.3
				CH_4	0.008	2.6
				CH_3CHO	0.296[e]	95.2
4	192	1	0.88[g]	CH_3Cl	0.002[h]	0.2
5	192[f]	1	1.79[g]	CH_3Cl	0.004[h]	0.2
6	32.6	422	0.284[i]	$(CH_3)_3N$	0.288	100
				polymer	<0.002	<1
7	29.3	15	0.252[i]	CH_3CHO	0.242[j]	96.5
				$(CH_3)_3N$	0.252	100
				polymer	<0.002	<1
8	28.2	181	0.311	Cl_2	<0.003	<1

a. Between irradiation and analysis. Earlier work (Ref. 4) has shown that, for a given radiation dose, the percent decomposition is dependent upon this time.
b. Sum of products found on gas-liquid chromatograms.
c. Estimated from decompositions measured in similar samples.
d. Sum of (in mmoles): CH_3CHO (0.022), acetal (0.133), crotonaldehyde (0.023; equiv. to 0.046 CH_3CHO), paraldehyde (0.050; equiv. to 0.150 CH_3CHO).
e. Sum of (in mmoles): CH_3CHO (0.011), acetal (0.076), crotonaldehyde (0.004; equiv. to 0.008 CH_3CHO), paraldehyde (0.067; equiv. to 0.201 CH_3CHO).
f. Dose rate 116×10^5 rads/hr.
g. Based on amt. CH_3CHO observed from the irrad. of 500 mg (3.53 mmoles) of choline chloride.
h. At lower total doses there was no detectable CH_3Cl.
i. Determined by counting undecomposed choline-^{14}C on paper chromatogram.
j. Sum (in mmoles) of: CH_3CHO (0.004), acetal (0.091), crotonaldehyde (0.003; equiv. to 0.006 CH_3CHO), paraldehyde 0.047 (equiv. to 0.141 CH_3CHO).

References

1. B. M. Tolbert et al., J. Am. Chem. Soc. 75, 1867 (1953).
2. R. M. Lemmon and M. A. Smith, ibid. 85, 1395 (1963).
3. A. J. Swallow, Radiation Chemistry of Organic Compounds (Pergamon Press, New York, N. Y., 1960), pp. 61-75.
4. R. O. Lindblom, R. M. Lemmon, and M. Calvin, J. Am. Chem. Soc. 83, 2484 (1961).
5. J. C. McLennan and W. L. Patrick, Can. J. Res. 5, 470 (1931).

5. IDENTIFICATION OF SOME NEW PRODUCTS FORMED BY THE IRRADIATION OF SOLID BENZENE WITH ACCELERATED $^{14}C^{+}$ IONS

Helmut Pohlet, Wallace Erwin, Tz-Hong Lin and Richard M. Lemmon

We are continuing our studies of the chemical consequences of the interaction of accelerated carbon ions with benzene (previous discussions appeared in our preceding annual report: UCRL-16806, March 1966, pp. 54-49). Recent gas-liquid chromatography (GLC) tracings of the target material after such irradiations has shown that there are a number of major products formed that have longer retention times than the previously reported benzene, toluene, and cycloheptatriene. Some evidence was given indicating that one of these products was diphenylmethane, and it was further predicted that another was phenylcycloheptatriene. In this report data will be given showing that these two products are indeed formed, and also that phenylacetylene is another of the major "post benzene" products--i.e., compounds appearing after benzene, on GLC. We interpret other data to be compatible with the presence of benzocyclopropene or perhaps another of the three possible isomeric bicycloheptatrienes:

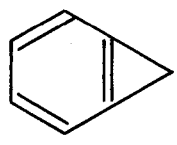

benzocyclopropene

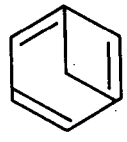

bicyclo [3.1.1] - heptatriene-1, 3, 5

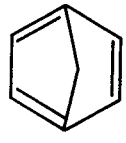

bicyclo [2.2.1] - heptatriene-1, 3, 5

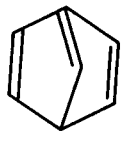

bicyclo [2.2.1] - heptatriene-2, 5, 7

The formation of such a C_7 compound (excited) on the interaction of an energetic $^{14}C^{+}$ ion (or atom) with benzene, followed by ejection of a C_1 species, is a possible mechanism for the appearance of benzene-^{14}C.

Experimental Procedure

The present target of the ion accelerator consists of a 1-cm-diam by 1/2-cm-long brass cylinder was silver soldered to the face of the cold finger. The 3/4-in.-diameter gold target disk was attached to this pedestal with silver paint, giving thermal and electrical contact.

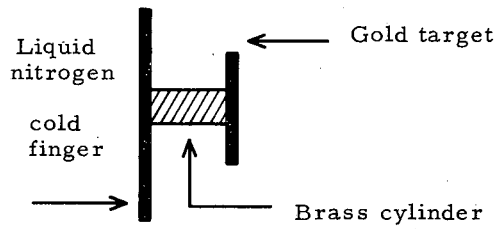

The benzene was deposited on the gold target from four nozzles arranged around the edge of the gold disk. It was hoped this arrangement would give a more uniform deposit of benzene over the entire surface of the gold disk. However, the result was four hills of solid benzene reaching towards the nozzles with a thinly coated area in the center:

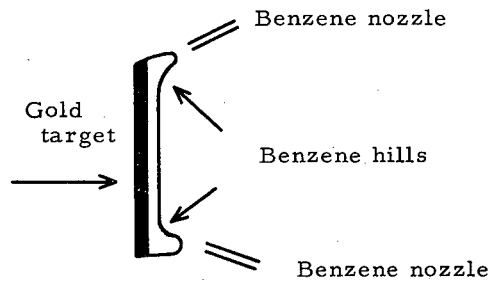

In the irradiation, the ion beam (approximately 1 μA) was focused near the center of the target. Approximately 200 μl of benzene was fed to the target before the irradiation started, and the input of benzene during the irradiation was 90 to 100 μl/hr. The irradiation lasted for 2.75 hr. The benzene recovered from the target in the sample collection vial was 250 to 300 μl. To this recovered benzene, several unlabeled carriers were added--30 μl toluene, 30 μl cycloheptatriene, 30 μl phenylacetylene, 30 mg diphenylmethane, 30 mg 7-phenylcycloheptatriene, and 30 mg biphenyl. All of these materials, with the exception of the 7-phenylcycloheptatriene, were commercial products.

We prepared the phenylcycloheptatriene

following the manner described by Doering and Knox:[1] When 25 g of cycloheptatriene was brominated, 73.7 g of dibromotroplidene (n_D = 1.5968^{25}) was obtained. Heating this dibroma compound at 65 to 70° under 1 mm yielded 10 g (21.3% yield) of tropylium bromide, m. p. 205–210°. Tropylium bromide was further reacted with phenyl-lithium to give 10 g of crude phenylcycloheptatriene (69% yield). Vacuum distillation of the crude product at 0.7 mm gave the following fractions:

1. below 25°, 0.9 g;
2. 65 to 86.5°, 2.9 g;
3. 86.5 to 87°, 4.1 g;
4. 87 to 100°, 1.5 g.

Fraction 3 crystallized after standing at room temperature overnight. This crystal was filtered and gave a mp 27–28°; on recrystallization from methanol the purified white crystal (3 g) melted at 28–29°. Figure 5-1 shows the NMR spectrum of this compound. There are absorptions at δ = 6.75 to 6.55 (triplet), 6.33 to 5.95 (complicated doublet), 5.50-5.17 (quartet), and a triplet around 2.65, with the peak ratio of 5:2:2:2:1. These are in agreement with the data reported by Ter Borg and Kloosteriziel[2] and Tezuka[3] for 7-phenylcycloheptatriene.

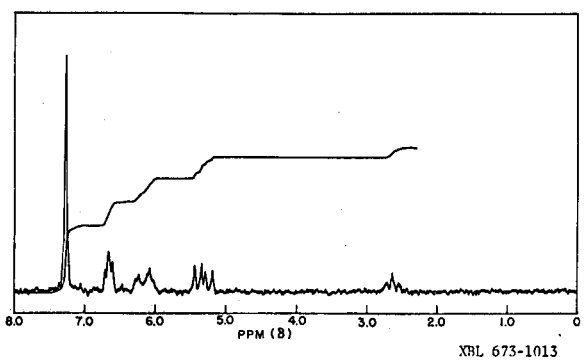

Fig. 5-1. Lower line, NMR spectra of 7-phenylcycloheptatriene in carbon tetrachloride; upper line, integrated hydrogen absorptions.

Figure 5-2 shows the GLC radioactivity and mass tracing from a 3-µl aliquot of the target benzene containing the added carriers. It can be seen that not only do radioactivity and mass peaks agree for benzene, toluene, and cycloheptatriene, but also that there are radioactivity peaks matching phenylacetylene, diphenylmethane, and phenylcycloheptatriene or biphenyl (these two have approximately the same retention time). From two separate aliquots, which were taken from two separate ion accelerator irradiations, this biphenyl-phenylcycloheptatriene peak was trapped. Then, to each of these samples 250 µl of pentane and approx 1 mg of PtO_2 were added, and the sample was hydrogenated for 1 hr at room temperature and 30 lb H_2 pressure. In all cases approx 90% of the radioactivity was converted to a new material chromatographing with an identical retention time to phenylcycloheptane, the hydrogenation product of the phenylcycloheptatriene carrier (see Fig. 5-3). A small peak of radioactivity always remained in the biphenyl region; however, we have not determined whether this actually is biphenyl or, what would be even more likely to be formed, methyl-biphenyl. The same treatment was given to the diphenylmethane peaks trapped from the chromatograph, but no changes occurred in these radioactivity peaks. In this case two chromatographic systems (Carbowax-20M and SE-30) were used to show the agreement between a radioactivity peak and the diphenylmethane mass peak. The phenylacetylene peak was trapped, hydrogenated, and rechromatographed, giving only mass and radioactivity peaks with retention times identical to that of ethylbenzene. This latter material has been checked only on aliquots from one irradiation because we did not know earlier what carriers to add. It should be mentioned also that there was no possibility of confusing this radioactive peak with that of phenylethylene, because phenylethylene has a retention time which falls between those of phenylacetylene and ethylbenzene, and which is completely separated from both of these materials.

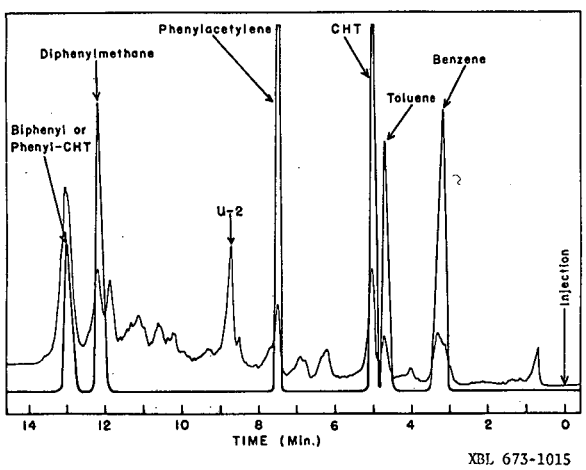

Fig. 5-2. GLC tracings for 30 µl of bombarded benzene, and added carriers, on Carbowax 20M. Smooth curve: mass (thermal conductivity) detection. Jagged curve: radioactivity (proportional counter) detection.

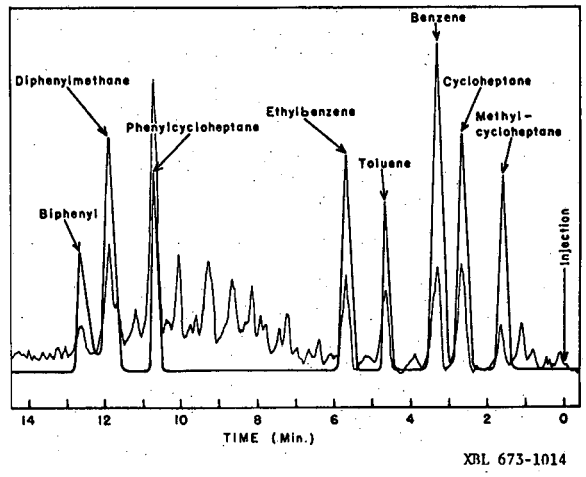

Fig. 5-3. GLC tracings for hydrogenated bombarded benzene, and added carriers, on Carbowax 20M. Smooth curve: mass (thermal conductivity) detection. Jagged curve: radioactivity (proportional counter) detection.

Figure 5-3 shows the radioactivity and mass tracings obtained when a 25-μl aliquot of the irradiated benzene was first hydrogenated and then chromatographed. Methylcyclohexane was an additional carrier added to this sample. By comparing Figs. 5-2 and 5-3, it can be seen that the radioactivity associated with the toluene mass peak has increased for the hydrogenated material, and also that a new radioactivity peak, which may be methylcyclohexane, has appeared. This hydrogenated chromatogram supplies not only confirmation of the identity of the parent compounds we have been discussing, but it may also give us information concerning compounds that might have been destroyed during the chromatography of the unhydrogenated material. Several new peaks have appeared for which we seem to have no parents in the unhydrogenated material.

We have trapped the area marked U-2 in Fig. 5-2, hydrogenated the trapped sample, and rechromatographed the hydrogenate. In two separate trappings (from one irradiation) two new radioactive peaks appeared, one corresponding to toluene and the other perhaps being methylcyclohexane. (This was not cochromatographed, but the retention times were compared.) We have attempted to repeat the trapping of U-2 so we could add methylcyclohexane as well as toluene to the sample to be hydrogenated. However, since we have no carrier to add, we have had several failures by apparently losing the compound. This means we have not yet confirmed our suspected formation of methylcyclohexane, although little doubt seems to exist concerning the formation of toluene.

Benzocyclopropene (see first page of this report) was considered a good possibility for the identity of U-2. A sample of this unusual hydrocarbon was kindly supplied to us by Professor E. Vogel, Organic Chemical Institute, University of Cologne, Cologne, Germany. However, this compound proved to be not identical (by cochromatography) with U-2. Neither did it coincide with any of the other radioactive peaks on our chromatograms.

References

1. W. von E. Doering and L. H. Knox, J. Am. Chem. Soc. 76, 3202 (1954).
2. A. P. Ter Borg and H. Kloosterziel, Rec. Trav. Chim. 82(8), 741 (1963).
3. Takahiro Tezuka, Bull. Chem. Soc. Jap. 37[8], 1113 (1964).

6. OPTICAL PROPERTIES OF RIBONUCLEIC ACIDS PREDICTED FROM OLIGOMERS†

C. R. Cantor, S. R. Jaskunas, and I. Tinoco, Jr.

A chemical explanation of the biological mode of action of RNA is contingent upon an understanding of the molecular structure. The general chemical structure of RNA is known. The complete details of the nucleotide sequence of four RNA's are now available, and the problem of determining the sequence of many other RNA's is being actively pursued. To understand the structure of an RNA, one additional problem remains. This is the determination of the molecular conformation under a variety of conditions which, one hopes, approximate the in vivo state. The problem of RNA conformation is complicated by the wide range of sizes and functions found for RNA's. If the dominant interactions which determine the conformation of an RNA in solution can be identified and characterized, the problem will be greatly simplified. At one time, the interaction between the bases of an RNA strand to form hydrogen-bonded base pairs was considered to be the sine qua non of RNA structure. Many hypothetical RNA conformations have been constructed by using a set of rules which attempts to maximize the number of A-U and G-C pairs, consistent with the constraints of the geometry of the RNA strand. Recently, it has been recognized that base stacking between the neighboring bases on a polynucleotide strand contributes a major part of the stability of the secondary structure. Thus we were interested to see if experimental conditions could be found whereby single-strand stacked conformations would predominate over base-paired regions.

A large number of possible conformations have been suggested for RNA's and polynucleotides. These include multiple-strand helices, single-strand helices, random coils, and more complicated folded arrangements. In view of the complexity of the problem of RNA conformation, what is needed is a set of simple model systems. These are the oligoribonucleotides. We expect that most of the properties of RNA should eventually be explainable in terms of the properties of its smaller components. Towards this end we are studying the conformational properties of oligonucleotides. In this paper we shall use some of the results obtained with oligomers to analyze the properties of polymers.

Many different experimental methods have been used as probes of RNA structure. They include chemical and enzymic reactivity, optical properties, hydrodynamic properties, small-angle x-ray scattering, hydrogen exchange, and nuclear magnetic resonance. Here we shall be mostly concerned with ultraviolet optical properties. The major advantage of ultraviolet spectra and optical rotatory dispersion is that experiments can be performed with very small quantities of material. Thus there is available a wealth of experimental data. Unlike many of the properties mentioned above, optical properties are readily suited to attempts to generalize from oligomers to polymers. In this work we shall extend the nearest-neighbor methods developed to account for the optical properties of oligomers.[1] These simple empirical calculations fairly well explain the optical properties of single-strand polymers. In addition, it should be possible to extend these methods to take into account double-strand and more complex conformations.

The yeast alanine sRNA with its 77 nucleotides and known sequence is a good molecule to illustrate our methods. We constructed a three-dimensional model of the alanine sRNA which included both the stacking of bases on a single strand, and the possibility of base pairing. Thus we used strong springs to connect bases which we believed were stacked, and interlocking rings to connect unstacked bases. The latter permit relatively free rotation of linked residues; the former will tend to keep stacked sections rigid. The bases were constructed from metal blocks, which are larger for purines than pyrimidines. The result is an approximate scale model.

We were able to construct conformations for the alanine sRNA which have considerably more hydrogen-bonded pairs than the models proposed previously. In addition, the model contains the additional constraints of base stacking. This conformation was selected by using the following rules. Uracil does not stack as strongly as the other three normal bases, and thus all U's were connected by rings instead of springs. The stacking of bases similar to U (T, dihydro U, and ψ) is also weak, but all purines stack strongly. Base pairs in which one base is I, T, dihydro U, or dimethyl G are allowed, although some of these interactions may be weaker than normal base pairs.

We have at our disposal the measured ORD of the alanine sRNA (Vournakis and Scheraga, 1966, Abst. Tenth Ann. Meet. Biophys. Soc., p. 54). We would like to compare this with the ORD calculated for the conformation proposed. In order to do this, we must

first compute the ORD of the single strand. The following approximations were made. We assume that the contribution to the ORD from unusual bases is the same as from the normal base they resemble. Thus we replaced I, MeI, MeG, and DiMeG by G; ψ and T by U. Since dihydro U does not contain a chromophore which absorbs in the 260-mμ region, we assumed it was a blank. Since the unusual bases are not present in large amounts, we expect that these approximations are not very severe, but to permit more accurate calculations it will be worth while to measure the ORD of dimers which contain unusual bases. The ORD calculated for single-strand alanine sRNA is compared with the experimental results of Vournakis and Scheraga at pH 6.83, 0.1 M phosphate, 0.15 M KCl, in Fig. 6-1. In this case, the experimental results in salt are shifted far to the blue compared with calculated or single-strand values.

However, if the contribution to the optical rotatory dispersion of the double stranded regions is added, the calculated results are significantly altered. The agreement in the shapes of the experimental and calculated optical rotatory dispersion for double strand is now excellent. By adding the contributions of double strands to the ORD, we are able to shift the single-strand calculations until they have almost the same peak, trough, and crossover as the experimental curve. The magnitude of the calculated curve is less satisfactory, since it is larger than the observed ORD. It is possible that this may be due to the choice of extinction coefficients, but a much more likely explanation is that the methods we have used here are so roughly approximate. There are undoubtedly errors in our calculation of the ORD of the double strand, since he have used only two of the ten contributing interactions. In addition, our model for the conformation may be far from the truth. The assumptions we made to count the contribution of unusual bases are also open to question. Thus we are pleased that the agreement between calculation and experiment is as good as it is. Whether or not it is fortuitous remains to be seen; however, it is clear that ORD is potentially a very powerful tool for studying the fine details of the conformation of RNA in solution.

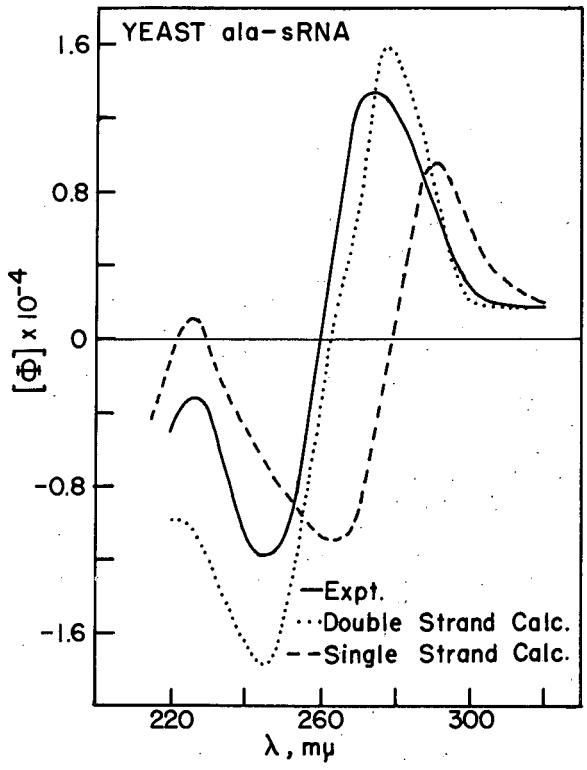

Fig. 6-1. Optical rotatory dispersion of the yeast alanine sRNA. ————, Experimental results of Vournakis and Scheraga (1966, Abst. Tenth Ann. Meet. Biophys. Soc., p. 54); ------, calculated ORD of single-strand RNA; ....., calculated ORD of a partially double-strand RNA.

References

†Condensed from C. R. Cantor, S. R. Jaskunas, and I. Tinoco, Jr., J. Mol. Biol. 20, 39 (1966).

1. C. R. Cantor and I. Tinoco, Jr., J. Mol. Biol. 13, 65 (1965).

7. CHLOROPHYLL-CHLOROPHYLL INTERACTIONS†

Edward A. Dratz, Alfred J. Schultz, and Kenneth Sauer

Introduction

Isolated chlorophyll molecules in solution are unable to carry out the energy-converting photoreactions characteristic of photosynthetic organisms. These organisms provide lipoprotein matrices (chloroplast grana or lamellae; bacterial chromatophores) in which the chlorophylls, carotenoids, and some important oxidation-reduction cofactors are brought together in a highly specific relationship to one another. Any attempt that the experimenter makes to alter this relationship almost invariably leads to complete loss of the photosynthetic activity. This applies to solvent extraction, treatment with most detergents, mild heating, etc. On the other hand, chloroplasts from leaves which have been fixed chemically with glutaraldehyde are found to retain a substantial fraction of their ability to carry out quantum conversion via the Hill reaction.[1]

The evidence at hand points to an important role for the particular way in which the pigments and cofactors are arranged spatially. The pigment molecules, for example, cannot be considered to be isolated from one another even as a good first approximation. Typical lamellar fractions contain 6 to 8% chlorophyll by weight, and pigment concentrations run in excess of 0.1 mole/liter.

Evidence from absorption spectra of chloroplasts from higher plants and algae as well as of photosynthetic bacteria suggests that in vivo the chlorphyll is at least partially aggregated. For example, low-temperature spectroscopy of plant material resolves several absorption maxima in the long-wavelength region, but the extracted chlorophyll a has only a single peak.[2] Fluorescence excitation spectra of those samples suggest that a part of the chlorophyll a, absorbing on the short-wavelength side of the main band, is unaggregated and highly fluorescent, while the chlorophyll a absorbing on the long-wavelength side of the main band is weakly fluorescent and is supposed to be aggregated.

Studies aimed at elucidating the nature of the pigment associations and their environments have met with only partial success. Oriented chloroplasts or fragments from them show little or no dichroism for most of the pigment absorption.[3-5] The fluorescence of the chlorophyll in these organelles is found to be almost completely depolarized. A long-wavelength form of chlorophyll a which is dichroic and gives rise to polarized fluorescence involves only a small fraction of the total chlorophyll in chloroplasts.[4-6] This fraction may, however, be of utmost importance to the energy conversion process.

Studies of nuclear magnetic resonance, infrared, and visible absorption spectra and of apparent molecular weights of purified chlorophylls in solution show that dimers and higher aggregates form readily under some conditions.[7-10] These aggregates have greatly enhanced optical activity compared with the monomers, and have been studied by optical rotatory dispersion (ORD) in the case of chlorophyll a.[11] The chlorophyll in chloroplast subunits also shows optical activity which is large compared with that of the extracted chlorophyll,[11,12] and this has been used as additional evidence for the presence of aggregated chlorophyll in vivo. It has been recognized, however, that the large optical activity of the chloroplast lamellar fragments (quantasomes) could be due to chlorophyll-protein or chlorophyll-lipid interactions, as well as to chlorophyll-chlorophyll interactions. The circular dichroism (CD) measurements reported here are particularly useful, because they reflect a specific kind of chlorophyll-chlorophyll interaction, the degenerate exciton interaction, in a much more sensitive way than ORD or absorption measurements. The degenerate interaction causes a splitting of the monomer absorption band in the aggregate, and results in a double circular dichroism that crosses zero in the region of the absorption maximum. In the presence of a large amount of other nondegenerate interactions the crossing point may be shifted, but it is still clearly seen. The degenerate interaction is important because it cannot be caused by chlorophyll-protein or chlorophyll-lipid interactions. It can only be due to chlorophyll-chlorophyll interactions. Furthermore, the degenerate interaction carries geometrical information about the aggregate which one has some hope of interpreting in a detailed way. Small exciton splittings that are not directly resolvable in the absorption spectra result in a double CD under most circumstances. The CD spectra of the chlorophylls in quantasomes and chromatophores contain large degenerate contributions which are strong evidence for chlorophyll-chlorophyll interactions in these systems.

Experimental Procedure

Materials

The preparation of chlorophyll a,

chlorophyll b, and bacteriochlorophyll are described elsewhere.[10] Carbon tetrachloride was reagent grade and was used without purification.

The suspension of microcrystalline chlorophyll a was prepared by adding isooctane to a small sample of the solid chlorophyll. After vigorous stirring, the suspension was spun in a clinical centrifuge at top speed for 5 min, and the supernatant suspension was used directly. No noticeable settling occurred during the half-hour period of measurement.

Chromatophores from Rhodospirillum rubrum and Rhodopseudomonas speroides were obtained by washing 5-day-old cultures free of growth medium, followed by sonication for 3 min at 0°C with a Biosonik oscillator. Fragments sedimenting between 40 000 g (30 min) and 180 000 g (50 min) were washed and resuspended in 0.05 M phosphate buffer, pH 7.5.

Barley was grown from seed in a phytotron under controlled illumination and temperature, and was harvested about 3 weeks after germination. The normal (Lyon) and the mutant strain (Chlorina 2), which is missing chlorophyll b,[13] were grown under identical conditions and harvested at the same time. Chloroplasts were isolated from the homogenized leaves essentially by the procedure of Park and Pon.[14] Sonication of the chloroplast suspension was followed by isolation of a fraction sedimenting between 9 000 g (10 min) and 110 000 g (30 min), resuspension in 10^{-3} M phosphate buffer, pH 7.5, and clarification at 9 000 g (10 min).

Methods

Absorption spectra were recorded by a Cary 14 spectrophotometer. For scattering samples the Model 1462 Scattered-Transmission Accessory was used. Optical rotatory dispersion spectra were obtained by using a Cary 60 instrument modified with a special red-sensitive photomultiplier.

The circular dichroism instrument is one of our own design. A detailed description of the apparatus appears elsewhere.[15] A few general features of the instrument are worth mentioning here. The apparatus employs a Cary 14 monochromator and a Pockels cell polarization modulator driven at 400 Hz.[16] Energy variations are compensated by controlling the PM voltage. Most measurements are made at a band width of about 1 mμ. The noise level of the instrument varies with wavelength at fixed resolution, but is approximately $\pm 1\times10^{-5}$ od units at 1 mμ band width over much of the wavelength range of 0.21 to 1.2 μ. The sensitivity of the instrument is further increased by averaging many scans of the spectrum, using a Nuclear Data ND800 Enhancetron. Under this mode of operation, the monochromator scan is controlled by the Enhancetron time base. Multiple scans reduce the noise level to $\pm 1\times10^{-6}$ od units in a reasonable period of time (about 2 hr). A Dumont 6011 PM tube is used for near infrared work, and an EMI 95580/A is used from 210 mμ to about 800 mμ.

Results and Discussion

Circular Dichroism Spectra of Chlorophyll Dimers

In vitro measurements of the CD of chlorophyll a, chlorophyll b, and bacteriochlorophyll in most solvents show extremely small optical activity (nearly unmeasurable by CD methods). In carbon tetrachloride, however, increasing concentration results in spectral changes and enhanced circular dichroism. The circular dichroism and absorption spectra of chlorophyll a, chlorophyll b, and bacteriochlorophyll solutions containing about 85% dimer are given in Figs. 7-1, 7-2, and 7-3. We can determine the molar circular dichroism of the dimers from measurements on these concentrated solutions, since the solutions are stable and we know the extent of dimerization from the equilibrium constants measured by using absorption spectra.[10] Precise CD measurements on dilute solutions, free of aggregates, have not yet been possible in carbon tetrachloride because of decomposition of the chlorophyll during the prolonged time of measurement. Measurements on dilute solutions in the same solvent can be made rapidly, to avoid decomposition, but with a resulting decrease in signal-to-noise ratio. The dilute solutions show essentially no dichroism, with an upper limit of 5 to 10% of the concentrated signals.

The dimers give large circular dichroism signals in the relatively isolated far red band as well as in the more complex Soret band, which is a composite of two nearby electronic transitions. We shall concentrate, initially, on interpreting the CD of the far red bands of these compounds. All three chlorophyll dimers show very similar CD spectra. This is consistent with all the evidence from NMR, IR, and absorption measurements,[7,10] that the three dimers have very similar structure. All three chlorophylls show a double circular dichroism spectrum that reverses sign close to the center of the absorption band. This behavior is due to the degenerate exciton interaction of the long-wavelength transition moments of the two monomers in the dimer.[17] The same interaction leads to the observed splitting of the absorption band in the dimer. The degenerate exciton interaction observed

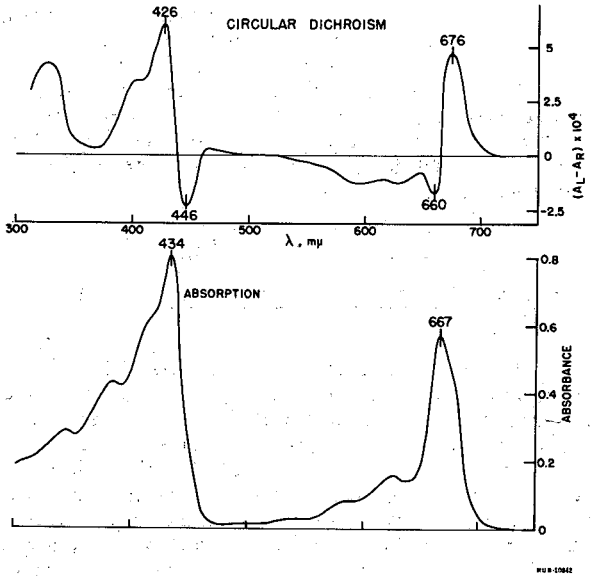

Fig. 7-1. Absorption and CD spectra of chlorophyll a dimers in carbon tetrachloride (CD: 1.37×10^{-3} M, 0.1-mm cell).

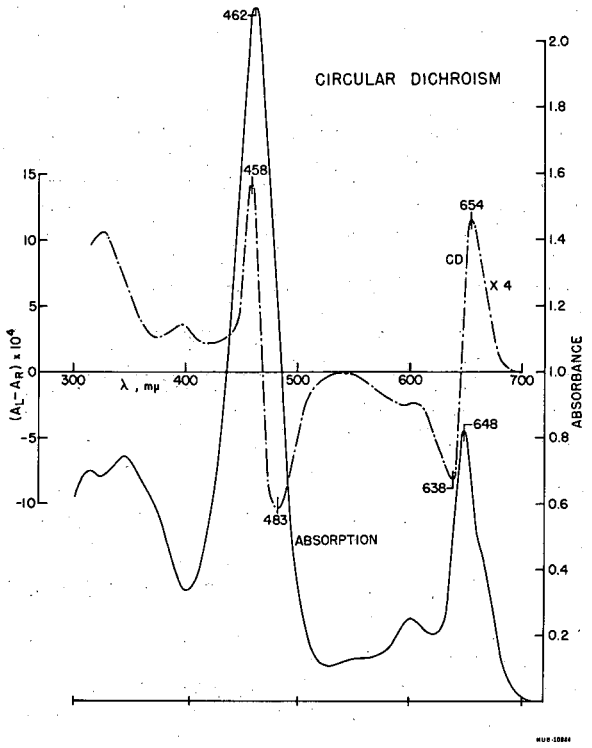

Fig. 7-2. Absorption and CD spectra of chlorophyll b dimers in carbon tetrachloride (CD: 3.70×10^{-3} M, 0.06-mm cell). The CD spectrum shown at wavelengths longer than 530 mμ has been multiplied by 4.0.

Fig. 7-3. Absorption and CD spectra of bacteriochlorophyll dimers in carbon tetrachloride (CD: 1.00×10^{-5} M, 0.125-mm cell). The CD spectrum shown at wavelengths longer than 700 mμ has been multiplied by 0.5.

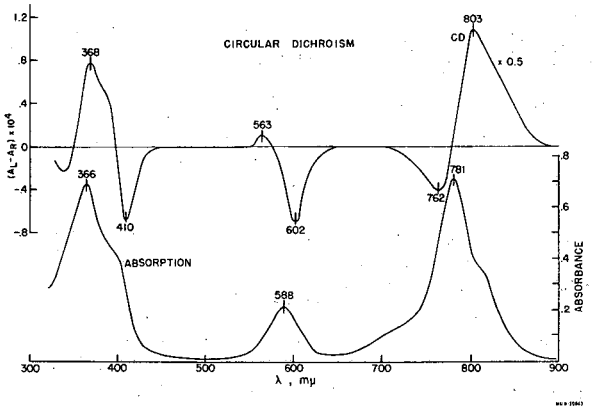

in the CD indicates that the monomer transition moments are not parallel nor are the chlorophyll rings coplanar in the dimer. Furthermore, the magnitude and sign of this degenerate CD component is related to the detailed geometry of the dimer in a relatively simple way. The CD spectrum is not symmetrical in amplitude above and below zero because of interactions of each chlorophyll with the electrostatic field and polarizabilities (that result from higher energy transitions) presented by the other.[18] This is the same interaction that gives rise to the observed hyperchromism in the dimer.[10,18,19] It is difficult to assign geometrical significance to the CD asymmetry effect because it originates in the interactions of the transition of interest with very many higher-energy transitions as well as a complicated static field interaction.[18]

The degenerate (double CD) contribution can be extracted from the experimental CD spectrum by a straightforward procedure. We fit the CD spectrum to a linear combination of a degenerate component (double CD, as in I in Fig. 7-4) and a nondegenerate component (single CD curve, as in II in Fig. 7-4) whose shape is assumed to be that of the monomer absorption. The degenerate component is recognized in the CD by a change of sign near the absorption maximum, while in the ORD the degenerate component merely gives an asymmetry to the apparent single Cotton effect unless the degenerate component is larger in amplitude than the nondegenerate part. The above degenerate contribution is extracted with a linear least-squares computer program.[20] In the calculation ν_0, the mean frequency of the exciton components, is obtained from an analysis of the absorption spectra.[10]

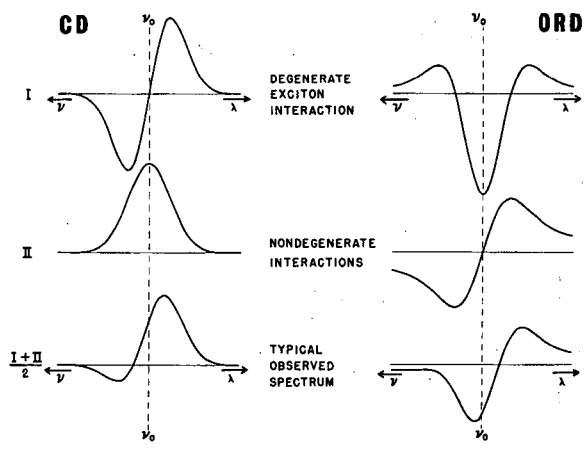

Fig. 7-4. Typical CD and ORD curves resulting from degenerate (I) and non-degenerate (II) interactions. These curves are obtained by decomposing the corresponding lower curves (I+II)/2, which approximate those observed for chlorophyll dimers.

Geometry of Dimers

A double CD spectrum that is caused by dimorization demonstrates that there is a degenerate interaction between the monomers in the dimer. The most general theory tells us that the chromophores are not coplanar and that the monomer transition moments are not parallel or exactly perpendicular in the dimer. Furthermore, with the aid of a particular theoretical model we may relate the degenerate CD to the detailed geometry of the dimer in a relatively simple way. The interaction may be treated as between point dipoles as a first approximation.[17] This approximation is not exact, but is useful as a start because it is simple and tractable, and may work satisfactorily.

For the point dipole approximation the dimer dipole approximation the dimer dipole strengths ($D_\pm$), rotational strengths ($R_\pm$), and absorption frequencies ($\nu_\pm$ in cm^{-1}) of the two exciton components resulting from monomer transitions at ν_0 are given[17] by

$$D_\pm = \mu^2 \pm \vec{\mu}_1 \cdot \vec{\mu}_2 = D_0 \pm \vec{\mu}_1 \cdot \vec{\mu}_2, \quad (1)$$

$$R_\pm = \mp \frac{\pi}{2} \nu_0 (\vec{R}_{12} \cdot \vec{\mu}_1 \times \vec{\mu}_2), \quad (2)$$

$$\nu_\pm = \nu_0 \pm V_{12}/hc, \quad (3)$$

$$V_{12} = \frac{1}{R_{12}^3}\left[\vec{\mu}_1 \cdot \vec{\mu}_2 - \frac{3(\vec{R}_{12} \cdot \vec{\mu}_1)(\vec{R}_{12} \cdot \vec{\mu}_2)}{R_{12}^2}\right], \quad (4)$$

where $\vec{\mu}_1$ is the electric dipole transition moment of monomer one and $\vec{R}_{12}$ is a vector connecting the centers of the two monomers in the dimer. If the exciton splitting, V_{12}, is smaller than the band width, most of the rotational strength cancels, owing to the strong overlap of components with opposite signs of rotation, as illustrated in Fig. 7-5. In order to get the theoretically useful quantity, the degenerate rotational strength ($R_\pm$), from the experimental values, we must know the exciton splitting of the transition. This is the

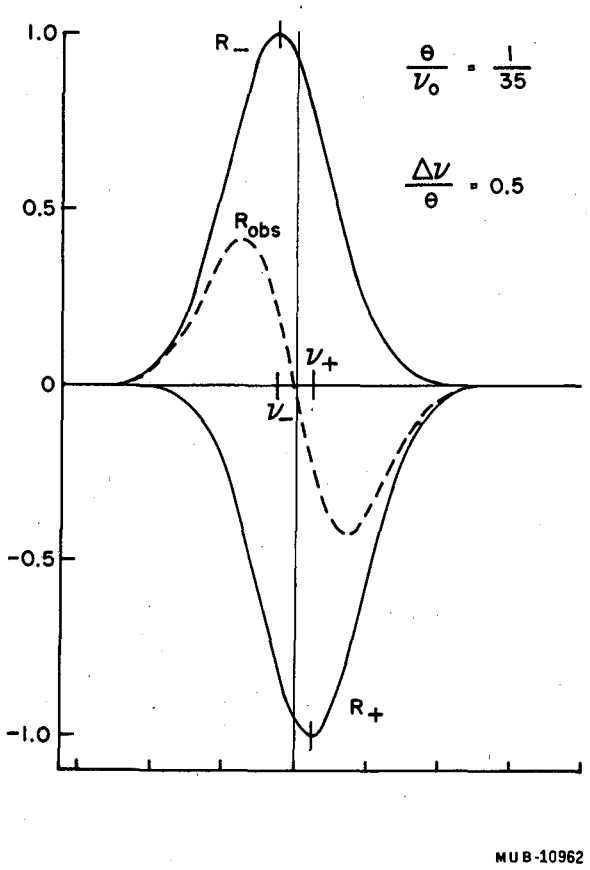

Fig. 7-5. Typical double CD component for an exciton split transition where the splitting is small compared with the band width. The cancellation of rotational strength in the center of the band is illustrated. Both R_+ and R_- have Gaussian shapes with half-width θ, and they are separated by $\Delta\nu$.

most difficult and uncertain part of the calculation, but fortunately, in the chlorophyll dimers, we can get experimental values for the exciton splitting from the absorption spectrum. The exciton splittings and the degenerate rotational strengths of the three chlorophylls are given in Table 7-I.[10] The exciton splitting

$$\Delta\nu = \nu_+ - \nu_- = \frac{2V_{12}}{hc}$$

is assumed to be positive for the purpose of Table 7-I. The quantities D_+/D_- and $R_\pm/D_0\nu_0$ depend only on the geometry of the dimers and not on the intensities or positions of the absorption bands. The similarities of these quantities for the three chlorophylls support the conclusion that their dimer structures are similar.[10] The absorption measurements imply an angle of about 80 deg between the red transition moments of the two chlorophylls in the dimers for the point dipole model.[10] The angle between the transition moments derived from the CD spectra is about 12 deg if we assume that the monomer planes are parallel in the dimer. Within the limitations of the point dipole model, the angle between the transition moments of 80 deg found from the absorption spectra is not dependent on any assumption about the parallelism of the monomer planes. The large discrepancy between the intertransition moment angle found from the absorption spectra (80 deg) and the angle found from the CD spectra assuming parallel planes (12 deg) seems much too large to ascribe completely to inadequacies in the point dipole model, since the exciton splitting is experimentally observed. We are forced to the conclusion that the chlorophyll planes are not parallel in the dimer.

If we attach a coordinate system to one monomer, two angles and a distance are needed to specify a vector from the center of the fixed monomer to the center of the other monomer. Three additional angles are sufficient to specify the orientation of the second monomer in this coordinate system. Six parameters--five angles and a distance--are needed to specify the dimer geometry in the general case. The observable parameters available for each absorption band are the degenerate rotational strength, $R_\pm$, the ratio of the dipole strengths, D_+/D_-, and the exciton splitting, V. Thus, there are three interaction parameters for each absorption band that exhibits exciton interaction. We can specify the geometry of the dimer from the interaction parameters for two independent transitions polarized along different directions in the molecule.

Bacteriochlorophyll has a distinct electronic transition at 590 mμ polarized in the molecular plane, but polarized perpendicular to the previously discussed 780-mμ transition.[21, 22] The 590-mμ transition is fairly strong (oscillator strength, f = 0.11) and shows a double CD component. The six interaction parameters for the two bands of bacteriochlorophyll are given in Table 7-I, and the analysis of these data is in progress. The available evidence indicates that chlorophyll a, chlorophyll b, and bacteriochlorophyll form nearly identical dimers.[7-10] If a structure of the bacteriochlorophyll dimer can be determined, we can propose this structure for the other chlorophyll dimers with some confidence and test it against the CD and absorption data.

Table 7-I. Spectral properties of the exciton split components of the dimers of three chlorophylls in carbon tetrachloride. (λ_0 and ν_0 refer to the average of the two exciton band positions.)

Molecule	λ_0 (mμ)	ν_0 (cm^{-1})	$\Delta\nu$ (cm^{-1})	D_+/D_-	$R_\pm \cdot 10^{40}$ cgs	$\frac{R_\pm}{D_0\nu_0} \cdot 10^8$ cgs
Chlorophyll a	674	14848	363	1.48	≈ ±20	±0.74
Chlorophyll b	655	15259	398	1.81	≈ ±18	±0.79
Bacteriochlorphyll	796	12565	490	1.32	±44.5	±0.95
	590	16940	470	0.9	± 6.9	

Crystalline Chlorophyll a

Figure 7-6 shows the absorption and CD spectra for chlorphyll a microcrystals in suspension. The crystal structure is not yet known for any of the chlorophylls; however, the CD measurement has definite qualitative interest in relation to the observed quantasome chlorophyll CD. As chlorophyll a is slightly soluble in isooctane, the suspension medium, there is a small monomer peak at 666 mμ. In the crystal absorption spectrum this peak is shifted to 745 mμ. This large red shift of the crystal over the monomer is probably due to the enormous polarizability of the crystalline environment compared with the solvent surrounding the monomer. It is a general observation that $\pi^-\pi^+$ transitions of molecules in polarizable solvents are red-shifted relative to those in solvents of low polarizability.[23]

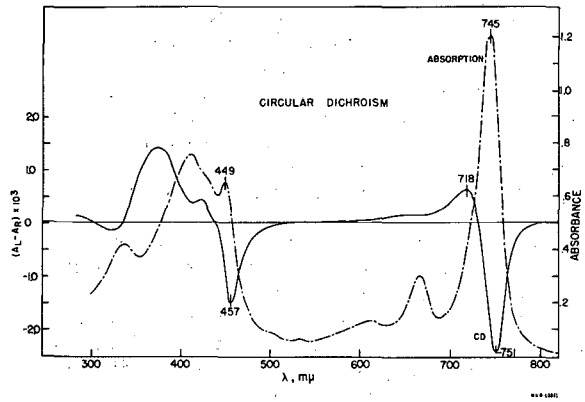

Fig. 7-6. Absorption and CD spectra of a suspension of chlorophyll a microcrystals in isooctane. Path length, 1.0 cm.

These red shifts are experimentally observed for the chlorophyll transitions. Increasing chlorophyll aggregation leads to increasing red shift of the absorption. A 10-to-15-mμ red shift for the dimer relative to the monomer is observed in carbon tetrachloride. At very high concentrations in carbon tetrachloride the bacteriochlorophyll absorption and CD show evidence of higher aggregates, red-shifted 30 mμ relative to the monomer. The molecule in the crystal is essentially dissolved in chlorophyll, a very polarizable medium, and the large red shift (80 mμ for chlorophyll a) results.

An analysis of the crystal CD shows that the degenerate component crosses zero within 1 mμ of the observed absorption peak. Therefore, the weak short-wavelength shoulder observed in the crystal absorption spectrum (≈ 720 mμ) is not an exciton split peak and must be vibrational in origin. The Gaussian half width is only about 25 cm^{-1} larger than for the monomer in CCl_4, so the exciton splitting in the crystal must be quite small.

Quantasomes from Barley Chloroplasts and from a Mutant Deficient in Chlorophyll b

Analysis of the optical properties of a preparation from higher plant chloroplasts is complicated by the presence of chlorophyll a, chiefly responsible for the absorption maxima at 678 and 436 mμ, and chlorphyll b, which gives rise to the distinct shoulder near 650 mμ and another at about 470 mμ. The carotenoids present have absorption maxima at 485, 455, and 428 mμ.[24] Figure 7-7 shows the ORD and absorption spectra of suspensions of lamellar fragments (quantasomes) of chloroplasts from normal barley as well as from a mutant that is completely missing chlorophyll b.[13] In the visible region of the spectrum, the mutant and normal quantasomes have identical ORD and absorption spectra except for the chlorophyll b regions near 650 and 470 mμ, where there and large differences. Figure 7-8

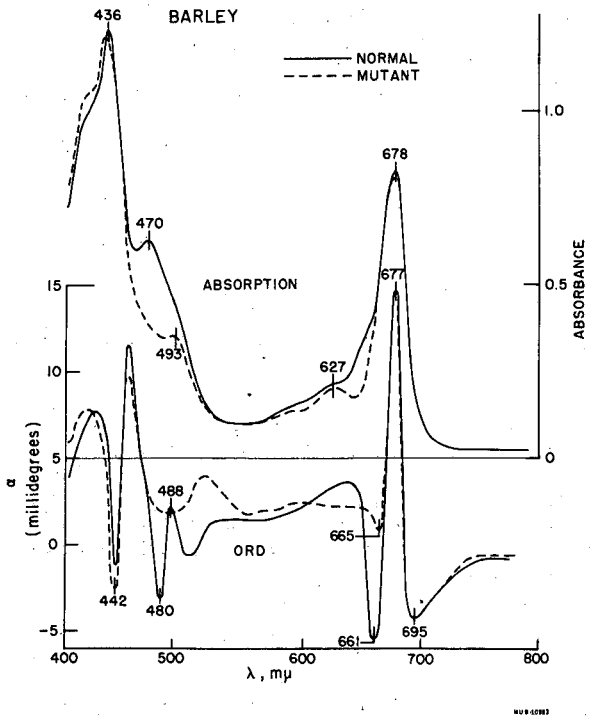

Fig. 7-7. Absorption and ORD spectra of quantasomes from normal barley (solid curves) and from a mutant lacking chlorophyll b (dashed curves).

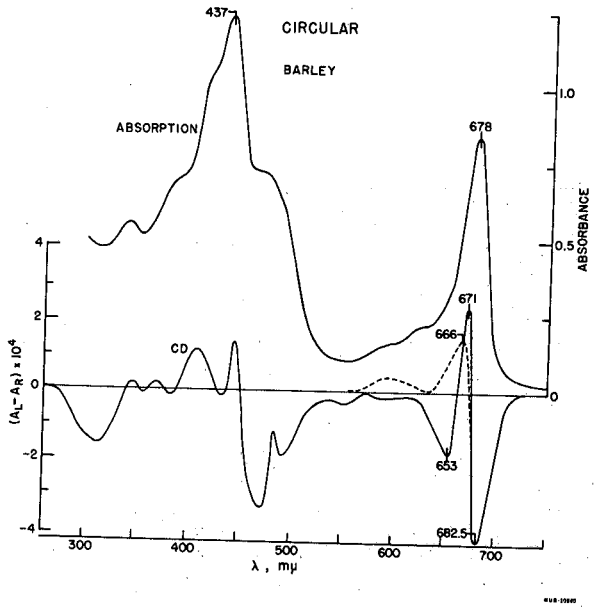

Fig. 7-8. Absorption and CD spectra of quantasomes from normal barley (solid curves) and CD spectrum of quantasomes from a mutant lacking chlorophyll b (dashed curve).

shows the CD spectra of these same materials. The chlorophyll a part of the CD spectrum in the mutant appears to be identical to the chlorophyll a region in the normal barley.

The chlorophyll a in the quantasomes shows a large double CD component, as we saw in the dimers and crystals. Presence of the double CD component in the chlorophyll a absorption region is good direct evidence for chlorophyll a-chlorophyll a interaction in quantasomes. Chlorophyll-protein or chlorophyll-lipid interactions would lead only to single CD bands and, if present, would only increase or decrease the asymmetry of the observed double CD component. The presence of a double CD implies that the interacting chlorophylls are not coplanar, nor are the red chlorophyll a transition moments parallel or exactly perpendicular in the quantasomes. The double CD component crosses zero at about 685 mμ. This is the average frequency of the exciton bands $\nu_0 = (\nu_+ + \nu_-)/2$ that give rise to the double CD. Thus, the interacting chlorophyll a molecules absorb on the long-wavelength side of the quantasome absorption peak at 678 mμ. The chlorophyll that absorbs on the short-wavelength side of the main peak is thought to be unaggregated, because it has relatively high fluorescence efficiency.[2]

The shape of the chlorophyll CD in quantasomes is reminiscent of the shape of the crystalline chlorophyll CD, which suggests that the chlorophyll a molecules in quantasomes and in the crystal have similar geometries. However, the interacting chlorophyll a in quantasomes is not aggregated exactly like a three-dimensional crystal because the absorption is not red-shifted as far as is the three-dimentional crystal. Chlorophyll a monolayers have their absorption shifted to 680 mμ.[25] The red shift of the chlorophyll that gives rise to the double CD in the quantasomes is about the same as the red shift in the monolayer. It may be, therefore, that the aggregated chlorophyll in the quantasomes is only one molecule thick, corresponding to a geometry like a two-dimensional chlorphyll a crystal.

The CD amplitude is small for quantasomes compared with that for a crystal suspension with equal peak absorption. A decrease in CD amplitude in a one- or two-dimensional crystal is expected relative to a three-dimensional crystal of otherwise identical geometry. The exciton forces giving

rise to the CD effects are relatively long range,[26] and therefore depend on the extent of the aggregate.

The quantasomes chlorophyll a CD (Fig. 7-8) is of about the same amplitude as that of the chlorophyll a dimer CD (Fig. 7-1) for equivalent total red absorption. It would be useful to subtract the absorption of the non-aggregated chlorphyll in the quantasome to determine the aggregate CD amplitude per unit of aggregate absorption. However, we have no direct evidence on the fraction of the total chlorophyll a that is aggregated in the quantasome. The exciton splitting evidenced by the CD is not resolved in the crystal or quantasome absorption at normal temperatures. However, the liquid-nitrogen-temperature derivative spectra of plant material resolves peaks at 673 mμ, 683 mμ, and about 695 mμ.[2] The double CD component crosses zero at about 685 mμ, and the observed absorption peak in the 673 mμ region is too far away to contribute to the double CD of the aggregate. The 673-mμ peak, estimated by Brown and French[27] to be about 50% of the total chlorophyll a absorption, is a reasonable approximation to the amount of unaggregated chlorophyll a. It is consistent with the CD evidence to propose that both the chlorophyll a 683 and 695 mμ are exciton peaks resulting from the same aggregate. If this were true, about one half of the chlorophyll a is in the aggregate. Assuming that at most one half of the chlorophyll a in the quantasome is aggregated, the CD amplitude of the aggregated chlorophyll a is at least twice that of the solution dimer.

The chlorphyll a dimer CD has a shape similar to the quantasome chlorophyll a CD, although the dimer CD has opposite sign. The opposite sign is not an indication of any great difference in the two geometrical structures, for it could be given by a mirror-image relationship. We take the similarity in shape of the dimer and quantasome CD to mean that the two geometrical structures are similar. A long-wavelength shoulder is clearly seen in the dimer spectrum, while the spectrum of plant material does not show a shoulder except at low temperature. The plant material shoulder must be somewhat obscured by absorption from unaggregated chlorophyll. The large amplitude of the quantasome chlorophyll a CD suggests a more extensive aggregate than a dimer. Helices, which are analogs of a one-dimensional crystal, are predicted to have a relatively large dependence of the rotational strength on chain length.[28] Two-dimensional systems might be expected to have an even stronger dependence on aggregate size. It is possible that the quantasome aggregates are dimers with a geometry that leads to larger rotational strength than the solution dimer. The aggregated chlorophyll a in the quantasomes is at least a dimer, and is most probably a more extensive aggregate in one or two dimensions.

Plants can be grown with altered amounts of the different chlorophyll components. From the CD of those materials we may be able to determine the absorption of the aggregated components, find out how much of the chlorophyll a is aggregated and, in principle, determine the geometry of the aggregate.

The predominant interaction of chlorophyll a is with itself, since the CD in the chlorophyll a region is identical in the normal and chlorophyll b-free mutant. The chlorophyll b region also has a degenerate component in the quantasome CD that is seen in the difference between the normal and the b-free mutant CD curves. This double CD in the chlorophyll b region indicates that in the normal barley at least some of the chlorophyll b is interacting with other chlorophyll b molecules.

One must not ignore the possibility that the observed CD in quantasomes is not due to degenerate interaction between chlorophylls, but rather due to more than one type of independent noninteracting chlorophyll. This explanation would require two types of chlorophyll environment, one absorbing at long wavelength with negative CD and the other at short wavelength with smaller positive CD. The close relation between the chlorophyll a dimer and the crystal CD, where only chlorophyll-chlorophyll interactions are present, and the quantasome chlorophyll a tends to favor the chlorophyll-chlorophyll interaction origin of the CD in quantasomes. Experimental investigation of plant material having altered amounts of the different chlorphyll components should answer this question directly.

Chromatophores from Photosynthetic Bacteria

Figure 7-9 shows the CD spectrum and absorption spectrum of Rhodospirillum rubrum chromatophores, and Fig. 7-10 shows the absorption spectrum of chromatophores of Rhodopseudomonas spheroides, together with portions of the ORD and CD spectra. The near infrared peaks of chromatophores from both species of bacteria show pronounced double CD components, indicating strong bacteriochlorophyll interactions. The double CD shows that the interacting bacteriochlorophylls are not coplanar and that their transition moments are not perpendicular to one another.

R. rubrum chromatophores exhibit a double CD band (Fig. 7-9) that crosses zero very close to the main absorption peak at 880 mμ. This indicates that at least some of the

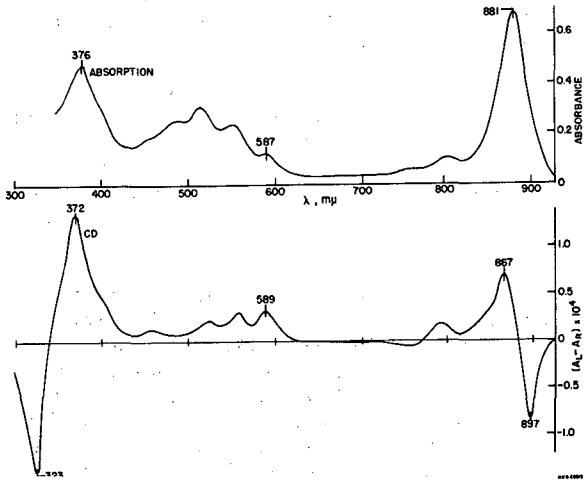

Fig. 7-9. Absorption and CD spectra of chromatophores from Rhodospirillum rubrum.

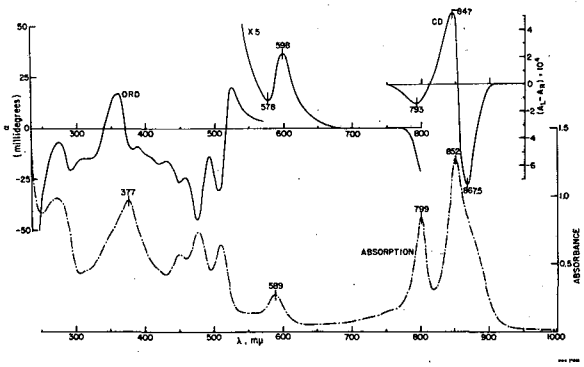

Fig. 7-10. Absorption, CD, and ORD spectra of chromatophores from Rhodopseudomonas spheroides.

bacteriochlorophyll with absorption centered at the main peak is aggregated with an exciton splitting small compared with the band width. Little unaggregated bacteriochlorphyll seems to be present, as this peak in the chromatophore spectrum is sharp and not spread out, as it would have to be if isolated and aggregated molecules were present together. The bacteriochlorophyll long-wavelength peak is slightly wider for the chromatophores than for the monomer absorption in carbon tetrachloride. If we assume a band shape like that in the monomer spectrum, the exciton splitting is of the order of 30 to 60 cm^{-1}.[1]

In R. rubrum, the 590-mμ bacteriochlorophyll CD peak has no obvious double CD component. However, the CD peak is red-shifted from the absorption peak. Since this is an allowed electronic transition, one would not expect vibrational effects to shift the CD maximum from the absorption maximum.[29] A negative component of the bacteriochlorophyll CD on the short-wavelength side of the 590-mμ peak may be obscured by the positive carotenoid CD. This could be the origin of the 2.5-mμ red shift of the positive bacteriochlorophyll CD peak. The CD curve at the bottom of Fig. 7-5 shows an example of the shift of a single CD peak centered at the absorption maximum by the addition of a double CD component. R. rubrum can be grown carotenoidless under the proper conditions.[30] Carotenoidless chromatophores would allow us to see the 590-mμ bacteriochlorophyll CD and absorption free of interference.

R. spheroides chromatophores (Fig. 7-10) show a particularly strong double CD in the longest-wavelength absorption band, indicating aggregation of the bacteriochlorophyll. The sharp peak on the short-wavelength side at 799 mμ seems to have a comparatively weak double CD component, judged by the shift to 793 mμ in the CD spectrum, with a magnitude approximately equal to that of the solution dimer. The 799-mμ band absorbs about where the solution dimers do, but shows no obvious splitting in the chromatophore absorption spectrum. The positions of the double CD and absorption indicate that the band may be due to dimers of bacteriochlorophyll. The small exciton splitting requires that the dimers have a different geometry from that of the solution dimers.

The long-wavelength absorption band at 852 mμ is red-shifted much farther than the solution dimer and, since the double CD indicates an aggregate, the bacteriochlorophyll absorbing here is undoubtedly a higher aggregate than a dimer. There is an obvious long-wavelength shoulder (about 880 mμ) on the main absorption band (852 mμ). The double

CD component crosses zero slightly to the long-wavelength side of the main absorption peak. Similar behavior is observed in all the chlorophyll dimers in solution. The long-wavelength shoulder may well be an exciton component split off from the main peak. Many photosynthetic bacteria show this long-wavelength shoulder, sometimes to an extent that varies with growth conditions.[31] Under these various conditions, either the bacteriochlorophyll aggregate geometry is altered or two different aggregated forms are present in variable amounts. Low-temperature absorption and CD measurements may distinguish between these alternatives.

Summary

The circular dischroism (CD) and absorption spectra of dimers of chlorophylls a and b and bacteriochlorophyll in carbon tetrachloride solution and of suspended crystalline chlorophyll a are presented. The dimers of all three chlorophylls seem to have a very similar structure by the criterion of these measurements. The chlorophyll-chlorophyll interactions in the dimer give rise to very large optical activity relative to the monomer. Our analysis of the dimer structure is not yet complete, but we can conclude with some confidence that the molecular planes are not parallel or coplanar in the dimer, nor are the transition moments parallel. The CD and absorption spectra of photosynthetic particles--barley quantasomes containing chlorophylls a and b, quantasomes prepared from a barley mutant that lacks chlorophyll b, and R. rubrum and R. spheroides chromatophores that contain bacteriochlorophyll--are also presented. The CD measurements give strong evidence for chlorophyll-chlorophyll interaction in all of the photosynthetic particles examined. We conclude that some of the chlorophyll a absorbing on the long-wavelength side of the main quantasome absorption band is aggregated. The aggregate is at least a dimer and may be a one- or two-dimensional analog to the chlorophyll a crystal. The chlorphyll a aggregate has the midpoint of exciton components at 685 mμ. We suggest that the chlorophyll a bands observed at 683 and 695 mμ observed in low-temperature derivative spectra may result from a single type of aggregate. The chlorophyll b shows evidence of interactions with other chlorophyll b in the quantasome. We open the possibility of finding the geometrical relationship of the interacting chlorophylls in the quantasome from further experiments. Bacteriochlorophyll appears to be aggregated in the two species of photosynthetic bacteria that were examined; however, the detailed structure of the aggregates is apparently different in these two cases.

Acknowledgments

The authors wish to acknowledge the kind of gift by Professor H. R. Highkin of the barley mutant seeds. Dr. Rodney Biltonen kindly provided us the use of his computer program for decomposing multiple CD spectra.

The work described in this report was supported, in part, by the U. S. Atomic Energy Commission.

Footnote and References

† In Proceedings of Brookhaven Symposia on Biology, No. 19, Energy Commission and the Photosynthetic Apparatus, June 6-9, 1966, 303-318, 196.

1. R. B. Park, J. Kelly, S. Drury, and K. Sauer, Proc. Natl. Acad. Sci. US 55, 1056 (1966).
2. W. L. Butler, The Chlorophylls, L. P. Vernon and G. R. Seely, Eds. (Academic Press, N. Y., 1966), p. 343.
3. J. C. Goedheer, Biochim Biophys. Acta 16, 471 (1955).
4. R. A. Olson, W. L. Butler, and W. H. Jennings, Biochim Biophys. Acta 58, 144 (1962).
5. K. Sauer and M. Calvin, J. Mol. Biol. 4, 451 (1962).
6. R. A. Olson, W. L. Butler, and W. H. Jennings, Biochim Biophys. Acta 54, 615 (1961).
7. J. J. Katz, G. L. Closs, F. C. Pennington, M. R. Thomas, and H. H. Strain, J. Am. Chem. Soc. 85, 3801 (1963).
8. G. L. Closs, J. J. Katz, F. C. Pennington, M. R. Thomas, and H. H. Strain, J. Am. Chem. Soc. 85, 3809 (1963).
9. A. F. H. Anderson and M. Calvin, Arch. Biochem. Biophys. 107, 251 (1964).
10. K. Sauer, J. R. Lindsay Smith, and A. J. Schultz, J. Am. Chem. Soc. 88, 2681 (1966).
11. K. Sauer, Proc. Natl. Acad. Sci. US 53, 716 (1965).
12. B. Ke, Nature 208, 573 (1965).
13. H. R. Highkin and A. W. Frenkel, Plant Physiol. 37, 814 (1962).
14. R. B. Park and N. G. Pon, J. Mol. Biol. 3, 1 (1961).
15. Edward A. Dratz, The Geometry and Electronic Structure of Biologically Significant Molecules as Observed by Natural and Magnetic Optical Activity (Ph. D. Thesis), UCRL-17200, Sept. 1966.
16. B. H. Billings, J. Opt. Soc. Am. 39, 802 (1949).
17. I. Tinoco Jr., Radiation Res. 20, 133 (1963).
18. I. Tinoco Jr., J. Chem. Phys. 33, 1332 (1960); Adv. Chem. Phys. 4, 113 (1962).

19. H. Devoe and I. Tinoco Jr., J. Mol. Biol. 4, 518 (1962).
20. R. Biltonen (Johns Hopkins University), private communication.
21. J. C. Goedheer, Thesis, Utrecht (1957).
22. M. Gouterman, J. Mol. Spect. 6, 138 (1961).
23. G. W. Robinson, in Light and Life, W. D. McElroy and B. Glass, Eds. (Johns Hopkins Press, Baltimore, 1961), p. 11.
24. K. Sauer and M. Calvin, Biochim Biophys. Acta 64, 324 (1962).
25. W. D. Bellamy, G. L. Gaines Jr. and A. G. Tweet, J. Chem. Phys. 39, 2528 (1963).
26. R. M. Hochstrasser and M. Kasha, Photochem. Photobiol. 3, 317 (1964).
27. J. S. Brown and C. S. French, Plant Physiol. 34, 305 (1959).
28. I. Tinoco Jr., R. W. Woody, and D. F. Bradley, J. Chem. Phys. 38, 1317 (1963).
29. W. Moffitt and A. Moscowitz, J. Chem. Phys. 30, 648 (1959).
30. G. Cohen-Bazire and R. Y. Stamier, Nature 181, 250 (1958).
31. R. K. Clayton, in Bacterial Photosynthesis, H. Gest, A. San Pietro, and L. P. Vernon, Eds. (Antioch Press, Yellow Springs, Ohio, 1963), p. 495.

8. DIMERIZATION OF CHLOROPHYLL a, CHLOROPHYLL b, AND BACTERIOCHLOROPHYLL IN SOLUTION

Kenneth Sauer, John R. Lindsay Smith, and Alfred J. Schultz

Analyses of the absorption spectra of three chlorophylls in carbon tetrachloride solution demonstrate the existence of monomer-dimer equilibrium in the concentration range from 10^{-6} to 10^{-3} mole/liter. The dimerization constants, $K_d = C_d/C_m^2$, are $1.0\pm0.4)\times 10^4$ liters/mole for chlorophyll a, $(0.8\pm0.3)\times10^4$ for chlorophyll b, and $(2.2\pm0.7)\times10^4$ liters/mole for bacteriochlorophyll at 24 ± 2°C, corresponding to standard free energies of dimer formation of -5.4, -5.3, and -5.8 kcal/mole, respectively.

The absorption spectra of pure monomer and pure dimer in carbon tetrachloride are calculated for each pigment. For each of the chlorophyll dimers the long-wavelength absorption band consists of a principal peak centered at approximately the position of the monomer absorption maximum, and a shoulder to long wavelengths. The relative oscillator strengths of the split components indicate that the corresponding transition moments for the two molecules in each dimer are nearly perpendicular to one another. The proton magnetic resonance spectrum of aggregated bacteriochlorophyll in $DCCl_3$ exhibits characteristic features similar to those previously reported for aggregated chlorophylls a and b. The evidence from these investigations to the conclusion that the structures of the dimers are nearly identical for the three chlorophyll molecules.

---

†Abstract of paper published in J. Am. Chem. Soc. 88, 2681 (1966).

9. HILL REACTION OF CHLOROPLASTS ISOLATED FROM GLUTARALDEHYDE-FIXED SPINACH LEAVES[†]

Roderic B. Park, Jeffrey Kelly, Susan Drury, and Kenneth Sauer

Experiments show that quantum conversion leading to O_2 evolution in the Hill reaction can occur in chloroplasts isolated from glutaraldehyde-fixed leaves with about 25% the efficiency of unfixed chloroplasts. The Hill reaction seems normal in that it is DCMU-inhibited, its rate is dependent on the presence of phosphorylation acceptors or uncouplers, and it exhibits a red drop in efficiency. The fixed chloroplasts do not change morphology upon acetone extraction, and therefore offer the possibility of performing lipid reconstitution experiments. Glutaraldehyde-fixed Chlorella cells are also active in the DCPIP Hill reaction. These results indicate not only that quantum conversion and electron transport in photosynthesis are explainable in terms of a rigid protein framework with lipid dispersed through it, but also that conformational changes as such are not necessary for quantum conversion leading to oxygen evolution and dye reduction.

[†]In Proceedings of Brookhaven Symposia on Biology, No. 19, Energy Conversion and the Photosynthetic Apparatus, June 6-9, 1966, 303-318, 196.

10. FREEZE-ETCHING OF CHLOROPLASTS FROM GLUTARALDEHYDE-FIXED LEAVES†

Roderic B. Park and Daniel Branton

Freeze-etching as a preparative technique for electron microscopy has been in use almost 12 years.[1] Its initial application was to studies of virus morphology, but improvements in methodology have opened many new applications.[2,3] The technique basically consists of rapidly freezing biological material and then breaking the frozen specimens in a vacuum. The surface so exposed is replicated, and the replica is observed by electron microscopy. The degree of etching is controlled by the time elapsed between breakage and replication and by the temperature of the specimen. Studies on chloroplast morphology by this technique have been reported by Mühlethaler, Moor, and Sarkowski[4] and by Branton and Park.[5] These two studies, although based on almost identical data, have produced very different interpretations. The major points of interpretive disagreement between the two studies are reviewed here, and some new data pertinent to the arguments are presented.

The freeze-etch morphology of isolated chloroplasts seen in cross section is shown in Fig. 10-1 and 10-2. Such cross sections yield dimensions and thylakoid configurations very similar to those obtained in studies of chloroplast thin sections. The compressed chloroplast in Fig. 10-1 was isolated in the pyrophosphate medium of Jensen[6] and is typical of chloroplast preparations with high CO_2 fixation capacity and high proportions of class I chloroplasts.[7] The chloroplast in Fig. 10-2 was isolated in sucrose phosphate medium[8] and is considerably swollen compared with that in Fig. 10-1. Such chloroplasts yield much lower CO_2 fixation rates than the type shown in Fig. 10-1. Undoubtedly the decreased CO_2 fixation capacity is associated with the morphological changes. Variations among the results of different experiments on the fixation rates of chloroplasts isolated in the pyrophosphate medium are also correlated with such changes in structure, the more swollen chloroplasts yielding lower rates.

The most interesting data from freeze-etching appear not in chloroplast cross sections but in breaks parallel to the thylakoid surfaces. The membranes provide planes of natural weakness in the frozen chloroplasts, and breaks often proceed along membrane faces. Such breaks are shown in Fig. 10-3, in which both cross sections and tangential breaks are evident. At least three typical faces are evident in both our[4] and Mühlethaler's pictures. We have labeled these A, B, and C, as shown in Fig. 10-2. B is a smooth surface with 175-Å-diameter by 90-Åparticles on its surface, though often these particles are removed during the break, leaving depressions. Surface A is at the same height as the tops of the large 175-Åparticles and apparently consists of the large particles surrounded by an embedding matrix. Surface C is a particulate surface made up of both the large 175-Åparticles and the smaller particles, and corresponds to the 175-Åparticles and their embedding matrix viewed from the side opposite the A face.

To what portion of the membrane do these faces correspond? Are they external surfaces representing the interface between the membrane and the external medium, or are they internal faces within the membrane?

Before this question is answered, an even more important question must be considered. Are the particles on these surfaces real, or do they arise perhaps from the freezing or contamination of the exposed surfaces during etching? The answer appears to be that the particles are real, and perhaps the best evidence for this is that they are not present in all membranes. Branton[9] has shown that myelin, the model for the unit membrane, is almost totally devoid of particles when viewed by freeze-etching. If contamination or freezing gave rise to the particles, they might be expected to yield particles on these membranes also. It is becoming apparent that membranes vary greatly with respect to their particulate nature, myelin being the least and thylakoids the most particulate thus far. It is tempting to speculate that the more complex the function of a membrane, the more particulate or micellar it is. A scale of membranes from the simplest to the most complex might then be as follows: myelin, tonoplast, and thylakoid.

Since the particles appear to be real, where are they located? Mühlethaler et al.[4] have placed them on the outside of a bimolecular leaflet of lipid (see Fig. 10-4), thus preserving the essential features of a Danielli-Davson[10] or unit membrane.[11] This would suggest that the particles are polar in character. We have argued that this interpretation is untenable for the following reasons.

1. The assumption that freeze-etch faces represent the surface between the membrane and the surrounding aqueous medium appears to be false. Branton[12] has clearly shown that most membranes do break down the center of

Fig. 10-1. Freeze-etch cross section of spinach chloroplast isolated in a pyrophosphate medium (Ref. 6).

Fig. 10-2. Freeze-etch cross section of spinach chloroplast isolated in a sucrose medium.

Fig. 10-3. Spinach thylakoid faces seen in a freeze-etch preparation of an isolated spinach chloroplast.

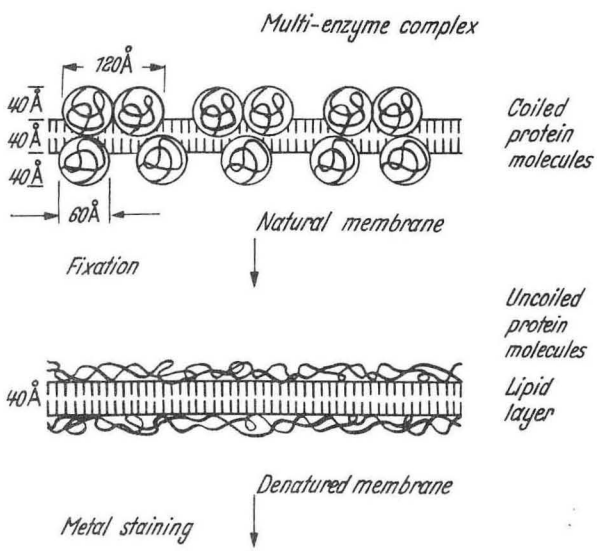

Fig. 10-4. Interpretation of thylakoid faces after Mühlethaler et al. (Ref. 4).

the membrane and not along the external faces. The exposed faces of membranes seen in freeze-etching actually are, in fact, internal faces which constitute planes of weakness in the frozen preparation.

2. The model proposed by Mühlethaler et al. would be highly birefringent as viewed in the light microscope, yet the observed intrinsic birefringence of chloroplast membranes is very low.[13] This indicates that the orientation of lipids cannot be as great as that proposed by Mühlethaler.[4]

3. The Mühlethaler model fails to explain why shadowed preparations of thylakoids demonstrate much less surface relief than the freeze-etch preparations. This difference in surface relief is due to the fact that the particles are embedded in the membrane matrix and exposed by the splitting process of freeze-etching mentioned above. This embedding of particles would also explain why undamaged thylakoids viewed by negative staining are so much less particulate than the freeze-etch preparations.[5]

4. As shown by data to be presented below, the membrane faces observed by freeze-etching are dependent on the presence of lipid in the membrane. Once the lipid is removed, breaks no longer occur along the membranes, the plane of weakness having been removed. Apparently the membrane faces are nonpolar in character, which, again, disagree with the Mühlethaler model, in which the faces seen by freeze-etching are placed in contact with water. The model proposed by Branton and Park to explain the freeze-etch data is presented in Fig. 10-5. The model consists of particles with two diameters, 175 Å and 100 Å, embedded in the membrane matrix. Surface A (an external surface) is apparent only where membranes are appressed and is never seen where the thylakoids are bounded by an aqueous environment. The model is, in many ways, similar to that proposed by Park and Pon[14] more than 6 years ago to explain the periodic structures seen in shadowed preparations. The 175-Å-diameter particles correspond to the quantasome seen in shadowed preparations[15] and occasionally exist in paracrystalline arrays.[5] They differ in that the quantasome was described for a complete membrane with the embedding matrix still surrounding the particle, whereas in freeze-etching the surrounding matrix is removed.

Thus far, the 175-Å particle is not only by far the largest particle seen on the surfaces of freeze-etched membranes, but it is also uniquely restricted to membranes containing chlorophyll or bacteriochlorophyll. Whether viewed in a number of higher plants or lower plants (Chlorella pyrenoidosa, Porphyridium cruentum, or Rhodospirillum rubrum) the particle appears to be about the same size.[22] All other membrane particles have thus far fallen

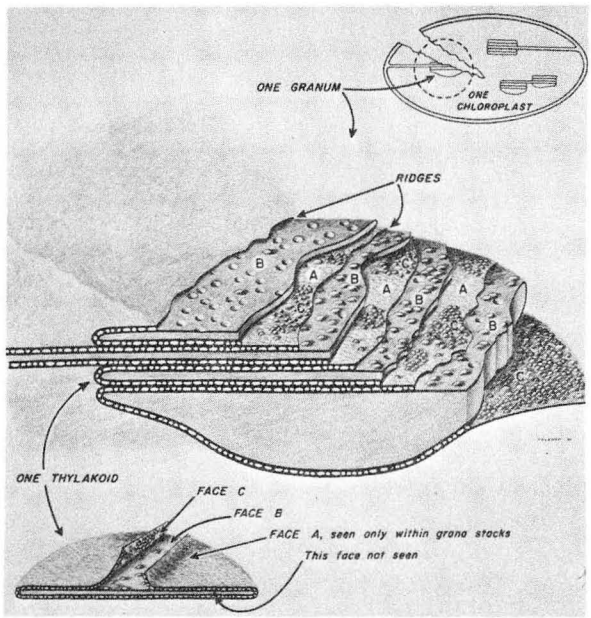

Fig. 10-5. Interpretation of thylakoid faces after Branton and Park (Ref. 5).

into the 100-Å-diameter range. The fact that the 175-Å particles exist not only in green plants but also in organisms with modified system II reactions or no system II reactions at all indicates that, although the particle may be uniquely involved in quantum conversion, it is not uniquely associated with O_2 evolution. Our initial thought[14] that the quantasome might be a representation of the Emerson and Arnold photosynthetic unit, though not excluded by the above observations, is made less likely. Also, the experiments by Isawa and Good[16] on DCMU inhibition of the Hill reaction indicate that there is only one O_2-evolving site per several quantasomes. The existence of isolated quantasomes in R. rubrum membranes of low chlorophyll content indicates that particles may be competent for system I quantum conversion and that in higher plants several of these electron transport chains may be associated with one O_2-evolving site. In such a model the number of reducing sites would exceed the number of oxidizing sites, a hypothesis which is borne out by Kok's studies on the P 700 concentration in chloroplasts.[17]

One approach to finding out more about the chemical composition and function of structures seen in Fig. 10-3 has been to extract selectively or digest certain substances within the thylakoids and to observe the modified membrane by sectioning or freeze-etch techniques. Bamberger and Park[18] have described such experiments with the hydrolytic

enzyme pronase and with a preparation from runner beans containing galactosidase and galactolipase. These experiments indicated that the smooth layer in surface B was galactolipid in nature and that the chlorophyll was associated with the large particles and their embedding matrix.

During the course of these experiments it became useful to fix the chloroplasts chemically with glutaraldehyde before enzyme treatment. Chloroplasts isolated from spinach leaves previously vacuum infiltrated with 6% glutaraldehyde for 1 hr appeared by freeze-etching almost identical to the best preparations of unfixed chloroplasts. Thus, glutaraldehyde does not appear to modify the surfaces along which thylakoids break, an indication that these surfaces might be nonpolar in character. These fixed chloroplasts also carry out an efficient indophenol Hill reaction, although the saturation rates are low.[19] During these studies on chloroplasts from glutaraldehyde-fixed leaves, we found that acetone extraction of the thylakoids, while removing pigment and presumably other lipids, did not alter the morphology of the chloroplasts as observed by light microscopy. This encouraged us to study chloroplasts from glutaraldehyde-fixed spinach leaves before and after lipid extraction, by both freeze-etching and conventional sectioning techniques. The results are presented in Figs. 10-6 through 10-9.

With respect to freeze-etching (Fig. 10-6), extraction of lipid completely removes the plane of weakness that exists in control membranes. Breaks no longer occur along membrane faces, but at random through the chloroplasts. The presence of lipid is essential to establish the weak layers along which breaks occur in freeze-etching. This result supports the view that the membrane faces seen are, for the most part, nonpolar surfaces which could result from liqid-lipid or lipid-protein interaction. This interpretation is consistent with the fact that these faces result from breaks along the interior of the membrane.[12]

Figures 10-8 and 10-9 are a comparison of $KMnO_4$-stained sections of glutaraldehyde-fixed chloroplasts before and after lipid extraction. Differences in the properties of the two fractions became evident during the fixation, when the control material reduced the $KMnO_4$ to a much greater extent than the extracted material. Thin sections of the control chloroplasts are very similar to chloroplasts seen in thin sections of $KMnO_4$-fixed leaves with respect to the thylakoid fine structure, starch grains, and the outer membrane. In the extracted material, however, the outer membrane is no longer evident, and the thylakoid staining is almost absent. The general morphology of the chloroplast is, nevertheless,

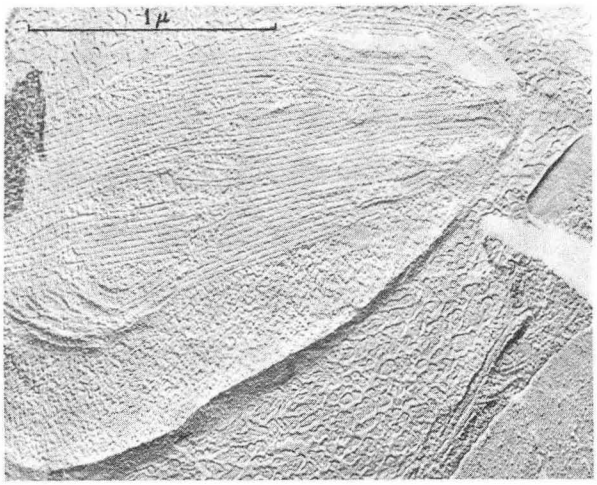

Fig. 10-6. Freeze-etch cross section of chloroplast isolated from a glutaraldehyde fixed spinach leaf.

Fig. 10-7. Freeze-etch cross section of chloroplasts isolated from a glutaraldehyde-fixed spinach leaf extracted with acetone.

Fig. 10-8. Cross section of a spinach chloroplast isolated from glutaraldehyde-fixed leaves, $KMnO_4$-stained and thin-sectioned.

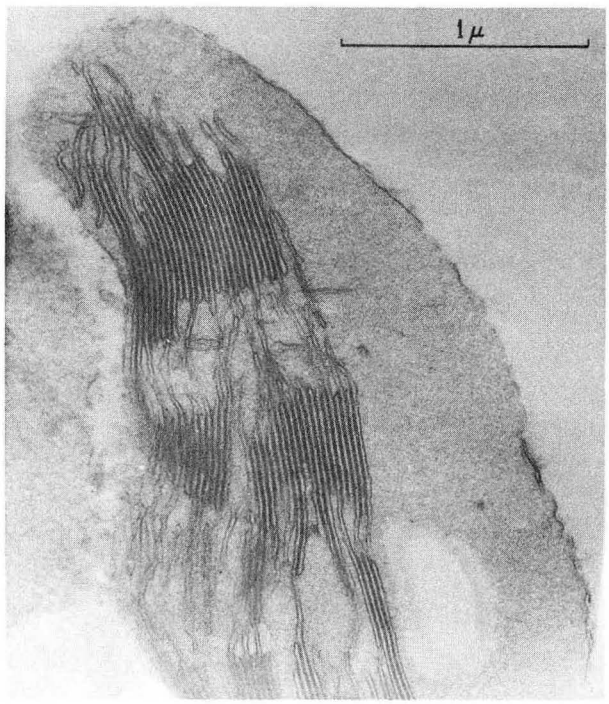

Fig. 10-9. Cross section of a spinach chloroplast isolated from glutaraldehyde-fixed leaves, extracted with acetone before $KMnO_4$ staining.

unaffected. Apparently lipid acts as a major reductant of $KMnO_4$ during chloroplast fixation, and its removal from the membrane greatly decreases the staining intensity. It is tempting to speculate that the dark regions of the $KMnO_4$-stained thylakoid are primarily lipid in character, which would place the lipid on the exterior of the membrane.[20]

Both $KMnO_4$ staining and freeze-etching of extracted membranes suggest that thylakoid lipids play a major role in both kinds of sample preparation. The lipids appear to be not only a major reductant of $KMnO_4$ but also necessary to produce the membrane faces observed in freeze-etching. Both observations are consistent with a membrane in which the external surface in contact with the aqueous phase consists primarily of the polar ends of lipids, which, in turn, are bound to nonpolar micelles within the membrane.

In conclusion, freeze-etching supports the view that the thylakoid is an example of a micellar membrane in which 175×90-Å and 100×90-Å particles are embedded in the membrane matrix. The 175-Å particles are confined to membranes which contain chlorphyll or bacteriochlorophyll. They appear to represent, with their embedding matrix, a quantum conversion and electron transport site, and correspond to the quantasome in shadowed preparations. The membrane surfaces seen in freeze-etching are dependent on the presence of lipid in the membrane. Removal of the lipid eliminates the weak face along which breaks occur, which suggests that the membrane faces seen in freeze-etching are nonpolar in nature.

Footnote and References

†In Proceedings of Brookhaven Symposia in Biology, No. 19, Energy Conversion and the Photosynthetic Apparatus, June 6-9, 1966.

1. R. L. Steere, J. Biophys. Biochem. Cytol. 3, 45 (1957).
2. H. Moor, K. Mühlethaler, H. Waldner, and Frey-Wyssling, A., J. Biophys. Biochem. Cytol. 10, 1 (1961).
3. H. Moor and K. Mühlethaler, J. Cell Biol. 17, 609 (1963).
4. K. Mühlethaler, H. Moor, and J. W. Sarkowski, Planta 67, 305 (1965).
5. D. Branton and R. B. Park, J. Ultrastruct. Res., in press.

6. R. G. Jensen and J. A. Bassham, Proc. Natl. Acad. Sci. U. S. 56, 1095 (1966).
7. D. Spencer and H. Unt, Australian J. Biol. Sci. 18, 197 (1965).
8. R. B. Park and N. G. Pon, J. Mol. Biol. 6, 105 (1963).
9. D. Branton, Exptl. Cell Res. 45, 703 (1966).
10. J. F. Danielli and H. A. Davson, J. Cellular Comp. Physiol. 5, 495 (1935).
11. J. D. Robertson, Symp. Soc. Study Develop. Growth 22, 1 (1964).
12. D. Branton, Proc. Natl. Acad. Sci. U. S. 55, 1048 (1966).
13. A. Frey-Wyssling and E. Steinmann, Biochim. Biophys. Acta 2, 214 (1948).
14. R. B. Park and N. G. Pon, J. Mol. Biol. 3, 1 (1961).
15. R. B. Park and J. Biggins, Science 144, 1009 (1964).
16. S. Izawa and N. E. Good, Biochim. Biophys. Acta 102, 20 (1965).
17. B. Kok, Biochim. Biophys. Acta 48, 527 (1961).
18. E. Bamberger and R. B. Park, Plant Physiol. 4, 1591 (1966).
19. R. B. Park, J. Kelly, S. Drury, and K. Sauer, Proc. Natl. Acad. Sci. U. S. 55, 1056 (1966).
20. R. B. Park, J. Cell Biol. 27, 151 (1965).
21. D. Branton, in Le Chloroplaste, C. Sironval, Ed. (Masson et Cie., Paris, 1967), p. 48.
22. W. DeBoer and D. Branton, Unpublished observations.

11. CHEMICAL TRAPPING OF A PRIMARY QUANTUM CONVERSION PRODUCT IN PHOTOSYNTHESIS †

Gerald A. Corker, Melvin P. Klein, and Melvin Calvin

Preliminary studies of a photochemical reaction between di-tertiary-butylnitroxide and chloroplasts isolated from spinach indicate that the nitroxide is coupling with the photoinduced radicals produced in these photosynthesizing systems. The exact fate of the nitroxide has not yet been determined but is being pursued by the use of a carbon-14-labeled nitroxide, with the object of determining the nature of the photoproduced radical, or radicals, with which it couples.

† Abstract of paper published in Proc. Natl. Acad. Sci. U. S. 56, 1365 (1966).

12. PHOTOSYNTHESIS BY ISOLATED CHLOROPLASTS. I. *

R. G. Jensen† and J. A. Bassham

Photosynthesis in green plants requires not only photoelectron transport, oxygen evolution, and photophosphorylation, but also the synthetic reactions whereby carbon dioxide is assimilated and reduced to a number of organic compounds via the photosynthetic carbon reduction cycle[1] and secondary biosynthetic pathways.[2] Complete photosynthesis with isolated chloroplasts has for many years been a goal of biochemists. Photosynthetic reactions could then be isolated from reactions of the cytoplasm, and the cell wall could be eliminated as a barrier to the assimilation of various added metabolites and chemicals. This achievement would greatly facilitate the study of the mechanism of enzymic transformations and metabolic control in the synthetic reactions of photosynthesis.

The photochemical transfer of electrons from water to artificial electron acceptors by subcellular particles from green plant cells was demonstrated many years ago by Hill and Scarisbrick.[3] Since that time, isolated chloroplasts and chloroplast particles have been found to be capable of photoelectron transport to NADP,[4-6] and of photophosphorylation.[7]

Although very high rates, exceeding those required for in vivo photosynthesis, have been demonstrated for photoelectron transport to both natural and artificial electron acceptors and for photophosphorylation, rates of carbon reduction during photosynthesis by isolated chloroplasts have been disappointingly low. Fixation of ^{14}C-labeled carbon dioxide into intermediate compounds of the photosynthetic carbon reduction cycle by isolated chloroplasts was reported by Allen et al. in 1955.[8] This ability to fix CO_2 was diminished with broken chlorplasts but could be restored by various cofactors,[9] and it was claimed that CO_2 fixation by chloroplasts could be accomplished in the dark if the cofactors ATP and NADPH were added.[10] A report from the same laboratory (in 1960) listed fixation rates of 4.5 to 6 μmoles CO_2/mg Chl/hr.[11] Others[12] found rates of about 4. It has long been assumed and is verified by experiment in this report, that spinach leaves should be capable of rates of CO_2 fixation exceeding 200 μmoles CO_2/mg Chl/hr.

Fixation of CO_2 has been stimulated by the addition of some intermediates of the carbon reduction cycle to broken chloroplasts,[9] or whole chloroplasts.[13] Walker[14] found a rate of 1.1 μmoles CO_2/mg Chl/hr to be increased to 24.3 (and later,[15] 36.9) upon the addition of ribose-5-phosphate to isolated chloroplasts prepared according to his method. With the addition of 71.5 μmoles of ribose-5-phosphate per mg chlorophyll to the reaction mixture, Walker's accelerated CO_2 fixation rate resulted in a total fixation of 6.0 μmoles CO_2 per mg chlorophyll during the 20-min period of incubation. Thus, the stimulated CO_2 fixation rate could result from the operation of only part of the carbon reduction cycle utilizing ATP from the photochemical reactions to convert ribose-5-phosphate to ribulose-1, 5-diphosphate, the carboxylation reaction substrate. It would appear that Walker's preparation had a limited capacity for conversion of other sugar phosphates to pentose phosphates.

Another type of stimulation of CO_2 fixation by chloroplasts was achieved by Heber and Tyszkiewicz,[16] who added a concentrated solution of soluble enzymes of the carbon reduction cycle to chloroplasts isolated in aqueous media and thereby obtained fixation rates of 4 μmoles CO2/mg Chl/hr, which were further stimulated to 12 μmoles CO_2/mg Chl/hr upon the addition of ATP and NADPH. Using chloroplasts from the marine chrysomonad Hymenomonas sp, Jeffrey et al.[17] measured a chloroplast fixation rate of 15.3 μmoles CO_2/mg Chl/hr, which was nearly 10% of the in vivo rate for that organism. Addition of chloroplast extract stimulated these chloroplasts to a rate of 34, or approximately 25% of the fixation rate of whole cells.

In the studies done for this experiment, efforts were made to obtain a well-defined, homogeneous preparation of chloroplasts with intact membranes, which would be capable of high rates of complete photosynthesis without the addition of either cofactors (other than inorganic ions) or enzymes. It was felt that such preparations would be more useful than reconstituted systems for studies of metabolic control and enzymic mechanisms.

Results and Discussion

Intact and freshly harvested and healthy spinach leaves gave a CO_2 fixation rate of 245 μmoles CO_2/mg Chl/hr. Chloroplasts prepared the same day from leaves from the same plants gave a fixation rate of 155 μmoles CO_2/mg Chl/hr. This rate with isolated chloroplasts was obtained over a period of 6 min following 3 min preillumination. Thus the isolated chloroplasts, for a limited period of time, assimilated carbon dioxide at a rate that was 63% of the in vivo photosynthetic rate.

The total carbon dioxide fixation during

various periods of time is shown in Fig. 12-1. The rate of photosynthesis declines continuously with time of photosynthesis, and by 30 min is 40 μmoles CO_2/mg Chl/hr.

The fixation rate becomes maximal with a bicarbonate concentration of about 3 mM (Fig. 12-2). The bicarbonate level for 1/2 maximum rate is 6×10^{-4} M, compared with 1.1×10^{-2} M reported[18] for isolated ribulose diphosphate carboxylase (E. C. 4.1.1.39). Thus, the isolated chloroplasts used in our experiments resemble much more nearly in vivo photosynthesis in their capability for carbon dioxide fixation than does the isolated, purified enzyme which catalyzes the primary carboxylation reaction of photosynthesis.

The saturation of CO_2 fixation rate with light intensity is shown in Fig. 12-3.

The appearance of the chloroplasts in the light microscope with phase optics is shown in Fig. 12-4. It can be seen that approximately 75% of the chloroplasts are of the class I type (highly refractive without clear grana) as defined by Spencer and Unt.[19] It seems probable that the biochemically active chloroplasts in our experiments are the class I chloroplasts, which retain an intact membrane and have not lost soluble protein. A large proportion of class I chloroplasts is not in itself sufficient to produce high rates of CO_2 fixation, since Spencer and Unt reported a rate of 2.88 μmoles CO_2/mg Chl/hr.

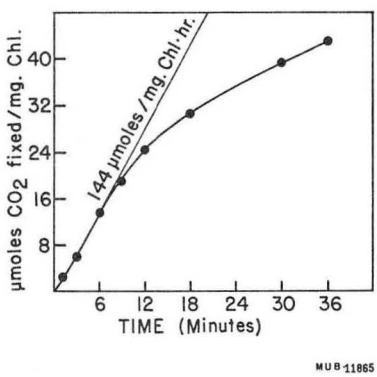

Fig. 12-1. Time course of carbon dioxide fixation by isolated chloroplasts.

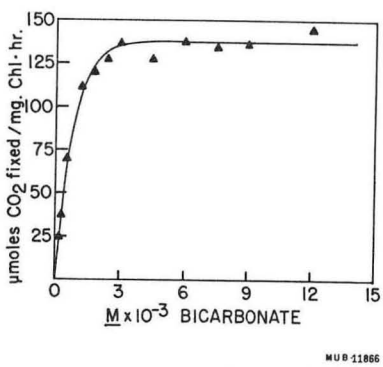

Fig. 12-2. Dependence of CO_2 fixation rate on bicarbonate concentration.

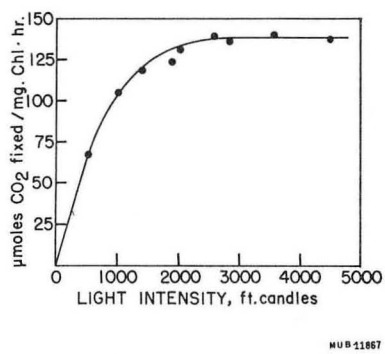

Fig. 12-3. Dependence of CO_2 fixation rate on light intensity. Light intensity given as incident intensity at surface of reaction flask. Light source was incandescent lamp varied by neutral density filters.

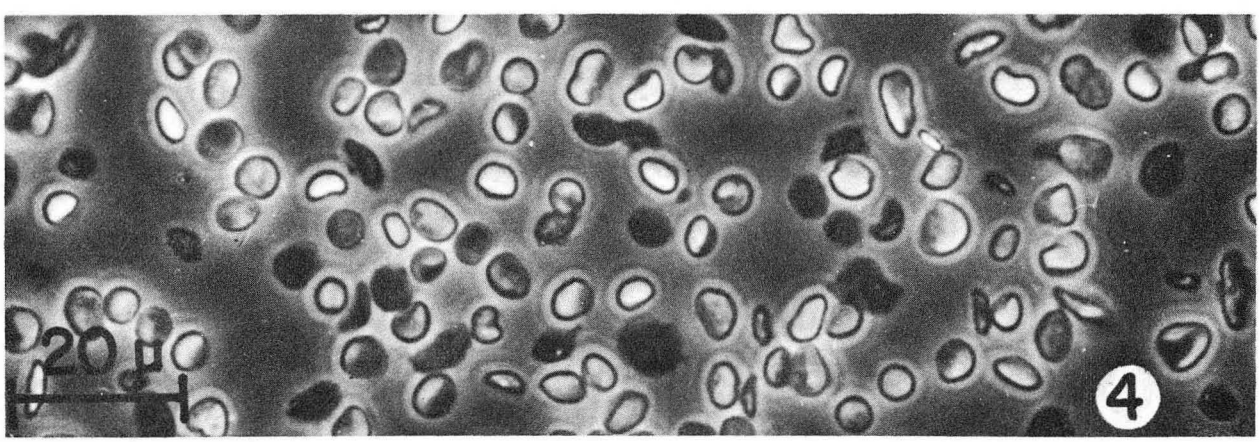

Fig. 12-4. Isolated chloroplasts under phase contrast in the light microscope. Class I chloroplasts appear bright and highly refractive with an outer, limiting membrane.

Electron micrographs prepared by using the freeze-etching technique with chloroplasts isolated as described in this paper are shown in Figs. 12-5 and 12-6. They both show the close stacking and unswollen configuration of the thylakoids which are typical of chloroplasts in vivo.

The products of CO_2 fixation during 10 min in whole spinach leave are shown in the radioautograph in Fig. 12-7. The pool sizes of intermediates of the carbon reduction cycle are relatively small, and the radiocarbon passes quickly on into larger pools of various secondary products such as sucrose, alanine, aspartic acids, other amino acids.

In contrast, the pattern of labeling in isolated chloroplasts, shown in Fig. 12-8, contains very high amounts of radiocarbon in intermediates of the carbon reduction cycle, particularly PGA, dihydroxyacetone phosphate, fructose and sedoheptulose diphosphates, and ribose-5-phosphate, as well as in glycolic acid. Work in progress indicates that these compounds are transported, or diffuse, rapidly from the isolated chloroplasts to the suspending medium. Hexose monophosphates and ribulose-1, 5-diphosphate are mostly retained in the chloroplasts. The labeling of secondary products of low molecular weight is rather small. Nonetheless, there is a significant amount of synthesis of macromolecules, as indicated by the large quantity of radiocarbon found at the origin.

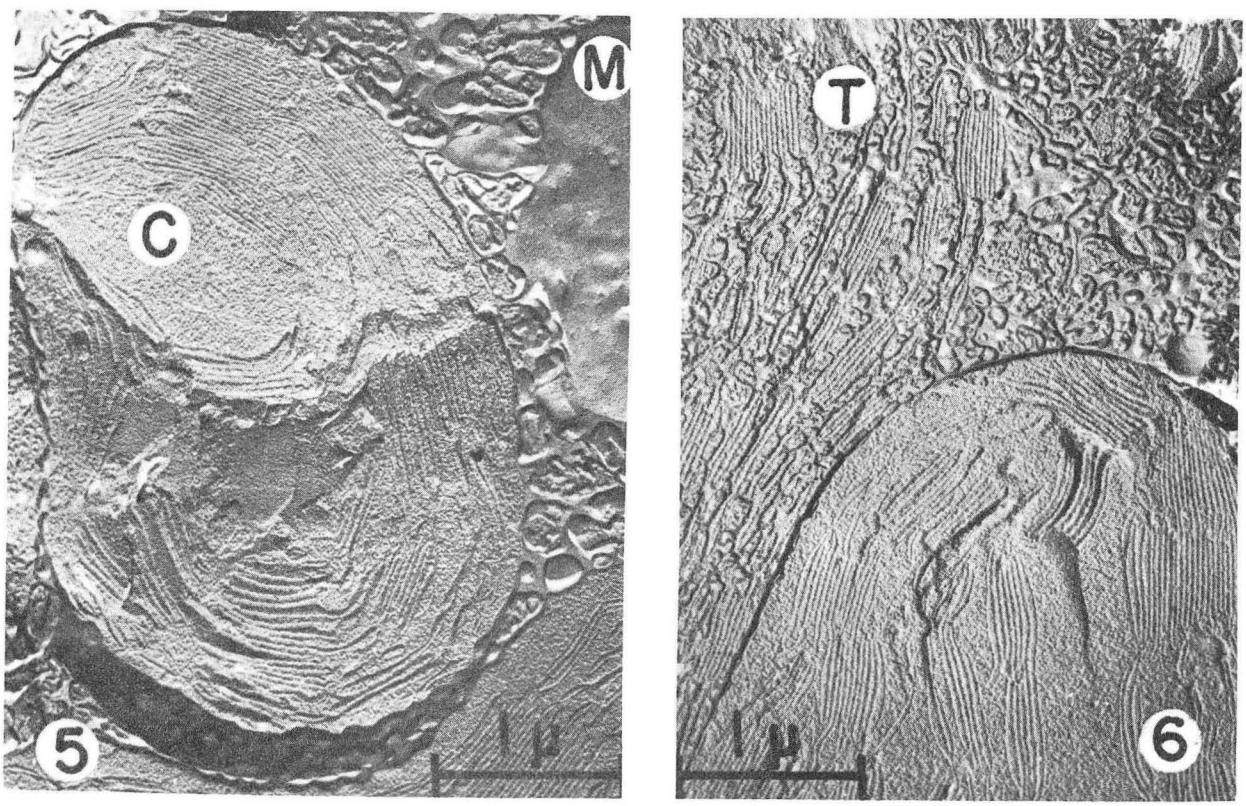

Fig. 12-5 and 12-6. Electron micrographs of isolated chloroplasts obtained by the freeze-etching technique.[23] These electron micrographs were prepared by Prof. Daniel Branton of the Department of Botany, University of California, Berkeley, and are reproduced by his courtesy. Fig. 12-5 is representative of chloroplast preparations giving high rates of CO_2 fixation. The chloroplasts (C) with closely packed thylakoids are surrounded by an intact outer membrane (M). In the upper right corner is another membrane surface left after the fracture process. Fig. 12-6 is representative of chloroplast preparations giving lower rates of CO_2 fixation. Although intact chloroplasts were found in this preparation, more plastids were without outer membranes. The thylakoids (T) are unswollen.

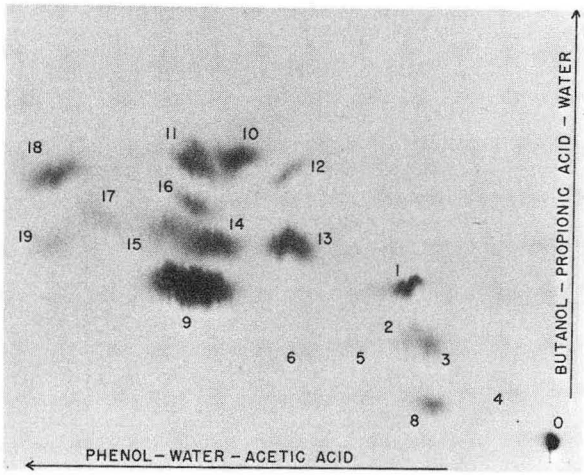

Fig. 12-7. Radioautograph of $^{14}CO_2$ photosynthetic products in whole spinach leaves. Detached spinach leaves were allowed to fix $^{14}CO_2$ for 10 min as described in text. After killing, the leaf material was analyzed by two-dimensional paper chromatography and radioautography.

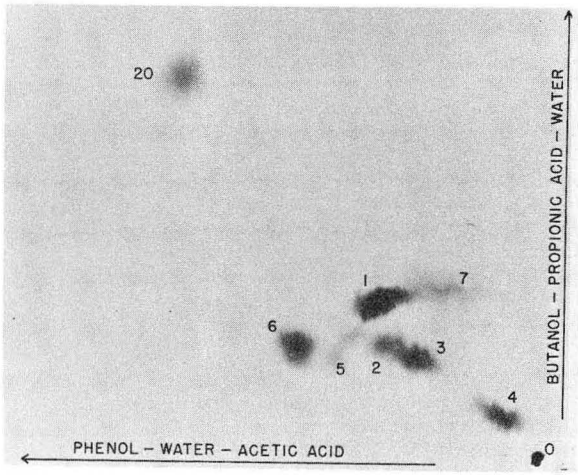

Fig. 12-8. Radioautograph of $^{14}CO_2$ photosynthetic products in isolated spinach chloroplasts. Isolated chloroplasts were allowed to fix $^{14}CO_2$ for 6 min as described in text. After killing, the leaf material was analyzed by two-dimensional paper chromatography and radioautography.

The numbers in Figs. 12-7 and 12-8 indicate the following compounds: 0, origin; 1, 3-phosphoglyceric acid; 2, fructose-6-phosphate; 3, sedoheptulose-7-phosphate and glucose-6-phosphate; 4, ribulose-1, 5-diphosphate, fructose-1, 6-diphosphate, and sedoheptulose-1, 7-diphosphate; 5, ribose-5-phosphate and ribulose-5-phosphate; 6, dihydroxyacetone phosphate; 7, 3-phosphoglyceraldehyde; 8, uridine diphosphoglucose; 9, sucrose; 10, malic acid; 11, glyceric acid (?); 12, itric acid; 13, aspartic acid; 14, serine; 15, glycine; 16, glutamic acid; 17, threonine; 18, alanine; 19, glutamine; 20, glycolic acid.

Footnotes and References

*Condensed from Proc. Natl. Acad. Sci. U. S. 56, 1095 (1966).

†NIH postdoctoral fellow (National Cancer Institute).

1. J. A. Bassham, A. A. Benson, Lorel D. Kay, Anne Z. Harris, A. T. Wilson, and M. Calvin, J. Am. Chem. Soc. 76, 1760 (1954).
2. M. Calvin and J. A. Bassham, The Photosynthesis of Carbon Compounds (New York: W. A. Benjamin, Inc., 1962).
3. R. Hill and R. Scarisbrick, Proc. Roy. Soc. (London) B129, 238 (1940).
4. W. Vishniac and S. Ochoa, Nature 167, 768 (1951).
5. L. J. Tolmach, Nature 167, 946 (1951).
6. D. I. Arnon, Nature 167, 1008 (1951).
7. D. I. Arnon, M. B. Allen, and F. R. Whatley, Nature 174, 394 (1954).
8. M. B. Allen, Daniel I. Arnon, J. B. Capindale, F. R. Whatley, and Lois J. Durham, J. Am. Chem. Soc. 77, 4149 (1955).
9. F. R. Whatley, M. B. Allen, L. L. Rosenberg, J. B. Capindale, and Daniel I. Arnon, Biochim. Biophys. Acta 20, 462 (1956).
10. Achim V. Trebst, Harry Y. Tsujimoto, and Daniel I. Arnon, Nature 182, 351 (1958).
11. M. Losada, A. V. Trebst, and Daniel I. Arnon, J. Biol. Chem. 235, 832 (1960).
12. Gibbs, Martin, and Nona Calo, Plant Physiol. 34, 318 (1959).
13. E. S. Bamberger and Martin Gibbs, Plant Physiol. 40, 919 (1965).
14. D. A. Walker, Biochem. J. 92, 22C (1964).
15. D. A. Walker, Plant Physiol. 40, 1157 (1965).
16. U. Heber and E. Tyszkiewicz, J. Exptl. Bot. 13, 185 (1962).
17. S. W. Jeffrey, J. Ulrich, and M. B. Allen, Biochim. Biophys. Acta, 112, 35 (1966).
18. A. Weissbach, B. L. Horecker, and J. Hurwitz, J. Biol. Chem. 218, 795 (1966).
19. D. Spencer, and H. Unt, Australian J. Biol. Sci. 18, 197 (1965).

13. PHOTOSYNTHESIS BY ISOLATED CHLOROPLASTS. II. DISTRIBUTION OF ^{14}C-LABELED PRODUCTS BETWEEN CHLOROPLASTS AND SUPERNATANT SOLUTION

J. A. Bassham, R. G. Jensen, and Martha Kirk

In the preceding paper we described conditions for obtaining high rates of photosynthesis with isolated chloroplasts, and preliminary experiments on the distribution of products between the chloroplasts and the medium in which they are suspended.

We have now carried out another more thorough experiment on the distribution of ^{14}C products of photosynthesis in isolated chloroplasts between the chloroplasts and the suspending medium. The distribution of labeled carbon in these products as a function of time of photosynthesis is given in this report.

Experimental Procedure

In these studies, chloroplasts were isolated from freshly grown spinach according to the methods described earlier.[1] These chloroplasts were then suspended in the usual assay medium.[1] In the first experiment, after a period of 3 min preincubation, ^{14}C-labeled bicarbonate was added to the chloroplasts and, over a period of 40 min photosynthesis, samples were taken for analysis. Most of these samples were subjected to a very quick centrifugation with a microfuge to separate the chloroplasts as a pellet from the suspending medium. Pellet and supernatant solution were then killed separately with 80% methanol as quickly as possible. The entire operation of withdrawing the sample, centrifuging, and killing required approximately 30 sec.

We recognized that this period of time is long enough for metabolic changes characteristic of light-dark transients to take place. Therefore additional samples of chloroplasts were taken and killed directly. The mixtures of methanol-water and chloroplasts or suspending medium were then analyzed by two-dimensional paper chromatography[1] and radioautography. The amount of ^{14}C in each compound of each sample was determined as a function of the time of sampling, and is plotted as μmoles ^{14}C/mg Chl in the Results section.

In a second experiment, chloroplasts were isolated and preilluminated as just described. However, ^{32}p-labeled phosphate was added at the beginning of the preillumination period and ^{14}C-labeled bicarbonate was added after 4 min of preillumination with the radiophosphorus. One sample was taken just before the addition of $^{14}CO_2$, and other samples were taken periodically after the addition of bicarbonate.

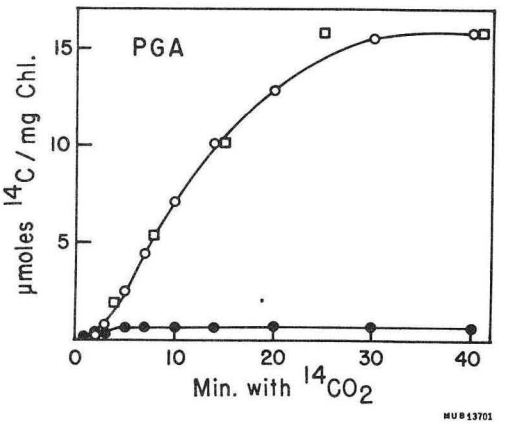

Fig. 13-1

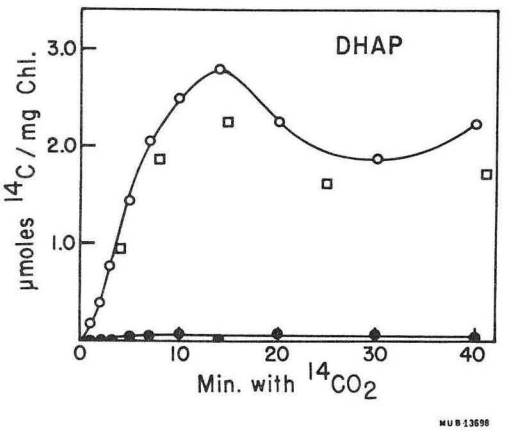

Fig. 13-2

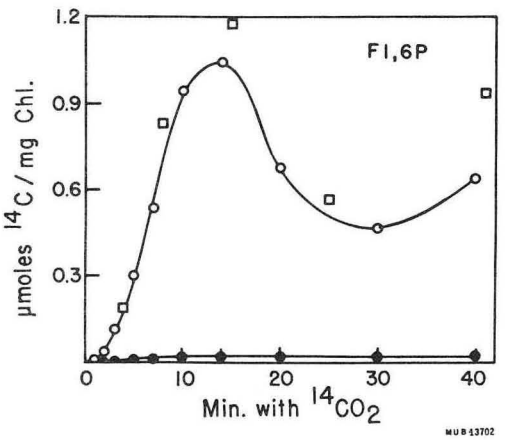

Fig. 13-3.

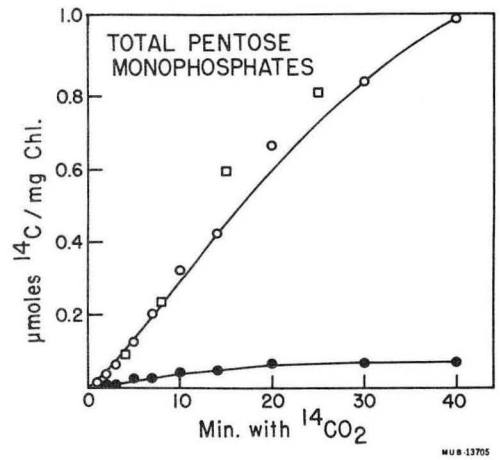

Fig. 4.

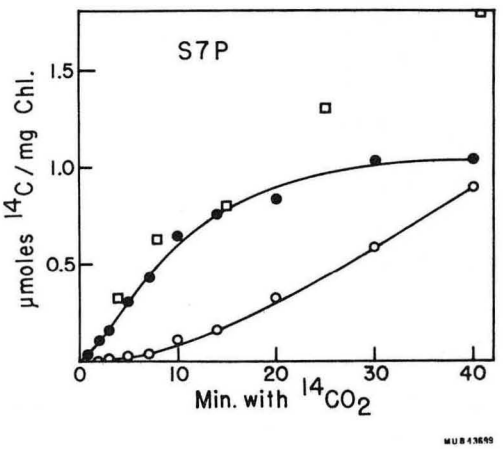

Fig. 7.

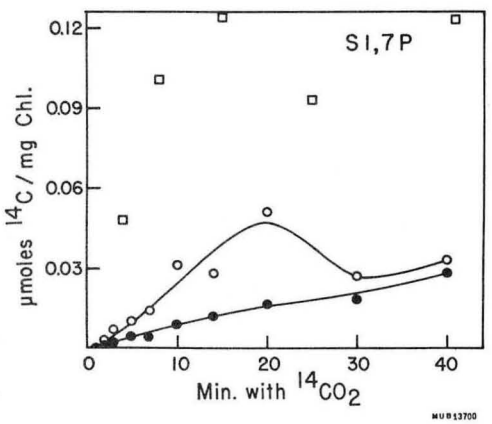

Fig. 5.

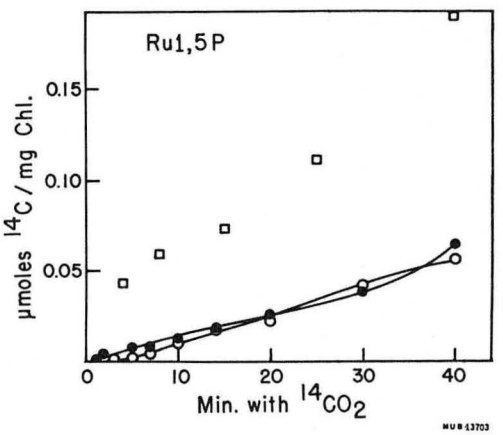

Fig. 8.

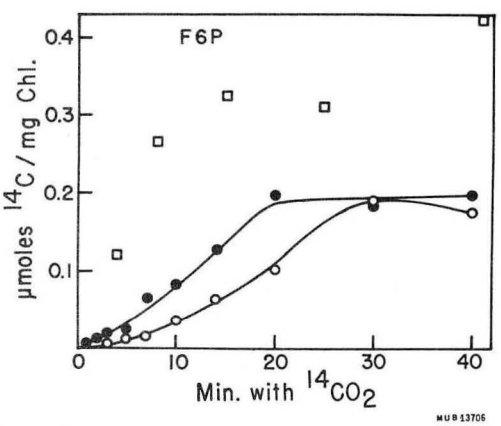

Fig. 6.

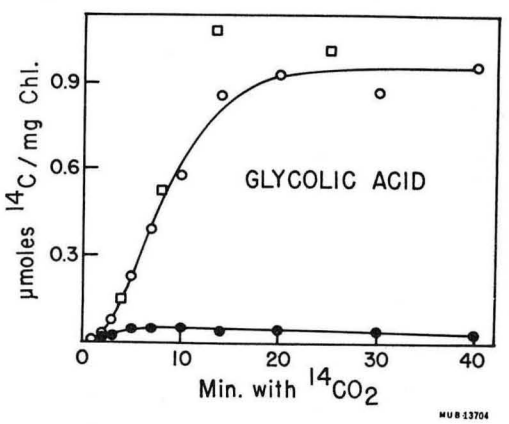

Fig. 9.

Figs. 13-1 through 13-9. Distribution of ^{14}C-labeled compounds between chloroplast pellet and supernatant solution during photoshythesis with isolated chloroplasts in the presence of ^{14}C-labeled bicarbonate. Open circles denote ^{14}C-labeling of compound in supernatant solution, closed circles denote ^{14}C-labeling of compound found in the pellet, and open squares denote ^{14}C-labeling of the compound in the samples that were not subjected to centrifugation. The identity of the specific compound is indicated in the figure.

At 14 min total illumination the light was turned off, and additional samples were taken in the dark. Finally, at 19 min the light was turned on again, and three more samples were taken. Each of these samples was separated by centrifugation as just described and analyzed by two-dimensional paper chromatography and radioautography. In this case the levels of ^{14}C and ^{32}p were counted with a Packard scintillation counter and the labeling of individual compounds with each tracer was determined. The results of this experiment were in some ways unsatisfactory, particularly with respect to the labeling of the sugar phosphates and other intermediates of the carbon cycle. This experiment is being repeated. However, the labeling of ADP and ATP provides some interesting information which is given in Results.

Results

The labeling with ^{14}C of intermediates of the carbon reduction cycle of photosynthesis and of glycolic acid in pellet and supernatant solutions in the first experiment (continuous illumination) are shown in Figs. 13-1 through 13-9. In each case the ^{14}C-labeling of the compound found in the supernatant solution is indicated by open circles and the ^{14}C-labeling of the compound found in the pellet is indicated by black dots. The ^{14}C-labeling of the compound found in the samples where the chloroplasts were not separated from the supernatant solution prior to killing are indicated by the squares.

In most cases the labeling of a given compound found in the sample which was not separated is roughly the sum of the labeling found in the pellet and supernatant curves. However, the sedoheptulose-1, 7-diphosphate and fructose-1, 6-diphosphate labeling was higher in the samples which were not separated than in the sum of the pellet and supernatant. At the same time, the labeling of dihydroxyacetone phosphate (DHAP) was lower in the unseparated sample than the sum of its labeling in pellet and supernatant. Thus it appears that some S-1, 7-P and some F-1, 6-p were converted to DHAP during the centrifugation. The level of ribulose-1, 5-diphosphate (Ru-1, 5-P) also apparently dropped during the centrifugation, presumably due to the continued carboxylation reaction. These changes, however, do not affect greatly the general conclusions which can be drawn from the pellet-supernatant curves.

Several intermediates of the carbon cycle and the glycolic acid are found very predominantly in the supernatant solution, [1] indicating that they are not well retained in the pellet. Most marked among these compounds are PGA (Fig. 13-1), DHAP (Fig. 13-2), and F-1, 6-P (Fig. 13-3). Also the total pentose monophosphate (Fig. 13-4), S-1, 7-P (Fig. 13-5), and glycolic acid (Fig. 13-9) are found predominantly in the supernatant solution.

In contrast to the compounds just mentioned, the ^{14}C-labeled fructose-6-phosphate (F6P) Fig. 13-6) and sedoheptulose-7-P (S7P) (Fig. 13-7) are found predominantly in the pellet. Ribulose-1, 5-diphosphate (Ru-1, 5-P) (Fig. 13-8) is about equally distributed between pellet and supernatant solution. In other earlier experiments the Ru-1, 5-P was found predominantly in the pellets. In this experiment the level of Ru-1, 5-P was much higher in the unseparated samples, and it is reasonable to suppose that most of this extra Ru-1, 5-P which was converted during the centrifugation was in the pellet.

A general pattern of behavior is beginning to emerge in which compounds lying between the carboxylation reaction of photosynthesis and the diphosphatase reaction are strongly exported from the chloroplast, or leak from the chloroplast into the supernatant solution. Less certain data are available for compounds which lie between the diphosphatase reaction and the carboxylation reaction, but it seems that these may be retained in the chloroplasts. Unfortunately we have not yet resolved the pentose monophosphates with sufficient accuracy to make a distinction between those which might be retained in the pellet and those which might leak out of the pellet. Work with special solvents is being carried out to try to effect a better separation of these compounds.

In order to obtain a better idea of the rate of formation of labeled compounds, we took the slope of the various labeling curves for pellet and supernatant and unseparated samples at 3 min after addition of ^{14}C and during the period between 5 and 10 min after addition of ^{14}C. These rates are listed in Table 13-I. These labeling rates and their sum provide a picture of what is happening to the radiocarbon as it is incorporated by the photosynthesizing chloroplasts with time. At 3 min it can be seen that a large part of the $^{14}CO_2$ taken up is being incorporated in the net synthesis of PGA and DHAP, which appears mostly in the supernatant solution. Even during the time between 3 min and the period 5 to 10 min, there is an accentuation of the formation of PGA at the expense of the formation of sugar phosphates, suggesting that some of the degeneration of the photosynthesis in the isolated chloroplasts is due to a slowing down of the reduction of PGA to DHAP.

The ratio of DHAP in the supernatant solution to DHAP in the pellet at 3 min is something like 40 to 1, and the ratio for F-1, 6-P is almost as high. These high ratios of export of sugar diphosphates and triose phosphate,

Table 13-I. Photosynthesis rates of product formation (μmoles ^{14}C/hr/mg Chl).

Compound	3 min after ^{14}C added			7 min after ^{14}C added		
	Pellet	Super-natant	Not separated	Pellet	Super-natant	Not separated
PGA	8.3	39.6	51.0	3.30	54.8	51.8
Total pentose monophosphate	0.21	1.79	1.70	0.20	2.94	2.70
DHAP	0.56	23.8	21.10	0.20	14.4	10.4
Glyceraldehyde P	---	1.69	1.11	---	1.27	.86
Ru-1, 5-P	0.07	0.03	0.45	0.07	0.09	0.17
Glycolic acid	0.71	3.94	4.65	0.06	4.62	4.72
S-1, 7-P	0.06	0.12	1.06	0.06	0.15	0.64
F-1, 6-P	0.19	6.66	3.90	0.10	7.92	6.92
F-6-P	0.38	0.17	2.94	0.73	0.27	1.32
S-7-P	4.30	0.27	4.80	4.33	1.02	4.10
GMP	1.60	0.21	2.04	1.98	1.00	3.46
Unknown sugar diphosphate	0.15	---	---	0.04	---	---
GDP	0.04	---	---	0.01	---	---
Total	16.57	78.28	94.84	11.12	88.50	87.13
	94.85			99.62		

together with the high retention of sugar monophosphates in the pellet, strongly suggest to us that the diphosphatase reaction is limiting from the beginning of the photosynthesis with isolated chloroplasts.

We are inclined to think that the export of compounds of the cycle lying between the carboxylation reaction and the diphosphatase reaction seen with the isolated chloroplasts is actually only an exaggeration of a naturally occurring phenomenon. Our hypothesis would be that the diphosphatase reaction is a point of metabolic regulation which controls the flow of carbon from the photosynthetic carbon reduction cycle to the region of biosynthesis of amino acids and fats which may be away from the immediate site of photosynthesis.

Whether or not this hypothesis proves to be correct, it is clear that the transport of carbon-labeled compounds from the isolated chloroplasts to the supernatant solution is not an indiscriminate leakage but rather a selective process of some kind.

The results of the second experiment, in which the light was turned off after 14 min, are shown in Figs. 13-10 and 13-11. Again, open circles represent labeling of compounds in the solution and black dots represent labeling of compound found in the pellet. It is apparent that both ATP (Fig. 13-10) and ADP (Fig. 13-11) rapidly diffuse between the pellet and the supernatant solution. When $H^{14}CO_3^-$ is added to preincubated chloroplasts, which have been deprived of bicarbonate, the level of ATP drops precipitously as the photosynthetic carbon reduction cycle requires the utilization of ATP for the kinase reactions with ribulose-5-phosphate and with PGA. Since the ATP in the supernatant solution drops very rapidly, it is clear that it is diffusing back into the chloroplasts where it must be used. A further drop in the level of ATP is seen when the light is turned off and a small rise in ATP occurs when the light is turned on again. The level of labeled ADP also drops upon addition of $H^{14}CO_3^-$, indicating that ADP also diffuses rapidly back into the chloroplasts. Moreover, the fact that it drops at the same time

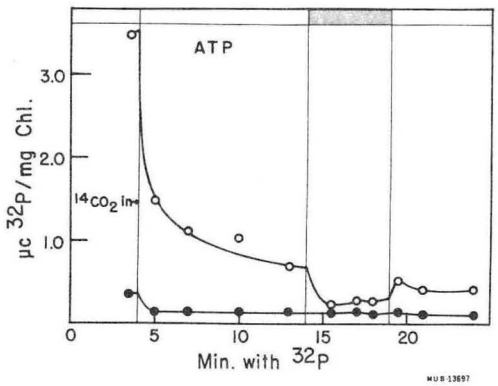

Fig. 13-10. Distribution of ^{32}P labeling of ATP and ADP between pellet and supernatant during photosynthesis with isolated chloroplasts. Open circles denote ^{32}P labeling of compound in supernatant solution, and closed circles denote ^{32}P labeling of compound in the pellet.

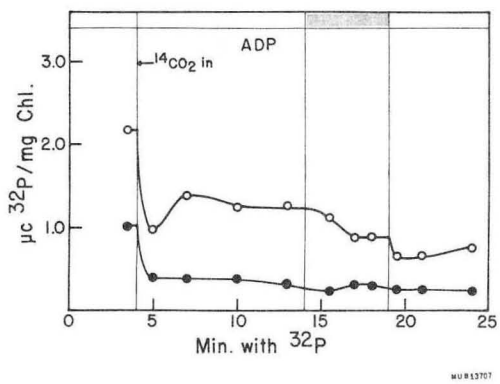

Fig. 13-11. Distribution of ^{32}P labeling of ATP and ADP between pellet and supernatant during photosynthesis with isolated chloroplasts. Open circles denote ^{32}P labeling of compound in supernatant solution, and closed circles denote ^{32}P labeling of compound in the pellet.

as ATP reinforces our previous observation[2] that there is apparently a very active myokinase, or adenylate kinase, reaction which interconverts ATP, ADP, and AMP to their equilibrium mixture.

Other results from this second experiment, as mentioned earlier were not satisfactory because of the deterioration of the chloroplasts by the time the light was turned off. A new experiment has been performed and is now being processed, in which the light was turned off earlier while the chloroplasts were still in a more active state. It is hoped that this experiment will give us a better insight into the light-dark transient changes occurring in intermediates of the photosynthetic carbon cycle, and the migrations in and out of the chloroplasts which may accompany these transient changes.

References

1. R. G. Jensen and J. A. Bassham, Proc. Natl. Acad. Sci. 56, 1095 (1966).
2. J. A. Bassham, R. G. Jensen, Martha Kirk, and Susan Gelb, LCBQ-9, p. 35 (1966).

14. BIOSYNTHESIS OF OPIUM AND TOBACCO ALKALOIDS

H. Rapoport, A. A. Liebman, B. Mundy, G. Blaschke, and H. I. Parker

Tobacco Alkaloids

Continuation of studies on nicotine biosynthesis with short-term exposure to $^{14}CO_2$ has established that the pyrrolidine ring does not have a symmetrical labeling pattern. A systematic degradation has been developed which permits isolation of each carbon atom of the pyrrolidine ring of nicotine. The independent synthesis of specifically labeled intermediates obtained during this sequence and their degradation have confirmed the integrity of the entire process. This degradation has been applied to numerous samples of nicotine obtained from short-term $^{14}CO_2$ biosynthesis with N. glutinosa, and in each experiment the pyrrolidine ring showed an unsymmetrical labeling pattern, a condition contrary to the accepted symmetrical-intermediate hypothesis of pyrrolidine ring formation. Ornithine feeding experiments, from which the symmetrical theory had evolved, were applied to N. glutinosa, and results were identical with those in other species. These experiments establish a greatly different labeling pattern in the pyrrolidine ring from CO_2 than from preformed precursors such as ornithine.

Opium Alkaloids

The final steps in the biosynthesis of morphine have been established as conversion of thebaine to codeine, which is then demethylated to morphine. Formation of codeine from thebaine must involve an additional intermediate, since two processes occur, reduction and demethylation. The nature of this intermediate depends upon which process occurs first. Thebaine could be reduced to codeine methyl ether followed by demethylation to codeine; or demethylation could occur first, yielding codeinone followed by reduction to codeine. Neither codeine methyl ether nor codeinone has been isolated from fresh plants; however, codeine methyl ether has been found in opium. We have now found evidence that codeinone is the intermediate in the biosynthetic conversion of thebaine to codeine. Thus, the later steps in the biosynthesis of morphine have been shown to involve seven compounds in the following sequence: reticuline → solutaridine → solutaridinol → thebaine → codeinone → codeine → morphine.

Reference

H. Rapoport, The Biosynthesis of the Pyridine and Piperidine Alkaloids, Abhandl. Deut. Akad. Wiss. Berlin, Kl. Chem. Geol. Biol. No. 3, 1966.

15. GENETIC CONTROL OF CATABOLITE REPRESSION

V. Moses and J. Palmer

The synthesis of the lactose enzymes of Escherichia coli is regulated by at least two factors in wild-type strains: the presence or absence of inducers, and the metabolic state of the cells. A variety of nutritional and physiological conditions, in which the cells contain excess quantities of certain metabolic intermediates, prevents the full expression of the lactose genes, even though an inducer may be present. This phenomenon, known as catabolite repression, may conveniently be studied by adding glucose to induced cells growing exponentially in a glycerol or other medium. When this is done, two phases of catobolite repression are observed. In the first, coinciding approximately with the shift-up in growth, synthesis of the lactose enzymes is severely repressed. After a variable period, depending on the particular strain under study, a partial relief of the severe repression is seen although the new steady differential rate of enzyme synthesis is always lower than the original rate before the introduction of glucose.[1] We may thus distinguish between the phases of initial "severe transient repression" and subsequent "mild permanent repression."

A study of the metabolic changes induced in the cells by the addition of glucose has suggested four possible candidates for the intermediary metabolite responsible for the repression.[2] Three of these are sugar phosphates directly concerned with glucose metabolism: glucose-6-phosphate, 6-phosphogluconate and fructose-1, 6-diphosphate. The fourth, reduced nicotine adenine dinucleotide phosphate, is involved in energy transfer and is of particular significance in glucose metabolism in relation to the operation of the pentose phosphate cycle.

Of parallel interest is the nature of the regulatory mechanism whereby the repressing intermediary metabolite is able to prevent the formation of the lactose enzymes. Recent studies with various regulatory mutants in the lactose operon have permitted an analysis of genetic regulatory factors controlling transient repression and have also suggested a hypothesis to explain the mild permanent repression. Since the genetic control of enzyme induction in the lactose operon is well understood,[3] it seemed worth investigating the possibility that either the transient or the permanent repressions, or both, were also modulated through the regulator (i) or operator (o) genes of this system.

Although transient and permanent repression is obtained with regulator constitutive strains (i^-) this does not ipso facto exclude the regulator gene from involvement in catabolite repression. Many such i^- mutations of the i-gene are known to be point mutants. Point mutations in other genes, e.g., the z gene coding for the enzyme β-galactosidase, do not result in the total absence of a gene product, but produce enzymatically inactive proteins which nonetheless possess many of the properties of the wild-type enzyme as witnessed by their ability to cross-react with antibody to native β-galactosidase. Similarly, it may be argued that a point mutation in the regulator gene, resulting in a constitutive phenotype, would also give rise to an inactive protein.

In the past, arguments have been used to exclude the i-gene from a role in catabolite repression on the basis of mating experiments.[4] If a strain carrrying i^+z^+ genes is mated with a lac deletion recipient, β-galactosidase synthesis during the first hour after mating is largely constitutive, yet subject to repression by glucose. The reason for the delay of expression of the i-gene in such experiments is not known, but since it was indeed not expressed, as judged by the constitutive enzyme synthesis, its role in glucose repression seemed doubtful. However, in the absence of further study such arguments may be countered by the suggestion that the i-gene product is activated by glucose metabolites. Thus, although insufficient i-gene product may be present to confer inducibility, the presence of glucose may enhance the effectiveness of the small amounts which are contained in the cells resulting in the repression of constitutive enzyme synthesis.

A more definitive approach to the role of the i-gene would require parallel mutants in one of which the i-gene was functional, while in the other it was not merely nonfunctional on the basis of being unable to confer inducibility, but was actually absent in the sense of being deleted. In our early studies of this problem,[5] the ideal strains (i^+ and i^{del}) were not available. However, a family of strains was available in which both the i-gene and the o-gene were deleted, and these could be compared with related wild-type and i^-o^+ strains. The effects on the differential rates of β-galactosidase synthesis of adding glucose to cells growing on glycerol was studied in the following four strains: (a) $i^+o^+z^+$ [wild type], (b) $i^-o^+z^+$ [regulator constitutive], (c)

$i^{del}o^{del}z^{+}$ [regulator and operator constitutive], and (d) a diploid strain $i^{+}o^{+}z^{-}/F\ i^{del}o^{del}z^{+}$. In the first two of these strains the addition of glucose produced the classical effect of a period of severe transient repression followed by a milder permanent repression. In the strains (c) and (d) the transient phase was absent although the mild permanent phase of repression remained. The differences in repression observed among these strains appeared to be specific to the lactose enzymes, and were not a consequence of an alteration in the pattern of glucose metabolism. Comparison of strains (b) and (c) showed that the effect of glucose on the induced synthesis of L-tryptophanase was unchanged. The growth response to glucose, and the metabolism of glucose via glycolysis and via the pentose phosphate cycle, was also identical in the two strains. We were therefore able to conclude that the severe transient phase of repression involved the operator gene, while the permanent phase did not.

The experiments did not allow an examination of the specific role of the i-gene. Since constitutivity of the operator gene is dominant for the cis-chromosome to the status of the i-gene,[3] the role of the i-gene cannot be studied in strains such as (c) and (d), which are fully operator-constitutive for the chromosome carrying z^{+}. Strain (c) possessed no i-gene; strain (d) carried a functional i-gene, yet did not exhibit transient repression. It thus appears that if the i-gene product is involved in transient repression it can only act when some functional character is present in the operator; total deletion of the operator precludes repression via the i-gene product. The i-gene product cannot be working at some site other than the operator, or a difference in repression pattern would have been observed between strains (c) and (d).

Further studies were made of permanent repression by isolating from strain (c) a mutant constitutive for the enzyme alkaline phosphatase. This enzyme, while showing no transient repression effects when glucose is added to growing cells, nevertheless does exhibit a reduction in the differential rate entirely analogous to that shown by β-galactosidase and quantitatively of approximately the same magnitude. It is not impossible that the permanent repression is neither specific for enzymes normally susceptible to catabolite repression, nor truly a repression. Both β-galactosidase and alkaline phosphates are enzymes completely irrelevant to cells growing on glycerol or glucose. No doubt when glucose is added to cells on glycerol a change occurs in the quantitative balance of proteins being synthesized; the faster rate of growth on glucose is correlated, for example, with a higher content of ribosomal protein.[6,7] If β-galactosidase and alkaline phosphatase syntheses are neither increased nor reduced when glucose is added to a strain constitutive for both these enzymes, yet the rates of synthesis of other proteins are increased, then on a differential basis the rates of synthesis of β-galactosidase and alkaline phosphatase will be reduced. We are currently investigating this possibility further.

Opportunities to investigate the i-gene as distinct from changes in the o-gene arose with the isolation of temperature-sensitive i-gene mutants[8] and "frame-shift" mutants of the i-gene.[9] Two types of temperature-sensitive mutants have been isolated: mutants (i^{TL}) in which the i-gene product is unstable at high temperatures (42°) but not at low temperatures (32°), and others (i^{TSS}) in which the synthesis of the i-gene product is prevented at 42° although, once made, the i-gene product is stable to heat and decays only slowly in metabolism.

We have studied two of these mutants and their immediate parents:[10] (e) i^{+} parent of i^{TL}, (f) i^{TL}, (g) i^{+} parent of i^{TSS}, and (h) i^{TSS}. At 32° strains (e) and (f) are inducible and strain (f) shows the classical response to the addition of glucose. At 42°, however, strain (f) is partly constitutive and fails to exhibit transient repression (permanent repression remains), although its parent strain (e) continues to do so. Thus temperature sensitivity leads to a loss of both inducibility and transient catabolite repression when the cells are cultured at 42°.

With strains (g) and (h) the situation is more complicated. Although strain (h) is constitutive at 42° it continues, with its parent strain (g), to exhibit transient repression at high temperature. However, it is also repressed at high temperature by o-nitrophenyl fucoside, a compound known to activate the i-gene product.[11] Such i^{TSS} cells cannot therefore be regarded as devoid of i-gene product at 42°, and the presence of a transient response to glucose indicates that the i-gene product may be involved in this effect. Thus, although we cannot yet be as certain that the i-gene is concerned in transient repression as we are about the o-gene, all our results are consistent with this being the case.

A formal i^{del} mutant has not been available for testing, but a functional deletion of the i-gene has been obtained in the form of a frame-shift mutant.[9] This mutant is fully constitutive, and the i-gene product has thus lost its affinity for the operator. The o-gene product in this train has also lost its affinity for inducer, as measured directly in binding experiments,[9] indicating that the effect of frame-shifting in the gene is very extensive. We have found that this strain also fails to exhibit

transient repression, although the permanent repression response is still present. These results provide supporting evidence for the involvement of the i-gene product in transient catabolite repression.

Our view of the molecular working of the i-gene product (repressor) must take into account three modes of interaction rather than the two originally envisaged.[3] One site on the repressor interacts with the operator and prevents initiation of transcription of the structural genes of the operon.[3] At another site the repressor may react with inducer, and when inducer is bound to the repressor the latter is allosterically altered in such a way that it will no longer bind to the operator.[12] We now propose an additional site on the repressor for the binding of the glucose metabolite. When this site is occupied we envisage a promotion of repressor binding to the operator so that the effects of the inducer and the glucose metabolite on the repressor will be competitive with one another. There is experimental support for such a competitive effect.[13,14]

Our model is consistent with existing kinetic data from living cells, but an ultimate test of its validity must await the preparation of a suitable cell-free system capable of synthesizing the lactose enzymes under inducible control. Meanwhile, the recent isolation of the lac repressor might permit a preliminary investigation of competitive binding effects without waiting for a cell-free system. We do not know whether other inducible enzymes exhibiting transient repression effects are controlled in a similar way to the lactose enzymes; nor has a formal investigation yet been made of the dilution hypothesis which we have proposed to account for mild permanent repression. Final elucidation of these phenomena will greatly increase our understanding of fundamental mechanisms for maintaining a proper balance among the many components making up a living cell.

References

1. V. Moses and C. Prevost, Biochem. J. 100, 336 (1966).
2. C. Prevost and V. Moses, Biochem. J., in press (1967).
3. F. Jacob and J. Monod, J. Mol. Biol. 3, 318 (1961).
4. W. F. Loomis, Jr., and B. Magasanik, J. Mol. Biol. 8, 417 (1964).
5. J. Palmer and V. Moses, Biochem. J. in press (1967).
6. O. Maaløe and N. O. Kjeldgaard, Control of Macromolecular Synthesis, N. A. Benjamin, Inc., (New York and Amsterdam, 1966), pp. 90-91.
7. H. G. Ungar and V. Moses, unpublished observations.
8. J. R. Sadler and A. Novick, J. Mol. Biol. 12, 305 (1965).
9. W. Gilbert and B. Müller-Hill, Proc. Natl. Acad. Sci., U. S. 56, 1891 (1966).
10. J. Palmer and V. Moses, submitted to Biochim, Biophys. Acta.
11. K. Jayaraman, B. Müller-Hill, and H. V. Rickenberg, J. Mol. Biol. 18, 339 (1966).
12. J. Monod, J. P. Changeux, and F. Jacob, J. Mol. Biol. 6, 306 (1963).
13. D. J. Clark and A. G. Marr, Biochim. Biophys. Acta 92, 85 (1964).
14. D. J. Clark, Biochim. Biophys. Acta 110, 554 (1965).

16. ATTEMPTED MODIFICATION OF RAT BEHAVIOR BY INJECTION OF BRAIN EXTRACTS FROM TRAINED DONORS

Ann M. Hughes, Edward L. Bennett, Marie Hebert, and Mark Lau

Previous experiments done in this Laboratory by Byrne, Samuel, and Hughes have shown that intraperitoneal injection of brain from appropriately trained rats can modify the behavior of the recipients. These experiments have been described in detail.[1] Briefly, the procedure is to use three groups of donor rats. One group is trained to press the left bar of a Grason-Stadler test chamber for a food reward, another to press the right bar, and a third donor group consists of naive rats which have never been placed in the test chamber. After the final training session, brains from two similarly trained rats are quickly removed after decapitation, homogenized together in cold 0.9% NaCl-0.01 M Tris, pH 7.5, and centrifuged, and the supernatant is injected intraperitoneally into a naive recipient. Subsequently the recipient is tested in a series of test sessions, first unrewarded, and then rewarded. The bar preference (left or right) and the corrected "Time to Learn" (TTL_{10}) (defined as the time to press one bar 10 times after the initial press for food reward) are determined. It is this latter measure (TTL_{10}) that discriminated between the recipient groups. Recipients from the right-trained donors had significantly smaller TTL_{10}'s than did recipients from either left-trained or naive animals. This enhanced rate of acquisition was found to be reproducible and to achieve statistical significance with 5 or 6 animals per group in the studies reported by Byrne and Samuel.

The purpose of the series of experiments presented here was to replicate and extend these observations. Ultimately, the objective is to obtain training, extraction, isolation, reinjection, and testing procedures that will permit a biochemical investigation of the behavior-modifying constituent(s) obtainable from "trained" brains. In view of the controversial nature of this area of research, it is essential that reliable and reproducible experimental procedures be devised. This report will attempt to describe the procedural details of the several experiments rather completely, since variation in detail may subsequently prove to be important.

Methods

The experiments reported by Byrne and Samuel had been done in the "student" laboratories in Tolman Hall. Animals were kept in one room; training and testing were done in an adjacent room. A rack of animals to be tested was wheeled from the colony room to the training room. Naive and recipient animals would not have heard the noises associated with the training and testing equipment. With the exception of EB-1, the present series of experiments have been done in Building 74 Trailer Annex. This is a 500-ft^2 facility consisting of approximately 200 ft^2 of colony room, an adjacent 200 ft^2 of general laboratory, and at the far end of the trailer, a 100-ft^2 training and testing room. In the trailer laboratory all rats are subjected to more of the training and testing sounds than in Tolman. The colony room is windowless and is maintained on a diurnal light-dark schedule (lights on from 0600 to 1800 hr). All rooms are air-conditioned and maintained at a temperature of 74°.

Ann Hughes has been primarily responsible for the maintenance, training, and testing of the rats. She was assisted by Stephanie Rosenbaum in Exp. 1, and by Mark Lau in Exps. 3 and 4. Marie Hebert has removed the brains (as in the majority of the earlier experiments reported by Byrne and Samuel), and Edward Bennett has homogenized the brains, and with Hiromi Morimoto assisted in the isolation and injection of the brain supernatants.

All rats used were male rats received from Holzman Laboratories, Madison, Wisconsin. Table I presents some "vital statistics" for these experiments.

Behavioral Treatment of Donors and Recipients

Since subtle differences in training and testing may influence the outcome of transfer experiments, the protocol for the donors of a typical experiment is given in Table II. The main deviations from this protocol were in EB-1, where the trained donors were recipients from an earlier experiment. In this experiment, rats which had a previous left dominance were trained as left donors, and those with a right dominance were trained for right donors. The naive donors were previously unused, younger animals, as in all other experiments of this group. Variations in the type of cages in which the animals were housed during training are also noted in Table I. Only in EB-1 and EB-4 were wire cages available for all rats. The plastic cages were translucent polypropylene cages which did not allow the rat to see out the sides.

The protocol for recipients is given in

Table I. Summary of experimental conditions of four experiments attempting to modify behavior by brain injections.

Experiment		EB-1	EB-2	EB-3	EB-4
Location		Tolman	Bldg. 74T	Bldg. 74T	Bldg. 74T
Types of cases: Donors		EC;[a] wire	EC; plastic	EC; plastic	EC; wire
Recipients		EC; wire	EC; plastic	EC; wire	EC; wire
Date and hour of sacrifice		Sept. 19, 1966	Nov. 7, 1966	Dec. 5, 1966	Feb. 1, 1967
		1740-1950	1830-2045	1700-1900	1630-1925
Time of injections		2025-2135	2145-2245	2000-2030	2000-2100
Age of donors on arrival (days)		70[b]	39	40	38
Age of donors at sacrifice (days)		83	57	60	57
Weight of donors at sacrifice (g):	(trained)	287	191	190	176
	(naive)	200	182	174	159
Age of recipients on arrival (days)		37	39	37	44
Age of recipients on injection		44	50	49	50
Weight at injection (g)		141	171	155	159
"85%" Weight (g)		143	162	156	160
No. of potential recipients		49	50	57	57
No. of recipients used		36	36	36	43
Time of test sessions (hr after inj.)[c]					
Unreinforced	1	13	12	13	12
	2	17	18	18	18
Reinforced	1	41	41	43	42
	2	65	65	67	66
	3	90	89	90	90
Feeding schedule (g after test)					
Unreinforced	1	0	0	0	0
	2	8	8	8	8
Reinforced	1	8	8	8	8
	2	8	8	8	7
	3	8	8	8	7

a. EC cages are large wire cages housing up to 24 rats and filled with rat "toys."
b. The naive donors for this experiment were 44 days of age on arrival and were 51 days at sacrifice.
c. In the IR series of experiments, reinforced test sessions were substituted for the first two unreinforced sessions, and they were given approximately 20 and 45 hr after injection.

Table II. Protocol for donors.

Donors received at 40 days of age (72 rats)	
Day 1:	Groups weighed, tagged, placed 24 to a cage in large Environmental Complexity (EC) cages. Given terramycin in water. Food ad lib.
Day 2:	Allowed to explore for 20 min in groups of about 12 in Hebb-Williams maze (Mazed).
Day 3:	Weighed. Given terramycin in water.
Day 4:	Mazed.
Day 5:	Weighed.
Day 6:	Mazed.
Day 7:	Weighed. Food is removed after weighing. The 85% weight is calculated individually. During subsequent training, supplemental food is provided to prevent loss of weight below this value on an individual basis.
Day 8:	Mazed. Rats are assigned to the appropriate group and housed in individual wire cages (note exceptions in Table I). Assignment includes particular training box (A, B, C, or D) as well as side of training. Rats to be trained are given group sessions for 15 min in training chamber; these sessions are unrewarded. Group sessions use 3 rats at a time. Ten pellets are placed in food cup. The purpose of these sessions is to familiarize the rat with training situation. Naive donors are never placed in test chamber. They are also housed in individual wire cages. Food allotment matched to rats being trained.
Days 9-12:	Begin hand shaping of rats. Rats are placed individually in appropriate training chamber for 20 min. During the first 5 min the rat is watched and pellets are manually dispensed when it is near the food cup or about to press a lever. The purpose is to familiarize the rat with the noise of the pellet dispenser, to teach it that food can be obtained in the box, etc. This procedure greatly facilitates subsequent training. Hand shaping continues on an individual basis until all animals have learned to press the bar. In some cases, "stupid" rat may require several shaping sessions.
Day 13:	Training begins. On the first day a rat is rewarded on a 1 to 1 reward schedule. That is, it gets 1 pellet every time it presses the correct bar. Training sessions are 20 min. Seven g of food are given after training sessions (avoid giving food immediately after session).
Days 14-20:	Each day the reward schedule is increased by 1, until finally 8 presses are required to receive a food pellet. Animals are weighed daily, and given sufficient food in addition to the allotment (7 g decreasing to 4 g) routinely given to keep weight above 85% of initial weight. Training sessions are randomized with respect to left group being trained first or right group being trained first. Some sessions are given at night.

Table III. Main deviations from this protocol were the number of days prior to injection that the rats were received. This varied from 7 in EB-4 to the more desired 11 or 12 in EB-2 and EB-3 (see Table I). Recipients were housed in plastic cages in EB-2. In all other experiments, wire cages were available.

Table III. Protocol for recipients.

Recipients received at 40 days of age, about 12 days prior to planned injection. A 30% excess of potential recipients was obtained.	
Day 1:	Weighed and tagged. Placed 24 to a cage in large Environmental Complexity (EC) cages. Given terramycin in water. Food ad lib.
Days 2, 4, 6:	Allowed to explore for 20 min in groups of 12 in Hebb-Williams maze.
Days 3, 5, 7:	Weighed. Also given terramycin on Day 3.
Day 8:	Mazed and weighed. "85%" weight calculated. Placed in individual cages and given 3 g food/rat.
Day 11:	Given 15 min unrewarded group sessions in testing box, 3 rats/group. Five g food/rat on return to cage.
Day 12:	Given unrewarded single 10 min sessions in testing box. The food cup had 5 pellets. The number of left and right presses recorded. Rats with either very few (usually zero or one presses) or rats with many (more than 10) presses rejected. This session was given within 4 hr prior to injection. Rats were weighed. Rats were given 8 g of food after injection (but not immediately). Supplemental food given if below 85% weight.

Preparation and Injection of Brain Extract

In all experiments, the rats were sacrificed and injections were made in the late afternoon and early evening, as summarized in Table I. Donor rats had been trained during the morning and early afternoon. In EB-1 and EB-2, the right-trained donors were trained first; in EB-3, the left-trained donors were trained first, and in EB-4, training was alternated. The sacrifice and homogenization procedures were as follows: A left-trained donor was decapitated and the brain removed (by Marie Hebert). The brain was immediately placed in 6 ml of ice-cold 0.9% NaCl-0.01 M Tris, pH 7.5 in a Potter-Elvehjem homogenizer tube (10 ml capacity). This was timed, and required 60 to 75 seconds. A second left-trained donor trained in the same box was then immediately sacrificed and the brain removed and added to the first in the homogenizer. Homogenization of the two like trained brains was then begun with the Teflon pestle powered by a Sunbeam Mixmaster motor (full speed in EB-1 and EB-2, speed setting at "8" in EB-3 and EB-4). The homogenizer was cooled in a bath of ice water in EB-1 and EB-2, but not in EB-3 or EB-4. Complete dispersion required 40 seconds to 1 minute, as judged by a visual inspection of the layer of homogenate which passed between the Teflon pestle and the wall of the glass homogenizer tube. The homogenate was poured into an 11 ml polypropylene centrifuge tube (cooled in ice). An additional 2.0 ml of cold buffer was added to the homogenizer, homogenized briefly, and added to the first homogenate. Code assignment was made at this time and consisted of a letter (A, B, C, or D) designating the box in which the donors had been trained and a code number. (Naive rats were balanced for testing boxes.) While two brains were being homogenized, a pair of right-trained rats were being sacrificed and the brains were placed in a different homogenizer. These brains were homogenized while naive rats were sacrificed, etc. After 8 homogenized samples had been obtained (16 rats), they were centrifuged for 30 min at 8000 rpm (7700 × g max) in a Sorval RC2-B centrifuge, head SS34 at 0°. This process was repeated until all rats had been decapitated and the brains had been homogenized and centrifuged. The dates and times for this procedure are summarized in Table I. It required approximately 2 hours to sacrifice 72 rats in a typical experiment.

After the samples had been centrifuged, the supernatants were decanted into clean 50 ml polypropylene centrifuge tubes and stored in ice. Shortly thereafter, in rapid sucession, these supernatants were injected intraperitoneally into the naive recipients. The volume of the supernatant, essentially all injected, was usually 5 to 5.5 ml. New disposable 5-ml syringes and No. 22 gauge needles were used. The recipient rats were then immediately returned to their individual cages. They were designated by the same code number as the sample injected, i.e., A-1, B-2, etc., indicating box and order in which to be tested. In EB-1, EB-2, and EB-3, one half of the rats were assigned IR code numbers which indicated that a modified test schedule was to be used as described below. After all rats had

been injected, they were individually given 8 g of food and individually supplemental food if they were below the 85% weight. A record was kept of supplemental food.

Test Procedure

Two test procedures were used in EB-1, EB-2, and EB-3. One test procedure, termed the "normal" test procedure (also used in EB-4), was that described by Byrne and Samuel.[1] In this procedure the rats are given two unrewarded 10-min test sessions approximately 12 and 18 h after injection. In these sessions, the numbers of left and right presses are recorded, but no food reward is obtained by pressing. Most rats only press the levers one or two times during these sesions, and many do not press at all. After the second session, the rats were given 8 g of food and supplemental food if below 85% weight. On the three successive days, the 20-min reinforced test sessions are given. During these sessions, the rat is rewarded by a pellet of food whenever it presses either lever. The first lever pressed, the time of first press, the time to press the lever ten times, and the lever which becomes dominant (the one the rat routinely presses) are recorded. Eight g of food are routinely given after each session. In EB-4, this was reduced to 7 g in order to increase the motivation of the rat. The times of these test sessions after injection are summarized in Table I.

In EB-1, EB-2, and EB-3, another test procedure, termed "immediate reinforcement" (IR) was used for one-half of the recipients. In this procedure, in lieu of the two unreinforced 10-min sessions, 20-min reinforced sessions were given. The same measures were taken as for the reinforced sessions of the "normal" test procedure. Only after all test sessions are completed and TTL_{10}'s have been calculated and checked from recorder tape obtained during testing, are the code assignments and sources of trained brain compared.

Results and Discussion

The primary purpose of these experiments was to satisfy ourselves that we could repeat the observations of Byrne and Samuel, particularly in view of change of some personnel and of site of experiments. Once this objective had been attained, experimental procedures would be modified in a stepwise fashion to find more optimum conditions if possible for isolating and characterizing the active substance(s) influencing behavior. In the experiments of Byrne and Samuel, five to six recipients in each of the three groups were sufficient. In the experiments presented here, we could train about 48 donor rats, and with 24 naive rats, about 36 recipients could be utilized. Therefore, in the first three experiments, we tested about 1/2 of the recipients by a modified procedure which eliminated the first two unrewarded sessions (immediate reinforcement). We thought that the rewarded testing within one day after injection of the brain homogenate might give enhanced results. As will be seen, this procedure was even less successful than the normal procedure in differentiating recipient groups.

In Tables IV through VII we have summarized the TTL_{10} data (both corrected and uncorrected) for all recipients. Uncorrected TTL_{10} is the time the rat required from the beginning of the reinforced test sessions to press one bar 10 times. The corrected TTL_{10} is the time required to press one bar 10 times after the first press on either bar. The ranks of the recipient rats for the several comparisons that can be made are given as well as the sum of ranks. We have relied upon the Mann-Whitney U test (one-tailed) to test for significance of differences between groups.[2] Rats which failed to press were eliminated from any statistical tests. This relatively easy statistical test has been employed by Rosenblatt et al.,[3] and Byrne and Samuel. Certain of the comparisons between groups might be made more rigorously by other statistical tests, such as an analysis of variance.

Table VIII presents a summary of the various tests for significance of differences between groups for each experiment. These comparisons are made for all rats that learned and all rats that pressed, using both uncorrected and corrected TTL_{10}. The measure used by Byrne and Samuel was the corrected TTL_{10} of all rats that pressed, and it is this measure that we will focus on. However, similar conclusions regarding the outcome of these experiments would be obtained by consideration of the other measures.

In EB-1, the right-injected recipients did learn faster than left-injected recipients; the significance of difference between groups was at the 0.03 level. However, the right-injected rats did not differ from naive injected animals while naive injected rats learned somewhat better than left-injected. These latter two results were not in accord with previous observations.

EB-2 was the first experiment to be done in the trailer laboratory. In this experiment, rats learned more slowly than in EB-1, and many rats pressed but did not learn. Right-injected rats did learn faster than either naive or left-injected, but no significant differences between groups were obtained.

The pattern of learning times in EB-3

Table IV. "Time to learn" data obtained by normal test procedure in EB-1.

Recip. Code #	Donor Training	Corr. TTL_{10} (min)	Uncorr. TTL_{10} (min)	Rank on Corrected TTL_{10}								Rank on Uncorrected TTL_{10}							
				R vs L		R vs N		L vs N		L+R vs N		R vs L		R vs N		L vs N		L+R vs N	
Pressed & Learned																			
C-33	N	2.6	8.8				1		1		1				4		2		4
A-8	N	5.2	5.9				2		2		2				1		1		1
A-27	R	5.5	18.7	1		3				3		7		9				11	
C-32	R	5.8	6.4	2		4				4		1		2				2	
A-7	R	6.8	7.9	3		5				5		2		3				3	
C-18	N	7.6	9.0				6		3		6				5.5		3.5		5.5
D-24	N	8.5	9.0				7		4		7				5.5		3.5		5.5
B-12	R	10.6	11.7	4		8				8		3		7				7	
C-17	R	12.1	13.2	5		9				9		4		8				8	
D-34	L	14.1	14.6		6			5		10			5			5		9	
B-28	L	15.0	15.7		7			6		11			6			6		10	
A-9	L	20.8	24.5		8			7		12			8			7		12	
A-26	N	21.2	39.8				10		8		13				11		11		17
D-22	L	24.9	27.6		9			9		14			9			8		13	
B-10	L	27.6	28.9		10			10		15			11			10		15	
C-16	L	28.1	28.7		11			11		16			10			9		14	
D-23	R	30.8	31.7	12		11				17		12		10				16	
Σ Ranks				27	51	40	26	48	18	124	29	29	49	39	27	45	21	120	33
Pressed but did not learn																			
B-11	N	>60					12		12		18				12		12		18
Σ Ranks				27	51	40	38	48	30	124	47	29	49	39	39	45	33	120	51

Table V. "Time to learn" data obtained by normal test procedure in EB-2.

Recip. Code #	Donor Training	Corr. TTL_{10} (min)	Uncorr. TTL_{10} (min)	Rank on Corrected TTL_{10}								Rank on Uncorrected TTL_{10}							
				R vs L		R vs N		L vs N		L+R vs N		R vs L		R vs N		L vs N		L+R vs N	
Pressed & Learned																			
C-2	R	6.6	30	1		1			1			3		3				4	
B-3	N	9.3	28				2	1		2					2		2		3
A-1	R	10.6	15	2		3				3		1		1				1	
B-2	R	11.8	74	3		4				4		7		8				10	
D-5	N	17.6	38				5	2		5					5		3		6
C-1	L	21.8	27		4			3		6			2			1		2	
B-4	R	30.1	31	5		6				7		4		4				5	
A-5	L	31	48		6			4		8			5			4		7	
D-1	N	37	68				7	5		9					6		5		8
D-4	R	57	70	7		8				10		6		7				9	
Σ Ranks				18	10	22	14	7	8	39	16	21	7	23	13	5	10	38	17
Pressed but did not learn																			
B-1	L				9			8		13.5			9			8		13.5	
D-3	R			9		10.5				13.5		9		10.5			8	13.5	
A-3	N						10.5	8		13.5					10.5		8		13.5
A-4	N						10.5	8		13.5					10.5		8		13.5
C-4	N						10.5	8		13.5					10.5				13.5
A-2	L				9			8		13.5			9			8		13.5	
Σ Ranks				27	28	32.5	45.5	23	32	79.5	56.5	30	25	33.5	44.5	21	34	78.5	57.5
Did not press--not included in any statistics																			
D-2	L																		
C-3	L																		

Table VI. "Time to learn" data obtained by normal test procedure in EB-3.

Recip. Code #	Donor Training	Corr. TTL_{10} (min)	Uncorr. TTL_{10} (min)	Rank on Corrected TTL_{10}								Rank on Uncorrected TTL_{10}							
				R vs L		R vs N		L vs N		L+R vs N		R vs L		R vs N		L vs N		L+R vs N	
Pressed & Learned																			
D-3	R	4.2	7.9	1		1				1		2		2				2	
C-1	R	4.6	7.2	2		2				2		1		1				1	
B-4	N	7.6	8.3				3		1		3				3		1		3
D-2	N	8.5	12.0				4		2		4				5		3		5
B-2	N	18.7	8.5				5		3		5				4		2		4
D-1	R	24.9	32	3		6				6		3		6				6	
A-5	N	41.9	42.6				7		4		7				7		4		7
Σ Ranks						9	19		10	9	19			9	19			9	19
Pressed but did not learn																			
D-4	L				5.5			5		9.5			5.5			5		9.5	
C-2	L				5.5			6		9.5			5.5			6		9.5	
B-5	R			5.5		8				9.5		5.5		8				9.5	
A-4	L				5.5			7		9.5			5.5			7		9.5	
Σ Ranks				11.5	16.5	17	19	18	10	47	19	11.5	16.5	17	19	18	10	47	19
Did not press--not included in any statistics																			
A-1	R																		
A-2	L																		
A-3	N																		
C-3	L																		
Poor injection--eliminated																			
C-4	N	46	49																
B-3	R	Did not learn																	

was similar to EB-1; that is, right and naive injected rats both learned faster than left-injected. In this experiment, again a number of rats pressed but did not learn, and more than the usual number did not press at all. As a result, the resulting N in each group was smaller than desired.

Accordingly, for EB-4 it was decided that all recipients would be tested by the normal test procedure. In this experiment, no significant differences were obtained between any of the groups. Wire cages were available for all animals, as had been the case for the experiments in Tolman, yet the TTL_{10} for all rats that pressed was not significantly different from similar rats in EB-2 and EB-3 where plastic cages were used for some animals (Table XV).

In Tables IX through XII, TTL_{10}'s and Mann-Whitney U tests for significance between groups are summarized for the immediate test procedures used in EB-1 through EB-3. No significant differences between groups were obtained by this procedure.

In Table XIII we have summarized the tests of significance obtained between groups when data obtained from rats that learned in all four normal test procedures are combined. While this method of treating the data should be viewed with caution, no significant differences between groups was evident. (With the larger N obtained, the Mann-Whitney U had to be transformed into a z score, and by use of appropriate tables, into a P value. [3]) Rosenblatt et al. have suggested that using the best 50% of the animals in each group may be a more valid indicator of a successful "transfer." Even by this technique, no significant differences were found.

In Table XIV, we have summarized the average TTL_{10} of all rats that learned for each experiment. Considerable variation is to be noted from experiment to experiment. The rats in EB-1 learned significantly faster than those in EB-2 or EB-4 (Table XV). The TTL_{10} of the rats in the other experiments did not differ significantly. When the right-injected groups are compared to left- and naive-injected groups using the combined data from all four experiments, very little difference in average learning time is noted.

We have not been able to find a relationship between the dominance (final bar

Table VII. "Time to learn" data obtained by normal test procedures in EB-4.

Recip. Code #	Donor Training	Corr. TTL_{10} (min)	Uncorr. TTL_{10} (min)	Rank on Corrected TTL_{10}								Rank on Uncorrected TTL_{10}							
				R vs L		R vs N		L vs N		L+R vs N		R vs L		R vs N		L vs N		L+R vs N	
Pressed & Learned																			
A-10	L	3.4	24.2		1			1		1			9			7		10	
A-9	R	3.6	25.2	2		1				2		10		6				12	
C-10	N	3.9	39.6				2		2		3				11		13		19
D-3	L	4.4	5.5		3			3		4			1			1		1	
D-10	L	5.1	9.1		4			4		5			5			4		5	
B-7	L	5.4	7.6		5			5		6			4			3		4	
B-10	L	5.5	7.3		6			6		7			3			2		3	
D-9	R	5.6	6.8	7		3				8		2		1				2	
B-9	N	6.7	15.2				4		7		9				3		5		7
B-6	N	8.9	25.1				5		8		10				5		8		11
B-2	L	11.3	26.6		8			9		11			11			9		13	
D-1	N	11.8	38.6				6		10		12				10		12		18
C-11	R	13.7	15.1	9		7				13		6		2				6	
C-4	L	17.4	42.6		10			11		14			15		12	14		20	
D-5	R	19.0	22.2	11		8				15		7		4				8	
A-7	L	19.7	67.0		12			12		16			19			17		25	
A-5	L	20.6	22.8		13			13		17			8			6		9	
B-4	R	21.4	66.1	14		9				18		18		14				24	
D-6	N	24.6	31.4				10		14		19				8		10		15
B-8	R	26.2	31.2	15		11				20		12		7				14	
C-6	N	26.5	67.8				12		15		21				15		18		26
C-5	R	30.1	35.1	16		13				22		13		9				16	
D-4	L	32.9	36.2		17			16		23			14			11		17	
C-1	L	43.3	46.6		18			17		24			16			16		22	
A-4	N	44.0	45.8				14		18		25						15		21
B-5	R	51.4	53.5	19		15				26		17		13				23	
A-6	R	54.6	75.5	20		16				27		20		16				27	
Σ Rank:				113	97	83	53	97	74	279	99	105	105	72	64	90	81	261	117
Pressed but did not learn																			
A-11	N						20		21.5		32.5				20		21.5		32.5
B-1	N						20		21.5		32.5				20		21.5		32.5
C-8	L				24			21.5		32.5			24			21.5		32.5	
C-2	N						20		21.5		32.5				20		21.5		32.5
C-7	R			24		20				32.5		24		20				32.5	
D-8	R			24		20				32.5		24		20				32.5	
A-1	R			24		20				32.5		24		20				32.5	
B-3	L				24			21.5		32.5			24			21.5		32.5	
D-2	R			24		20				32.5		24		20				32.5	
D-7	L				24			21.5		32.5			24			21.5		32.5	
Σ Ranks				209	169	163	113	161.5	138.5	506.5	196.5	201	177	152	124	153.5	145.5	488.5	214.5

Did not press--not included in any statistics

A-2	L
C-3	R
A-8	N
C-9	R

Escaped and got food during testing--not included in any statistics

A-3	N
D-11	N

Table VIII. "Normal" test procedure. Summary of tests for significance of differences by Mann-Whitney U Test.

Expt.	Comparison[a]	Rats that learned: Corr. TTL_{10} U	Corr. TTL_{10} P	Uncorr. TTL_{10} U	Uncorr. TTL_{10} P	Comparison	Rats that pressed: Corr. TTL_{10} U	Corr. TTL_{10} P	Uncorr. TTL_{10} U	Uncorr. TTL_{10} P
EB-1	R(6)[b] vs L(6)	6	0.03	8	0.07	R(6)[b] vs L(6)	6	0.03	8	0.07
	R(6) vs N(5)[b]	11	0.27	12	0.33	R(6) vs N(6)[b]	17	0.47	18	0.53
	L(6) vs N(5)[b]	3	0.02	6	0.06	L(6) vs N(6)[b]	9	0.09	12	0.20
	R+L(12) vs N(5)[b]	14	≈0.05	18	>0.05	R+L(12) vs N(6)	26	>>0.05	30	>>0.05
EB-2	R(5) vs L(2)	3	0.29	4	0.43	R(6) vs L(4)	6	0.13	9	0.30
	R(5) vs N(3)	7	0.5	7	0.5	R(6) vs N(6)	11.5	0.18	12.5	0.22
	L(2) vs N(3)	2	0.4	2	0.4	L(4) vs N(6)	11	0.46	11	0.46
	R+L(7) vs N(3)	10	0.5	10	0.5	R+L(10) vs N(6)	24.5	>>0.05	23.5	>>0.05
EB-3	R(3) vs L(0)	--	--	--	--	R(4)[b] vs L(3)	1.5	≈0.09	1.5	≈0.09
	R(3) vs N(4)	3	0.20	3	0.20	R(4) vs N(4)[b]	7	0.44	7	0.44
	L(0) vs N(3)	--	--	--	--	L(3) vs N(4)[b]	0	0.03	0	0.03
	R+L(3) vs N(4)	3	0.20	3	0.20	R+L(7) vs N(4)	9	0.21	9	0.21
EB-4	R(9) vs L(11)[b]	31	≈0.06	39	>>0.05	R(13) vs L(14)[b]	64	>0.05	72	>>0.05
	R(9) vs N(7)	25	>>0.05	27	>>0.05	R(13) vs N(10)	58	>>0.05	61	>>0.05
	L(11) vs N(7)	31	>>0.05	24	>>0.05	L(14) vs N(10)	56.5	>>0.05	49.5	>>0.05
	R+L(20) vs N(7)	69	>>0.05	51	>>0.05	R+L(27) vs N(10)	128.5	>>0.05	110	>>0.05

a. No. in ( ) after letter designating donor training indicates number of recipients.
b. Designates the better group when the significant level of difference is 0.1 or better by the Mann-Whitney U Test (one-tailed).

Table IX. "Time to learn" data obtained by immediate reinforcement test procedure in EB-1.

Recip. Code #	Donor Training	Corr. TTL_{10} (min)	Uncorr. TTL_{10} (min)	Rank on Corrected TTL_{10}: R vs L	R vs N	L vs N	L+R vs N	Rank on Uncorrected TTL_{10}: R vs L	R vs N	L vs N	L+R vs N
Pressed & Learned											
C-13	L	6.0	7.1		1	1	1		1	1	1
C-15	R	8.0	9.2	2	1		2	2	1		2
A-3	N	8.6	10.7		2	2	3		2	2	3
D-19	R	9.0	33.3	3	3		4	9	11		14
B-30	R	9.1	11.2	4	4		5	3.5	3		4
C-31	L	9.8	11.2	5		3	6	3.5		3	5
B-6	R	10.6	32.9	6	5		7	8	10		13
B-5	N	10.7	16.4		6	4	8		4	4	6
C-14	N	12.0	19.2		7	5	9		6	5	8
D-20	N	12.9	32.0		8	6	10		9	8	12
D-36	R	14.0	18.5	7	9		11	5	5		7
A-1	R	26.5	30.7	8	10		12	7	7		10
A-2	L	27.2	29.7	9		7	13	6		6	9
B-29	N	27.7	40.0		11	8	14		12	10	16
A-25	L	29.0	35.2	10		9	15	10		9	15
D-35	N	30.6	32.0		12	10	16		8	7	11
Σ Ranks:				30	25 32 46	20	35 76	60	35.5 19.5 37 41	19	36 80 56
Pressed but did not learn											
D-21	L				11	11	17		11	11	17
B-4	L				12	12	18		12	12	18
Σ Ranks:				30	48	43	35 111	60	35 43	42	36 115 56

Table X. "Time to learn" data obtained by immediate reinforcement test procedure in EB-2.

Recip. Code #	Donor Training	Corr. TTL_{10} (min)	Uncorr. TTL_{10} (min)	Rank on Corrected TTL_{10}								Rank on Uncorrected TTL_{10}							
				R vs L		R vs N		L vs N		L+R vs N		R vs L		R vs N		L vs N		L+R vs N	
Pressed & Learned																			
D-9	R	5.6	8.3	1		1				1		1		1				1	
C-9	L	11.8	17.1		2			1		2			3			2		3	
A-6	L	14.0	14.7		3			2		3			2			1		2	
A-9	N	19.5	24.6				2		3		4				2		3		4
C-8	R	26.2	37.0	4		3				5		4		4				6	
D-6	N	29.6	34.9				4		4		6				3		4		5
B-8	R	53.2	75.4	5		5				7		7		5		5		9	
B-5	L	66.9	69.6		6			5		8			5					7	
C-5	R	73.8	74.1	7		6				9		6		6				8	
Σ Ranks:				17	11	15	6	8	7	35	10	18	10	16	5	8	7	36	9
Pressed but did not learn																			
B-9	N						9.5		8.5		13.5				9.5		8.5		13.5
D-8	N						9.5		8.5		13.5				9.5		8.5		13.5
D-7	L				9.5			8.5		13.5			9.5			8.5		13.5	
C-7	N						9.5		8.5		13.5				9.5		8.5		13.5
B-7	R			9.5		9.5				13.5		9.5		9.5				13.5	
B-6	L				9.5			8.5		13.5					9.5	8.5		13.5	
A-7	N						9.5		8.5		13.5		9.5				8.5		13.5
A-8	R			9.5		9.5				13.5		9.5		9.5				13.5	
Σ Ranks:				36	30	34	44	25	41	89	64	37	29	35	43	25	41	90	63
Did not press--not included in any statistics																			
C-6																			

Table XI. "Time to learn" data obtained by immediate reinforcement test procedure in EB-3.

Recip. Code #	Donor Training	TTL_{10} (min)	Uncorr. TTL_{10} (min)	Rank on Corrected TTL_{10}								Rank on Uncorrected TTL_{10}							
				R vs L		R vs N		L vs N		L+R vs N		R vs L		R vs N		L vs N		L+R vs N	
Pressed & Learned																			
B-10	L	0.5	8.8		1			1		1			3			1		3	
A-3	L	3.4	25.7		2			2		2			5			7		9	
D-2	R	4.6	6.3	3		1				3		1		1				1	
C-1	L	5.7	59.2		4			3		4			9			12		15	
A-1	R	6.6	8.1	5		2				5		2		2				2	
D-3	N	8.2	9.8				3		4		6						2		4
A-4	N	9.0	11.5				4		5		7				3		3		5
C-3	N	14.0	14.8				5		6		8				4		4		6
D-4	L	16.5	19.2		6			7		9			4		5	5		7	
D-5	N	21.2	22.1				6		8		10						6		8
B-3	L	26.1	28.8		7			9		11			6		6	8		10	
D-1	L	34.3	39.4		8			10		12			7			9		11	
C-2	N	42.1	54.7				7		11		13				8		10		13
C-4	R	47.0	47.5	9		8				14		8		7				12	
B-1	N	53.7	54.8				9		12		15				9		11		14
Σ Ranks:				17	28	11	34	32	46	61	59	11	34	10	35	42	36	70	50
Pressed but did not learn																			
B-4	L				11.5			13		17.5			11.5			13		17.5	
C-5	R			11.5		11				17.5		11.5		11				17.5	
A-2	R			11.5		11				17.5		11.5		11				17.5	
B-2	R			11.5		11				17.5		11.5		11				17.5	
Σ Ranks:				51.5	39.5	44	34	95	46	131	59	45.5	45.5	43	35	55	36	140	50

Table XII. Immediate reinforcement test procedure. Summary of tests for significance of differences by Mann-Whitney U-Test.

Expt.	Comparison†	Rats that learned: Corr. TTL_{10} U	Corr. TTL_{10} P	Uncorr. TTL_{10} U	Uncorr. TTL_{10} P	Comparison	Rats that pressed: Corr. TTL_{10} U	Corr. TTL_{10} P	Uncorr. TTL_{10} U	Uncorr. TTL_{10} P
EB-1	R(6) vs L(4)	9	0.30	9.5	0.34	R(6)* vs L(6)	9	0.09	14.5	0.32
	R(6) vs N(6)	11	0.16	16	0.41					
	L(4) vs N(6)	10	0.38	9	0.30	L(6) vs N(6)	14	0.29	15	0.35
	L+R(10) vs N(6)	21	>>0.05	25	>>0.05	L+R(12) vs N(6)	33	>>0.05	35	>>0.05
EB-2	R(4) vs L(3)	5	0.43	4	0.31	R(6) vs L(5)	15	0.53	14	0.46
	R(4) vs N(2)	3	0.40	2	0.27	R(6) vs N(6)	13	0.24	14	0.29
	L(3) vs N(2)	2	0.27	2	0.40	L(5) vs N(6)	10	0.21	10	0.21
	L+R(7) vs N(2)	7	0.56	6	0.41	L+R(11) vs N(6)	23	>>0.05	24	>>0.05
EB-3	R(3) vs L(6)	7	0.36	5	0.19	R(6) vs L(7)*	11.5	0.10	17.5	0.34
	R(3) vs N(6)	5	0.19	4	0.13	R(6) vs N(6)	13	0.24	14	0.29
	L(6) vs N(6)	11	0.15	15	0.35	L(7) vs N(6)	17	0.31	15	0.22
	R+L(9) vs N(6)	16	>>0.05	25	>>0.05	R+L(13) vs N(6)	38	>>0.05	29	>>0.05

†No. in ( ) after letter designating donor training indicates number of recipients.

*Designates the better group when the significant level of difference is 0.1 or better by the Mann-Whitney U-test (one-tailed).

Table XIII. Summary of Mann-Whitney U Tests for four experiments combined.

Significance of differences between groups for all recipients that pressed[a]

Comparison (No. of recipients in parentheses)	U	z	P
R(29) vs L(27)	349	0.70	0.24
R(29) vs N(26)	369	0.13	0.45
L(27) vs N(26)	318	0.59	0.28

Significance of differences between groups for best 50% of each group

	U	P	Critical value for P=.05
R(14) vs L(13)	65	NS	56
R(14) vs N(13)	85	NS	56
L(13) vs N(13)	63	NS	51

a. The average TTL_{10}'s of the "learners" were R, 19.4 min; L, 18.5; and N, 16.4. The average TTL_{10}'s for the "top 50%" were 8.6, 12.6, and 9.0 min respectively.

Table XIV. Average "Time to learn" data obtained by normal test procedure; individual and combined experiments.

Expt.	Donor training	Numbers of rats: Learned	Pressed but did not learn	Did not press	Average TTL_{10} of learners (min)
EB-1	R	6	0	0	11.9
	L	6	0	0	21.8
	N	5	1	0	9.0
	Totals	17	1	0	14.5
EB-2	R	5	1	0	31.4
	L	2	2	0	26.3
	N	3	3	2	21.5
	Totals	10	6	2	27.4
EB-3	R	3	1	1	11.2
	L	0	3	2	--
	N	4	0	1	19.2
	Totals	7	4	4	15.8
EB-4	R	9	4	2	25.1
	L	11	3	1	15.4
	N	7	3	1	18.1
	Totals	27	10	4	19.3
EB-1 through EB-4 Combined	R	23	6	3	19.4
	L	19	8	5	18.5
	N	19	7	2	16.4

Table XV. Comparison of differences of TTL_{10} of all rats that pressed between experiments.

Experiments compared (No. of rats)	Mann-Whitney U	z	P	Critical value for P of .05
EB-1(18)[a] vs EB-2(16)	66		0.01	
EB-1(18)[a] vs EB-3(11)	72		>0.05	61
EB-1(18)[a] vs EB-4(37)	244	1.59	0.06	
EB-2(16) vs EB-3(11)	74		>0.05	54
EB-2(16) vs EB-4(37)	239	1.11	0.14	
EB-3(11) vs EB-4(37)	198	0.1	0.45	

a. Indicates faster learning group when significant at the 0.1 level by the Mann-Whitney U-test (one-tailed).

preference) of these rats and the source of injected material. In fact, in EB-3 and EB-4 nearly all rats were right-dominant.

In conclusion, in four experiments in which 61 rats learned and 21 additional rats pressed but did not learn, we have not been able to find any consistent evidence that brains from right-trained rats are able to improve the learning time of injected rats. The reasons for our failure to replicate the observations of Byrne and Samuel are unknown at this time. For the present, we are not planning further replications of this type of experiment.

References

1. W. L. Byrne and D. Samuel, UCRL-17135; submitted to Science.
2. S. Siegel, Nonparametric Statistics for the Behavioral Sciences (McGraw Hill Book Co., New York, 1956). In calculating U, we have not corrected for tied ranks. This correction would reduce the significance of difference between groups.
3. F. Rosenblatt, J. T. Farrow, and S. Rhine, Proc. Natl. Acad. Sci. U. S. 55, 548, 787 (1966).

17. EXPERIMENTAL COMPLEXITY, CEREBRAL CHANGE, AND BEHAVIOR†

Mark R. Rosenzweig,* Edward L. Bennett, Marian C. Diamond,‡
Hiromi Morimoto, Ann Orme, and Marie Hebert

Abstract

Three main topics are discussed in this paper:

(a) The evidence that even moderate enrichment of the environment of colony rats will benefit their problem-solving ability;
(b) New results concerning the chemical and anatomical plasticity of the brain as a consequence of enriched experience, and especially results on the time course of some of these changes;
(c) An interpretation of these cerebral effects, suggesting that in part they reflect the processes of consolidating the storage of memory.

Problem-Solving and Enriched Experience

Our previous findings that enriched experience improves problem-solving ability have now been strengthened and extended. In the 1965 Annual Report we reported results of experiments in which animals had one month of either enriched or impoverished experience before being tested on a visual reversal discrimination problem.[1] Animals in the enriched conditions (EC) lived in a group of twelve in a large cage provided with "toys," and they had daily exploration in a field with a new pattern of barriers each day. Animals in the impoverished condition (IC) lived in individual cages in an isolation room. The results for comparing EC with IC rats of two strains of rats are shown in Fig. 17-1 (left). In each strain the enriched-environment rats made significantly fewer errors than their deprived littermates. For the two strains combined, the difference between EC and IC animals was significant at beyond the 0.001 level of confidence.

Now, given such a difference between enriched and impoverished as that we reported last year, one can ask whether it is the enrichment that improves performance or the impoverishment that impairs it, or whether both kinds of effects occur. Similar questions had been asked about the cerebral effects of experience. We have sought in new experiments to investigate the behavioral problem just as we had the cerebral one--by using an intermediate group with normal colony experience. The SC (Social Control or Standard Colony) animals lived under usual colony conditions, three to a cage. After one month of either enriched or colony conditions, the littermates were given the visual reversal discrimination test. Figure 17-1 (center) shows the results. The EC/SC differences are almost as large as had been the EC/IC differences in the previous experiment. For the two strains combined, the enriched-experience animals perform better than colony littermates at beyond the 0.01 level of confidence.

In a further experiment, we gave enriched-experience and colony rats a battery of three successive tests--the Lashley III maze, the Dashiell checkerboard maze, and the visual reversal discrimination test (Fig. 17-1 (right). Here the first two tests showed relatively large differences in favor of the enriched-experience rats. Considering the two strains together, the EC were superior to the SC at beyond the 0.01 level on the Lashley test; on the Dashiell test the overall difference just missed being significant because of one S_3 EC animal that made an unusually poor score. By the time the rats reached the reversal discrimination test, however, they were all experienced problem-solvers, and there were no real differences left between the groups. Overall the errors on the reversal test in this experiment were only 60% as large as in the previous experiment. Due to its place in the battery, the reversal test no longer differentiated among the groups according to their previous condition. The initial tests, however, demonstrated again that one month of moderate enrichment improved the ability of rats over that of their brothers who had remained under colony conditions. Just as we previously proved that isolation is not necessary in order to produce cerebral differences from enriched animals, so now we can show that isolation is not required in these experiments to produce behavioral differences. The colony rat--the standard subject in so many behavioral experiments--can be improved significantly in problem-solving ability by experiencing only one month in a somewhat more complex environment.

Changes in the Brain with Experience

Methods

During the past six years we have been accumulating evidence that the brain changes in a number of ways as a consequence of experience. In most of these experiments, littermate rats have been assigned at weaning to either the enriched-experience or the

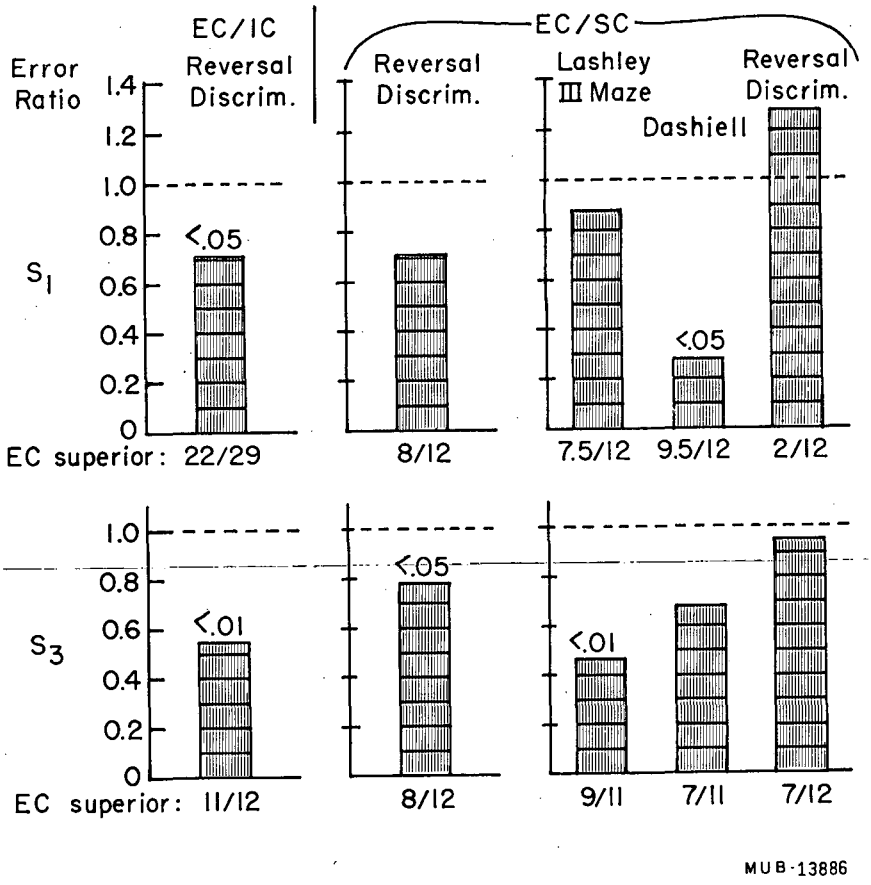

Fig. 17-1. Error ratios, enriched vs impoverished rats, for two behavioral tests. The left portion of the figure compares the error ratio of EC to IC, S_1 and S_3 rats on the reversal discrimination test; the center portion compares the error ratio of EC to SC rats; the right portion presents the results when EC and SC rats are given a series of different tests.

impoverished-experience condition. These conditions are as defined in the previous section, except that after the first month the enriched-experience animals receive one or two trials a day in a maze. We use in succession the Lashley, Dashiell, and Krech mazes. Since the animals are given training, we designate this condition as ECT. Both the ECT and the IC conditions provide food and water ad lib, and both last for 80 days. At the end of the 80-day period, the animals are sacrificed and the brains are analyzed chemically or anatomically. The animals are assigned at random to the conditions, and they are given code numbers that do not reveal their experimental treatment to the chemists or anatomists who perform the analyses.

Results

The brain changes measurably as a consequence of this differential experience. Table 17-I summarizes the changes that we have found in the occipital or visual region of the cerebral cortex; this region usually shows the largest effects. The changes are expressed as percentage differences between enriched-experience and impoverished-experience littermates. Next to each difference is indicated the probability that it could have arisen by chance and also the number of littermate pairs in which the ECT animal exceeded its IC littermate on the measure. The cortex is seen to gain significantly in weight and to increase by a similar amount in total protein.

Table 17-I. Effects of differential experience on visual cortex (difference between ECT and IC littermates of S_1 strain).

Measure	Difference (%)	P	No. ECT > IC
Weight	6.1	<0.001	106/141
Total protein	7.8[a]	<0.001	25/32
Depth	6.3	<0.001	36/41
Total AChE	2.3	<0.01	83/140
Total ChE	10.2	<0.001	77.5/98
No. neurons	-3.1	NS	7/17
No. glia	14.0	<0.01	12/17
Neuron area	13.4	<0.001	11.5/13

a. Weight difference 7.0% in these experiments.

(The increase in protein proves that the greater bulk of the enriched brains is synthesized material and not just water content, as has sometimes been suggested.) When anatomical sections of the brain are made, the depth of the cortex is found to grow by about the same percentage as the weight. Thus these three measures--wet weight, total protein, and depth--agree rather well in demonstrating that the enriched-experience rats develop more cortical tissue than do their deprived littermates. It should be noted that this increase in cortical bulk does not reflect a difference in body weight. On the contrary, at the end of the 80-day period the enriched-environment group weighs about 7% less than the impoverished-experience group.

Chemically, we have found differential effects in the activities of the enzymes acetylcholinesterase (AChE) and cholinesterase (ChE). Both enzymes increase in total activity as a consequence of enriched experience, but total AChE increases significantly less than does tissue weight, while ChE increase significantly more than tissue weight. In searching to understand this pattern of enzymatic changes, we realized that neurons contain more AChE than ChE, while glial cells contain more ChE than AChE. Therefore, we made counts of neurons and glial cells in the visual cortex, using an improved technique.[2] The results indicated that while the number of neurons per unit of area remains about the same, the glial cells proliferate in the enriched condition. We have also asked whether neuron cell bodies might increase in size, even though neurons do not increase in number. Our first results were negative,[2] but more recent measurements with higher magnification have given consistently positive results. The observed increase of 13% in area of the perikaryon indicates an increase of about 20% in its volume. This new finding is based on two experiments in which the experienced animal was observed to have larger perikarya in 11.5 out of 13 littermate pairs. The nucleus was seen to enlarge to about the same degree as the cell body. New experiments are now in progress to test further the exciting possibility that the nerve cell and its nucleus expand as opportunities for learning are provided.

Finally, we might mention two preliminary observations: First, in a single experiment we found increases in the diameter of cortical capillaries in the enriched-experience group.[3] This experiment is now being repeated. Secondly, there are the measurements of dendritic branching made by Dr. Ralph Holloway and by Dr. J. P. Schade on rats prepared in our laboratories. In two experiments Dr. Holloway has found indications that dendrites of neurons to enriched-experience animals branch and ramify more widely than do those of the impoverished-experience littermates. A third experiment on dendritic branching is now in progress. On the other hand, Dr. Schade has not found consistent differences in dendritic branching between ECT and IC animals, so final judgment on this variable must be reserved.

Cerebral Changes as Correlates of Stored Memory

Although not providing conclusive evidence, these results seemed to be consistent with the hypothesis that the observed cerebral changes reflect the long-term storage of memory in the brain. A number of investigators have speculated that learning induces neurons to strengthen existing synaptic connections or to develop new ones. Since many synaptic junctions are rich in AChE, an increase in synapses would probably entail an increase in total AChE activity. A neuron with a larger number of functional connections would require a more active cell body, and this might well demand an increase in size. More and more functions are being found for the glial cells, two well-acknowledged activities being to help nourish the neurons and to provide sheaths for neuronal branches. Either or both of these could account for the glial proliferation that we observe if neurons are increasing in activity and making new connections. The increased number of glia, increased size of perikarya, and perhaps also increases in capillary diameter and in neuronal branches could all help to account for the increased bulk of cortex. In sum, it was tempting to suppose that the cerebral effects we observed were correlates of memory storage. If this was true, then the following consequence should hold: The greater the opportunity animals have to learn, the greater will be the changes

in their brains. Recently we have attempted to test this deduction in the following form: The longer the duration of the differential environmental conditions, the greater the anticipated cerebral changes. For the measurements made so far, the hypothesis appears to be untenable, as we will show next.

Magnitude of Changes as Function of Duration of Experience

Varying the duration of the differential experience produced first a rise but then a fall in the magnitude of the cortical weight effect. Figure 17-2 indicates the development of cortical weight of rats put into our standard enriched or impoverished conditions at weaning (25 days of age) and then sacrificed at either 55 days, 105 days, or 185 days of age. The experiment of 30-day duration (sacrifice at 55 days) involved eleven S_1 litters, each litter supplying two rats to the enriched and two to the impoverished condition. Here there was 7.1% more total cortex in the brains of EC animals than in IC littermates. The effect fell to 4.1% in experiments of 80-day duration (sacrifice at 105 days). This result is based on thirteen "standard" ECT-IC experiments with 141 littermate pairs of S_1 rats. A further decrease to only 2.0% was observed when the animals remained in the ECT or IC environments for 160 days. This result is based on a single experiment with twelve littermate pairs of the S_1 strain. The results of the 30-day and 160-day experiments are not based on large numbers of rats, and further data may suggest some changes in the shapes of the curves. The main phenomenon is, however, corroborated by the results to be described next.

In a recent experiment, animals were placed in the differential environments at 60 days of age, and groups were sacrificed at 75, 90, 105, and 120 days (Table 17-II). In this experiment the enriched condition did not include any formal training. The 30-day effect is seen to be considerably larger than those of the shorter or longer periods, and the larger size of the 30-day effect is significant ($P<0.05$). Results of another experiment with only 30-day groups are also shown in the table. These two sets of 30-day results, plus the one illustrated in Fig. 17-2, are all larger than any of the effects for weight of total cortex that we have obtained in thirteen "standard" 80-day experiments. Further experiments are being done to define the time course more precisely, but we are already certain that the cerebral effects reach a peak and then descend.

Let us return briefly to the 160-day experiment for some further indications. This experiment included not only animals kept in the enriched and impoverished conditions

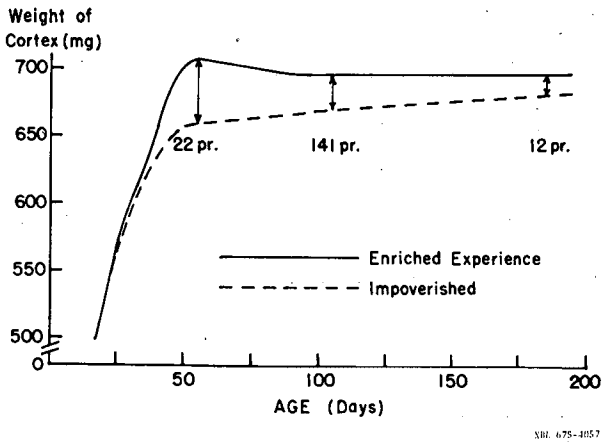

Fig. 17-2. Development of cortical weight of rats maintained in enriched or impoverished conditions from 25 days to 55, 105, and 185 days of age.

Table 17-II. Total cortical weight as function of duration of EC vs IC experience (S_1 rats, started at 60 days of age).

Experiment & N per group		Duration (days) 15	30	45	60
7465	EC	703	715	723	702
N=10	IC	682	669	696	681
	% diff.	3.1	6.9	3.9	3.1
	P	<0.05	<0.01	<0.01	NS
6819	EC	--	717	--	--
N=12	IC	--	660	--	--
	% diff.		8.7		
	P		<0.001		

throughout, but also littermates that spent either the first or the second 80 days in the colony condition and the other 80 days in the enriched condition. The design of the experiment is shown to the left in Table 17-III. Twelve litters each furnished one animal to each of the four conditions. The mean weights of total cortex are given in the right part of the table. Not too much should be made of these results, since none of the differences was statistically significant, but some trends may be noted. The animals that spent the second half of the experiment in the enriched condition (actually repeating the schedule of

Table 17-III. Weight of total cortex after four combinations of experimental conditions.

Age in days in different conditions		Cortical weight (mg)
25 to 105	106 to 185	
ECT	ECT	698
ECT	SC	699
SC	ECT	711
IC	IC	684

the first half) ended with the same cortical weight as the animals that spent the last 80 days in the colony condition. Apparently the continuation of the enriched condition was no more stimulating than the colony condition. Conversely, the animals that went from the colony condition to 80 days in the enriched condition had the greatest cortical weight. This group developed a cortical weight 3.8% greater than that of the impoverished animals--a difference very close to the 4.1% seen in our standard 80-day experiments. To make one more comparison, we might note that the second and third groups were both alike in receiving 80 days of enrichment and 80 days of colony life. Yet the order of the two treatments appears to have been important, since the group experiencing the enriched environment immediately prior to sacrifice had the greater amount of cortical tissue. Thus the indications from this experiment (although we must stress that they are not significant) are that it is novelty rather than complexity of the environment that induces the cortical effects.

We followed this experiment by two others in which some groups spent about 80 days in an extremely inpoverished environment and then were given 50 days in an enriched condition. Table 17-IV presents the design of these experiments and also the cortical weights. In both cases, the animals that had spent 80 days in extreme impoverishment and then 50 days in an enriched condition showed a rapid rise in cortical weight during the latter period. They yielded brain values like those of the rats that had spent the entire 130 days in the enriched condition; they differed significantly from the rats that remained in the impoverished condition throughout. In other words, the most recent environmental condition pretty well determines cortical weight, and the earlier condition leaves little if any trace--on this measure. The effects that must have been caused by the earlier treatments have disappeared during the later period.

What about the time course of measures other than cortical weight? In the rest of the

Table 17-IV. Effects of successive environments on weight of total cortex in two experiments.

Exper. & N per condition	Age in different conditions (days)		Cortical wt (mg)	P
4977	29 to 111	112 to 161		
	ECT[a]	---	719	<0.05
N=6	IEI[b]	---	687	
	ECT	ECT	730	<0.05
	IEI	IEI	692	<0.001
	IEI	ECT	751	
6379	26 to 110	111 to 159		
	EC[c]	EC	716	<0.05
N=10	IEI	IEI	686	<0.05
	IEI	EC	713	
	EC	IEI	695	

a. Enriched conditions with training, the "standard" ECT condition.
b. Isolated in extreme impoverishment.
c. Enriched condition, without training.

brain (or "subcortex") the 30-day experiments show small gains in favor of the enriched-experience animals, while the longer experiments show small losses (Table 17-V). The ratio of cortical weight to that of the rest of the brain has furnished particularly stable effects in the 80-day experiments. Since in the 30-day experiments subcortex as well as cortex gains in weight, the cortical/subcortical ratio does not show as large a percentage difference here as does cortical weight. Nevertheless, on the ratio measure also, as the bottom row in Table 17-V shows, the differences drop progressively as the experiments become longer in duration. Effects on total activities of AChE and ChE in all of these experiments follow time courses much like that of the weight effects. No histological results are as yet available from experiments of durations other than 80 days.

The discovery that the cerebral effects of experience are transitory poses a serious challenge to the hypothesis that these effects are correlates of memory traces. We had not adopted this hypothesis,[4] and our new evidence clearly opposes it. Both theoretical and empirical considerations indicate that transitory cerebral effects cannot be correlates of memory traces. Most learning theorists currently hold that consolidated memory traces should persist indefinitely, unless they are replaced by competing habits. That is, once a habit has been learned and consolidated, then either the originally learned material or a roughly

Table 17-V. Percentage differences in brain weights between enriched- and impoverished-experience S_1 littermates, for experiments of three durations.

Duration, days:	30	80	160
N (pairs):	22	141	12
Total cortex	7.1[a]	4.1[a]	2.0
Rest of brain	1.2	-1.1[b]	-2.8[c]
Total cortex / Rest of brain	5.8[a]	5.3[a]	4.9[a]

a. $P < 0.001$.
b. $P < 0.01$.
c. $P < 0.05$.

equivalent replacement should continue to be present. Empirically, we know that rats and other animals can remember habits for months, with little decrement. Not only should the rats in the complex condition retain what they have learned, but they should also be learning new material. Recall that after the first month they are run in three maze apparatuses. Nevertheless, the cerebral differences distinguishing them from the impoverished animals are declining at the same time.

Cerebral Changes as Correlates of the Processes of Memory Storage

If the temporary changes that occur in the brain as consequences of experience cannot be correlates of memory traces, can they be related in some more tenable way to the mechanisms of learning and memory? We would like to propose that the changes that wax and wane may be correlates of the processes of consolidation of memory. During the time when learning is occurring and stable traces (of some sort) are being laid down in the brain, temporary modifications of brain tissue may well arise in order to support these processes. This should be true whether one adopts a "connectionistic" approach (as we are inclined to do), or whether one takes the approach of "molecular psychobiology" and supposes that learning involves chiefly the formation of altered ratios of chemical products within the nerve cells. In either case the necessary increases in metabolic and synthetic activities would require more work of nerve cells and more support in terms of metabolic supplies. Enlargement of cell bodies and proliferation of the surrounding glial cells would be consistent with this picture. Once learning was completed and the resultant processes of consolidation had subsided, then the changes needed to support this extra activity would regress, and only the correlates of long-term memory would remain to differentiate the trained from the untrained brain.

Temporary brain changes that occur during learning could provide valuable guides to further studies of the mechanisms of long-term memory storage. They could indicate the locations and the relative magnitudes of active processes of consolidation. Regions of major temporary changes would seem to be the most promising sites at which to search for permanent chemical or anatomical modifications related to memory storage. The painstaking studies of dendrite branching, for example, are being done at the occipital cortex because this is the region that shows the largest transient changes in cortical weight and enzymatic activities. It is also conceivable that there are both temporary and permanent components of the increases in neuronal size and glial number. That is, although the changes diminish between 30 and 160 days, permanent effects might nevertheless be found in experiments of longer duration. Figure 17-3 illustrates schematically three possible patterns of change--(a) permanent, (b) permanent plus temporary, and (c) temporary alone. At present we may speculate which measures follow each pattern. Thorough investigations of the time courses of changes in each of our measures will be required to determine which, if any, of these patterns actually describes the particular variable.

A reasonable objection to our interpretation, as stated thus far, should be considered here. This is the argument that, according to the hypothesis, the cerebral differences should not regress in our experiments, since one group continues to have new experiences while the other group remains in a uniform, impoverished environment. To answer this objection, we must give some further information and confess that the enriched environment does not present much that is novel after the first few weeks. The toys in the cage are drawn from a rather limited pool, and all soon become familiar. The pattern of barriers in the open field is changed daily, but some animals nevertheless go to sleep before their half-hour is over. Social relations among the group probably tend to stabilize early. Observation indicates that the animals are more active in the early weeks of the enriched situation than later. (Nor is this solely an effect of aging, for it is also seen among rats introduced to the experiment as young adults at 105 days of age.) Another indication that the animals soon habituated to the daily environmental changes was obtained by one of our students, Mr. William Love. Love found, in an experiment now being repeated, that 4 hours a day in the enriched environment was as effective as 24

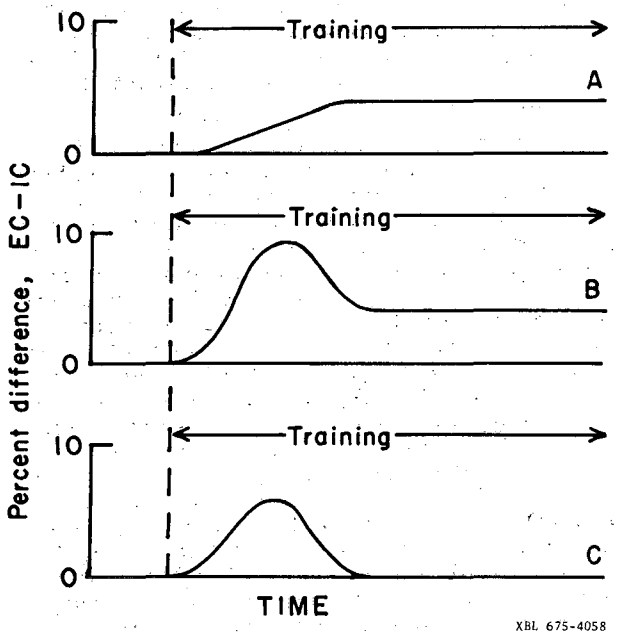

Fig. 17-3. Schematic representation of three possible patterns of brain change as a consequence of training: (a) permanent; (b) permanent plus temporary; and (c) temporary alone.

hours a day for producing cerebral changes. It should be easy to increase the complexity and variety of the experimental conditions. We believe not only that introducing greater novelty should increase the amplitude of the cerebral effects, but that, if opportunities for new learning are continually introduced, this should also prolong the "consolidation state" of the brain. Experiments to test these deductions are now projected.

Conclusion

In conclusion, the three main points are:

(a) The problem-solving ability of the colony rat can be improved significantly by giving it a month's experience in a somewhat more complex environment.

(b) An enriched environment leads to a number of measurable changes in the anatomy and chemistry of the brain. The changes whose time course we have followed reach a peak after about 30 days of enriched experience and then decline. Because these changes are now seen to be transitory, they cannot reflect stored memory.

(c) We propose instead that the transitory changes may reflect the processes of consolidation of memory. Localization of such processes may guide us to finding the mechanisms of permanent storage of memory.

Footnotes and References

†Paper was presented in Symposium on "The Role of Experience in Intellectual Development," AAAS Meeting, Washington, D. C., December 30, 1966.

*Department of Psychology, University of California, Berkeley, California.
‡Department of Physiology-Anatomy, University of California, Berkeley, California.

1. Edward L. Bennett, Marie Hebert, Hiromi Morimoto, and Ann Orme, Heredity, Environment, Learning, and the Brain in Chemical Biodynamics Annual Report, UCRL-16806, March 1966, p. 34.
2. M. C. Diamond, F. Law, H. Rhodes, B. Lindner, M. R. Rosenzweig, D. Krech, and E. L. Bennett, Increase in Cortical Depth and Glia Numbers in Rats Subjected to Enriched Environment, J. Comp. Neurol. 128, 117 (1966).
3. M. C. Diamond, D. Krech, and M. R. Rosenzweig, The Effects of an Enriched Environment on the Histology of the Cerebral Cortex, J. Comp. Neurol. 123, 111 (1964).
4. E. L. Bennett, M. C. Diamond, D. Krech, and M. R. Rosenzweig, Chemical and Anatomical Plasticity of Brain, Science 146, 610 (1964).

18. ORGANIC DEPOSITS FROM MUD LAKE, FLORIDA

Eugene D. McCarthy and William Van Hoeven

Introduction

The richly organic algal ooze from Mud Lake, Florida, has recently been considered to represent a modern-day precursor of oil shales of the type exemplified in the Green River Formation.[1] Microscopic characteristics of the oil shale of the Green River Formation and its fossil micro-organisms indicate that the precursor of such oil shales might indeed be such an algal ooze, accumulating gradually in shallow lakes. The theory that algal oozes could give rise to oil shales is not new. Algae have less cellulose and a correspondingly greater proportion of fats and soaps. The contemporary alga Botryococcus is present in microscopic remains in organic oozes. To complement this geological and paleobotanical evidence, the organic geochemist can isolate and identify the constituents of the genera of the blue-green algae known to be present in Mud Lake, and compare them with the organic compounds isolated and identified in Mud Lake and at a later stage of "diagenetic" degradation in the Green River Formation. (Diagenesis = alteration taking place on organic constituents after deposition.) A comparison of the findings from these sources would, if the algal ooze precursor theory is justified, represent the detailed and precise analysis of the changes taking place at the molecular level from the contemporary genera of blue-green algae, through the post-Pleistocene deposits of the Mud Lake deposits, to the Eocene Period of the Green River Formation. This report represents our preliminary findings.

Experimental Procedure

The samples from the Mud Lake Deposits were kindly supplied by Dr. W. H. Bradley of the United States Geological Survey, Washington. Mud Lake is 1 mile in diameter and 2 to 3 feet deep. The algal ooze is 3 feet thick; underneath this algal ooze is a layer of peat.

Samples for analysis are designated as:
MW-O = Mud Lake algal ooze at the mud-water interface,
MW-1→6 = Mud Lake algal ooze at 1→6 feet, respectively, below the mud-water interface.

1. The elemental analyses of the various levels are indicated as:

Constituent	MW-O (%)	MW-2 (%)	MW-3 (%)	MW-6 (%)	Oil shale (%)
C	40.06	40.36	41.17	52.20	80.50
H	6.39	6.45	6.87	5.32	10.30
O					5.75
N	4.16	3.82		1.39	2.39
S	1.13	2.62		2.59	1.04
Ash				11%	

2. The C^{14} ages of the sediments are:

MW-1	1900 ± 200 years
MW-3	2280 ± 200 years
MW-4	4100 ± 250 years
MW-6	5200 ± 250 years

(The data for these two tables were kindly supplied by Dr. H. W. Bradley.)

3. The following represents the scheme we have employed in the isolation of the organic components from the Mud Lake sample, MW-2:

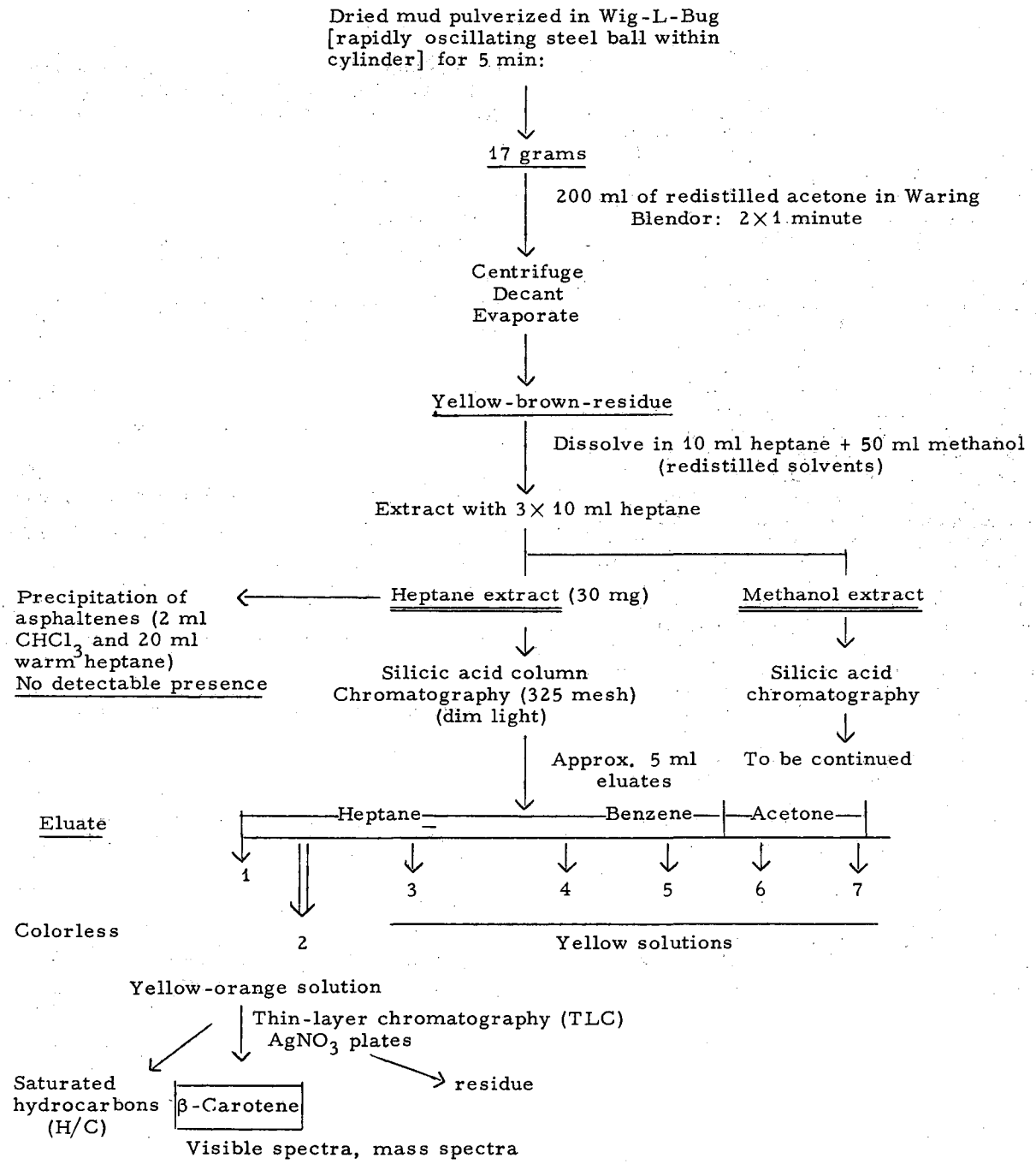

Other extraction schemes have been utilized, and the efficiencies of these procedures are reported:

A. 2.17 g (MW-3) ⟶ [benzene: methanol (4:1 v/v), sonicate 45 min] ⟶ 120 mg total extract.

17 mg heptane-solubles.

B. 8.28 g (MW-6) ⟶ [benzene: methanol (4:1 v/v), sonicate 30 min] ⟶ 98 mg total extract.

Results (Heptane Extract)

Our analysis has been confined to the heptane-soluble organic material obtained from the heptane extract in the partition between the solvents heptane and methanol. Further separation of the organic constituents in this extract by silicic acid column chromatography has provided convincing evidence for the presence of β-carotene in the Mud Lake deposit, MW-2. The visible spectrum of this compound is identical with a similar compound isolated from the level MW-O. The spectroscopic evidence for the presence of β-carotene is indicated below:

A. Mass Spectrometric Analysis

All samples were determined on a modified C. E. C. mass spectrometer, Model 21-103 C, with ionizing voltage 70 eV, and an inlet heated to about 200° C.

Standard: m/e 536 (M); m/e 368 (M-168); m/e 236 (M-300).

Mud Lake Sample: m/e 536 (M), m/e 420 (M-116); m/e 368 (M-168); m/e 236 (M-300). Also molecular ions present at m/e 548, 550, and 629.

B. Visible Spectra

All spectra, recorded on a Cary-14 spectrophotometer (values in mμ).

Solvent		MW-2	MW-O	Standard β-Carotene		Literature (Karrer) (Ref. 2)	Literature (Ref. 3)
Hexane	max.	474	476	Heptane solvent	479	477	479
	min.	466	466		469		467-468
	max.	448	449		451	450	451
	sh.	429	428-29		430	425	430-32
Benzene	max.	489	490		492		494
	min.	482	480		484		482
	max.	463	462		465		463
	sh.	442	442		441		440-444
CS_2	max.	505	506		506		
	max.	480-1	481		482		
	sh.	456	457		458		

max. = maximum, min. = minimum, sh. = shoulder.

C. Thin-Layer Chromatography

The visible spectra recorded above represent the spectral characteristics of the heptane eluate[2] [see Isolation Scheme] from silicic acid column chromatography. Subsequent purification by thin-layer chromatography using silica gel G plates, impregnated with 12% silver nitrate after the methods of De Vries,[4] Morris,[5] and Eglinton,[6] indicates that this fraction contains some saturated alkanes and a small amount of unsaturated material, in addition to the β-carotene which remains at the origin.

	Material	Rf values
Heptane eluate 2	Saturated alkanes	0.9 → 0.95
	Unsaturated alkanes	0.1 → 0.15
	β-Carotene	0

TLC Conditions

a. prewashed with ethyl acetate

b. 118°/30 min.

c. 0.001% Rhodamine B: Detector

d. 95% iso-octane–5% benzene: Developer

D. Gas-Liquid Chromatography

We have previously done work on the saturated alkanes identified in the Mud Lake deposit MW-O, and have noted the dominance of the n-C27, n-C29, and n-C31 alkanes in that sample, a feature which is also observed in the Green River Formation saturated alkanes. An odd-even normal hydrocarbon alternation is also observed in both the Mud Lake deposit and the Green River Formation, but in contrast to the latter sediment the Mud Lake deposit exhibits no predominance of the n-C_{17} alkane. The saturated alkanes from the MW-2 sample show great similarity to those isolated from the MW-O sample. The absence of the n-C_{17} alkane, a known constituent of blue-green algae of the Nostoc variety,[7] from the Mud Lake deposits remains anomalous, for blue-green algae of the Aphanothece, Oscillitoria-Limnetica, Microcystis, Incerta, Spirulina genera--though not of the Nostoc--predominate in the shallow Mud Lake waters. The analysis of the chemical components of these blue-green algae is presently in progress.

Discussion

These preliminary findings lead to the tentative suggestion that diagenetic degradation has not yet taken place to any extent in the Mud Lake deposits. The identification of β-carotane,[6] the fully saturated analog of β-carotane, in the Green River Formation lends credence to the theory that the Mud Lake deposits may indeed be modern counterparts of rich oil shales such as the Green River Formation, but at the post-Pleistocene period the transformation of the chemical constituents had not taken place to any significant extent.

References

1. W. H. Bradley, presented at Annual Meeting, Geological Society of America, November 1966.
2. P. Karrer and E. Jucker, Carotenoids (Elsevier Press, Amsterdam, 1950), Chapter 10.
3. L. Lang, Ed., Absorption Spectroscopy (Academic Press, New York, 1961), Vol. I, p. 58.
4. B. De Vries, Chem. Ind. (London) 1049 (1962).
5. L. J. Morris, Chem. Ind. (London) 1238 (1962).
6. G. Eglinton et al., presented at Annual Meeting, Geological Society of America, November 1966.
7. R. B. Johns et al., Geochim. Cosmochim. Acta 30, 1191 (1966).

19. SEARCH FOR δ-AMINOLEVULINIC ACID AS A PRODUCT OF METHANE-AMMONIA-WATER IRRADIATION

Margaret A. Smith, Ahmed Choughuley, and Richard M. Lemmon

Our understanding of how the porphyrins may have appeared on the primitive, prebiotic Earth is still in an unsatisfactory state. It is generally assumed that they may have appeared abiogenetically following the now established biosynthetic route.[1] In this route, glycine is known to condense with succinate to give δ-aminolevulinic acid (δ-ALA). Two of the latter molecules then condense to a substituted pyrrole, porphobilinogen; it, in turn, condenses with itself to give a porphyrin.[1] That a similar route may have been followed on the prebiotic Earth is indicated by the recent work of Szutka in this Laboratory. He found that the ultraviolet irradiation of δ-ALA, under primitive Earth conditions, converted about half of this compound to a pyrrolic compound--the latter was not specifically identified.

The question remains: is δ-ALA a product of CH_4-NH_3-H_2O irradiations? This report details our efforts, so far unsuccessful, to establish it as such a product.

Experimental Procedures

Carrier δ-aminolevulinic acid

Preliminary paper chromatography of some commercially supplied δ-ALA gave erratic results, with occasional evidence of decomposition or impurity. Another sample of δ-ALA was obtained from the California Corporation for Biochemical Research, Los Angeles, California. No impurities giving a positive ninhydrin reaction were detected after paper chromatography. The elemental analysis was: C, 35.95 (calc. 35.83); H, 5.87 (calc. 6.02).

Paper chromatography of δ-ALA

Two-dimensional paper chromatography on Whatman No. 1 paper using (1) 1-butanol–acetic acid–water (100:22:50) and (2) isopropanol-methanol-water (70:10:20) as developing solvents was used in our early work for the initial separation of the products from electron irradiation of CH_4-NH_3-H_2O. Attempts to establish RF values for δ-ALA, and other compounds thought to be possible products, failed with these solvent mixtures. Rf values differing by as much as a factor of two were observed. The use of 50 λ of a 1-mg/ml aqueous solution of orange II dye to produce a marker spot to which others could be related gave reasonably consistent results. Subsequently, even these values became erratic; however, this was found to have been caused by running too few papers, so that the chromatography box was not saturated with solvent vapor. Consequently, using three troughs and six papers in each box (in addition to using an orange II marker spot) became our standard procedure; this gave results which were acceptable although not entirely reproducible.

In order to ascertain if δ-ALA could be chromatographed, eluted, and rechromatographed without decomposition, six chromatograms of 100 μg each were developed two-dimensionally with (a) 1-butanol–acetic acid–water (100:22:50) and (b) isopropanol-methanol-water (70:10:20). Three of these chromatograms were sprayed with ninhydrin solution in order that they could be used as a guide for eluting the δ-ALA from the remaining three. Following elution with water, the δ-ALA was rechromatographed with the same two solvent mixtures. The resultant ninhydrin-positive spots had lower Rf values in both solvent systems than was previously observed for δ-ALA. At first we concluded that decomposition had occurred. As a further check, another series of chromatograms was processed in the same manner except that 50 μg δ-ALA, which had not been chromatographed, was added before the rechromatography. Instead of the two spots expected on the final chromatograms, only single spots were seen, again with the low Rf values in both solvent systems. We concluded that δ-ALA could be rechromatographed without suffering decomposition. However, Rf values vary from experiment to experiment--we don't yet understand why.

In our earlier work we had eluted the δ-ALA region and rechromatographed this material using (1) sec-butanol–propionic acid–water (160:25:50) and (2) sec-butanol–tert-butanol–water (43:48.4:8.6). A very badly streaked spot was obtained. We therefore decided that a better pair of solvents for rechromatography must be found. The following solvent systems were tried for two-dimensional chromatography of 100 μg δ-ALA on Whatman No. 1 paper:

(a) ethyl acetate–formic acid–water (105:30:15) and propanol-10 N ammonium hydroxide (7:3);

(b) ethyl acetate–formic acid–water (105:30:15) and tert-butanol–methyl ethyl ketone–10 N ammonium hydroxide–water (40:30:10:20);

(c) ethyl acetate–formic acid–water

(105:30:15) and 88% phenol in water–acetic acid–0.5 M K_2EDTA–water (840:10:2:100);
(d) 88% phenol in water–acetic acid-0.5 M K_2EDTA–water (840:10:2:100) and 1-butanol–propionic acid–water (92.5:45:61.3);
(e) 1-butanol–propionic acid–water (92.5:45:61.3) and the upper phase of a mixture of sec-butanol–tert-butanol–water (43:8.6:48.4).

All these solvent mixtures gave badly streaked spots. The pair of solvent mixtures giving excellent results, regardless of which was used for initial development, were ethanol–1 M acetic acid–pyridine–water (95:10:3:3), and the upper phase of a mixture of sec-butanol–tert-butanol–water (43:8.6:48.4). (This solvent works well in conjunction with the ethanol-HOAc, but not in conjunction with the butanol–propionic acid listed under (e) above.)

Electron irradiations of methane, ammonia, and water

The general procedure used for the electron irradiations was that previously reported.[2] The irradiation tube was charged with 20 ml 4 N NH_4OH, and approximately 1.3 mmole CH_4 containing either 0.5 or 1.0 mCi ^{14}C-labeled methane. The time of irradiation was varied, as will be indicated. In all cases, initial chromatography was done on Whatman No. 1 paper using (1) 1-butanol–acetic acid–water (100:22:50) and (2) isopropanol–methanol–water (70:10:20). Ninhydrin spray reagent (0.6 g ninhydrin in 100 ml methanol) was used for the chemical detection of carrier δ-ALA, and radioautography on x-ray film was used to detect labeled material.

To an 8-ml aliquot portion of the irradiated solution, removed after 45 min of irradiation, 100 μg carrier δ-ALA was added. An apparent positive result was obtained after the initial chromatography. There was a large amount of activity in the δ-ALA region, but the chromatogram was streaked and there was no discrete active spot corresponding to the δ-ALA. With this chromatogram used as a guide, the area which would contain any δ-ALA was cut from a chromatogram of a 2-ml aliquot portion removed after 30 min during the same irradiation. Following elution with water, 100 μg carrier δ-ALA was added, and the solution rechromatographed with the same solvent mixtures as before. No correspondence between the radioautograph and the sprayed chromatogram was observed, however; so little active material was present that this negative result was questionable.

During a subsequent irradiation, a 2-ml aliquot portion was removed after 30 min, 100 μg carrier δ-ALA was added, and paper chromatography was done as before. The radioautograph of this chromatogram, after a one-week exposure, showed a very faint trace of activity corresponding in location to the δ-ALA spot. The chromatogram was placed on film for 4 weeks. Again, there seemed to be activity present in the δ-ALA area; however, the ninhydrin-developed spot had faded so much that this positive result was questionable.

We decided to devote an entire experiment to the search for δ-ALA. After the addition of 100 μg of carrier compound, the total 20 ml of solution, which had been irradiated for 1 hour, was concentrated by evaporation, and a single chromatogram prepared. This chromatogram was overloaded and very badly streaked, as shown by the radioautograph. Spraying with ninhydrin revealed that the Rf values of δ-ALA had been greatly altered. In order to reduce the amount of chromatography-interfering substances, the experiment was repeated; this time, however, the solution was halved before chromatography and two chromatograms were prepared. One of these was sprayed in order that it could be used as a guide for eluting, the δ-ALA from the second. Again the chromatograms were overloaded and badly streaked. The sprayed chromatograms showed no δ-ALA spot--only a slight positive reaction over a large area. Apparently overloading and the large amount of polymeric material produced in a 1-hour irradiation made successful chromatography of δ-ALA impossible. Therefore, in the next experiment, the time of irradiation was reduced to 45 min and the irradiated solution was divided into six equal portions. One hundred μg carrier δ-ALA was added to each, and six chromatograms were prepared. Very little streaking was observed on the radioautographs of these chromatograms. Three were sprayed and the δ-ALA spots were found to have the expected Rf values. There were no active spots corresponding in location, size, and shape to the δ-ALA spots. Under our experimental conditions we could detect a yield of δ-ALA of as little as 0.05%. This negative result seemed reliable, in view of the good chromatography obtained, and no rechromatography in second solvent systems seemed necessary.

Results and Discussion

During a 45-min electron irradiation of methane, ammonia, and water, no detectable amount of δ-ALA is formed. This compound is difficult to paper chromatograph successfully, and this fact probably accounts for earlier indications of δ-ALA formation. We will now try to establish the irradiation conditions that give a maximum total yield of glycine

and succinic acid. Such conditions should also give the maximum probability of δ-ALA's appearance.

References

1. D. Shemin, in Proceedings of the 3rd International Congress on Biochemistry, Brussels, 1955, pp. 197-204, 1956.

2. C. Ponnamperuma, R. M. Lemmon, R. Mariner, and M. Calvin, Proc. Natl. Acad. Sci. U. S. 49, 737 (1963).

PUBLICATION LIST, 1966

Biophysical Chemistry

1. Kenneth Sauer, John R. Lindsay Smith, and A. J. Schultz, The Dimerization of Chlorophyll a, Chlorophyll b, and Bacterio--chlorophyll in Solution, J. Am. Chem. Soc. 88, 2831 (1966).

2. Roderic B. Park, Jeffrey Kelly, Susan Drury, and Kenneth Sauer, The Hill Reaction of Chloroplasts Isolated from Glutaraldehyde-Fixed Spinach Leaves, Proc. Natl. Acad. Sci. U. S. 55, 1056 (1966).

3. Roderic B. Park, Chloroplast Structure, in The Chlorphylls, Eds. L. P. Vernon and G. R. Seely (Academic Press, Inc., New York, 1966), p. 283.

4. P. L. Lintilhac and R. B. Park, Localization of Chlorophyll in Spinach Chloroplast Lamellae by Fluorescence Microscopy, J. Cell. Biol. 28, 582 (1966).

5. Roderic B. Park, Subunits of Chloroplast Structure and Quantum Conversion in Photosynthesis, Intern. Rev. Cytology 20, 67 (1966).

6. E. S. Bamberger and Roderic B. Park, The Effect of Hydrolytic Enzymes on the Photosynthetic Efficiency and Morphology of Chloroplasts, Plant Physiol. 41, 1591 (1966).

7. I. Tinoco, Jr. and S. L. Davis, Ultra-Violet Absorption Spectrum of Thymine in Ice, Nature 210, 1286 (1966).

8. I. Tinoco, Jr. and Myron Warshaw, Optical Properties of Sixteen Dinucleoside Phosphates, J. Mol. Biol. 20, 29 (1966).

9. I. Tinoco, Jr., C. R. Cantor, and S. R. Jaskunas, Optical Properties of Ribonucleic Acids Predicted from Oligomers, J. Mol. Biol. 20, 39 (1966).

10. E. A. Dratz and Melvin Calvin, Substrate and Inhibitor Induced Changes in the Optical Rotatory Dispersion of Aspartate Transcarbamylase, Nature 211, 497 (1966).

11. Gerald A. Corker, Melvin P. Klein, and Melvin Calvin, Chemical Trapping of a Primary Quantum Conversion Product in Photosynthesis, Proc. Natl. Acad. Sci. U. S. 56, 1365 (1966).

Organic Chemistry and Radiation Chemistry

12. Marieanne Byrn and Melvin Calvin, Oxygen-18 Exchange Reactions of Aldehydes and Ketones, J. Am. Chem. Soc. 88, 1916 (1966).

13. Catherine Fenselau and Melvin Calvin, Selectivity in Zeolite Occlusion of Olefins, Nature 212, 889 (1966).

14. John R. Lindsay Smith and Melvin Calvin, Studies on the Chemical and Photochemical Oxidation of Bacterio-chlorophyll, J. Am. Chem. Soc. 88, 4500 (1966).

15. P. E. Brown, M. Calvin, and J. F. Newmark, Thymine Addition to Ethanol: Induction by Gamma Irradiation, Science 151, 68 (1966).

16. R. M. Lemmon, The Search for Radiation Deaminations in DNA, Nature 212, 1481 (1966).

Chemical Physics

17. H. H. Wickman, M. P. Klein, and D. A. Shirley, Paramagnetic Hyperfine Structure and Relaxation Effects in Mössbauer Spectra: ^{57}Fe in Ferrichrome A, Phys. Rev. 152, 345 (1966).

18. C. S. Fadley, S. B. M. Hagstrom, M. P. Klein, and D. A. Shirley, Chemical Shifts of Core Electron Binding Energies in Iodine and Europium, Bull. Am. Phys. Soc. 11, 884 (1966).

19. E. Matthias, D. A. Shirley, M. P. Klein, and N. Edelstein, Detection of Nuclear Magnetic Resonance in a 235-nsec Excited Nuclear State by Perturbed Angular Correlation, Phys. Rev. Letters 16, 974 (1966).

20. W. Easley, N. Edelstein, M. P. Klein, and D. A. Shirley, Nuclear Spin and Moment of ^{110m}Ag by Paramagnetic Resonance, Phys. Rev. 141, 1132 (1966).

Plant Biochemistry

21. Marianne Byrn, John R. Lindsay Smith, and M. Calvin, The Role of Bacteriochlorophyll in Photosynthetic Hydrogen Transfer, J. Am. Chem. Soc. 88, 3178 (1966).

22. J. A. Bassham, Photosynthesis, in Survey of Progress in Chemistry, Ed. A. F. Scott (Academic Press, Inc., New York, 1966), 3, p. 1.

23. R. G. Jensen and J. A. Bassham, Photosynthesis by Isolated Chloroplasts, Proc. Natl. Acad. Sci. U. S. 56, 1095 (1966).

24. Tor A. Pedersen, Martha Kirk, and J. A. Bassham, Inhibition of Photophosphorylation and Other Photosynthetic Reactions by Fatty Acids and Esters, Biochim. Biophys. Acta 112, 189 (1966).

25. Tor A. Pedersen, Martha R. Kirk, and J. A. Bassham, Light-Dark Transients in Levels of Intermediate Compounds During Photosynthesis in Air-Adapted Chlorella, Physiol. Plantarum 19, 219 (1966).

26. J. E. Plamondon and J. A. Bassham, Glycolic Acid Labeling During Photosynthesis with $^{14}CO_2$ and Tritiated Water, Plant Physiol. 41, 1272 (1966).

27. J. A. Bassham and Martha Kirk, Rapid Inhibitor-Induced Changes in the ^{14}C-Labeled Compounds Formed by the Photosynthetic Carbon Reduction Cycle, Advan. Tracer Methodol. 3, 211 (1966).

28. J. Biggins and R. B. Park, CO_2 Assimilation by Etiolated Hordeum vulgare Seedlings During the Onset of Photosynthesis, Plant Physiol. 41, 115 (1966).

29. H. Rapoport, The Biosynthesis of the Pyridine and Piperidine Alkaloids. The Tobacco Alkaloids, Deut. Akad. Wiss. Berlin, No. 3, 1966.

Brain Biochemistry

30. D. Krech, M. R. Rosenzweig, and E. L. Bennett, Environmental Impoverishment, Social Isolation, and Changes in Brain Chemistry and Behavior, Physiol. Behavior 1, 99 (1966).

31. E. L. Bennett, M. C. Diamond, H. Morimoto, and M. Hebert, Acetylcholinesterase Activity and Weight Measures in Fifteen Brain Areas from Six Lines of Rats, J. Neurochem. 13, 563 (1966).

32. M. C. Diamond, F. Law, H. Rhodes, B. Lindner, M. R. Rosenzweig, D. Krech, and E. L. Bennett, Increases in Cortical Depth and Glia Numbers in Rats Subjected to Enriched Environment, J. Comp. Neurol. 128, 117 (1966).

33. W. L. Byrne and 22 others, Memory Transfer, Science 153, 658 (1966).

34. K. Schlesinger, E. L. Bennett, M. Hebert, and G. McClearn, Effects of Alcohol Consumption on the Activity of Liver Enzymes in C57 BL/Crgl Mice, Nature 209, 448 (1966).

35. K. Schlesinger, R. Kakihana, and E. L. Bennett, Effects of Tetraethylthiuramdisulfide (Antabuse) on the Metabolism and Consumption of Ethanol in Mice, Psychosom. Med. 28, 515 (1966).

36. William L. Byrne, David Samuel, Edward L. Bennett, Mark R. Rosenzweig, and E. Wasserman, Attempts to Transfer Learning in Rats with Extracts Containing Ribonucleic Acid with Brain Homogenates, UCRL-16754, March 1966.

Molecular Biology of Bacteria

37. D. C. H. McBrien and V. Moses, Effect of Isopropylthiogalactoside on the Induction of the Galactose Operon by D-Fucose in a Lactose Deletion Mutant of E. coli, J. Bacteriol. 91, 1391 (1966).

38. V. Moses and P. Sharp, Effect of Actinomycin on the Synthesis of Macromolecules in Escherichia coli, Biochim. Biophys. Acta 119, 200 (1966).

39. V. Moses and C. Prevost, Catabolite Repression of β-Galactosidase Synthesis in Escherichia coli, Biochem. J. 100, 336 (1966).

40. C. Prevost and V. Moses, The Action of Phenethyl Alcohol on the Synthesis of Macromolecules in Escherichia coli, J. Bacteriol. 91, 1446 (1966).

41. V. Moses and K. K. Lonberg-Holm, The Study of Metabolic Compartmentalization, J. Theoret. Biol. 10, 336 (1966).

42. V. Moses, Die Augfliederung des Stoffwechsels der Zelle aug Verschiedene Reaksionsraüme, Naturw. Rundschau 19, 441 (1966).

Chemical Evolution

43. Dean H. Kenyon, Gary Steinman, and Melvin Calvin, The Mechanism and Protobiochemical Significance of Dicyanamide-Mediated Peptide Synthesis, Biochim. Biophys. Acta 124, 339 (1966).

44. Melvin Calvin, Chemical Evolution of Life and Sensibility, UCRL-17132, Sept. 1966.

45. A. S. U. Choughuley and R. M. Lemmon, Production of Cysteic Acid, Taurine, and Cystamine Under Primitive Earth Conditions, Nature 210, 628 (1966).

46. G. Eglinton, P. M. Scott, T. Belsky, A. L. Burlingame, W. Richter, and Melvin Calvin, Occurrence of Isoprenoid Alkanes in a Precambrian Sediment, in Advances in Organic Geochemistry 1964, Eds. G. D. Hobson and M. C. Louis (Pergamon Press, London, 1966), p. 41.

47. William Van Hoeven, Pat Haug, A. L. Burlingame, and Melvin Calvin, Hydrocarbons from Australian Oil, 200 Million Years Old, Nature 211, 1361 (1966).

48. R. B. Johns, T. Belsky, E. J. McCarthy, A. L. Burlingame, P. Haug, H. Schnoes, W. Richter, and Melvin Calvin, Organic Geochemistry of Ancient Sediments. II, Geochim. Cosmochim. Acta 30, 1191 (1966).

THESES

Work for the following Ph. D. theses was completed during 1966:

1. Charles R. Cantor, Sequence-Dependent Properties of Oligonucleotides, UCRL-16701, May 1966.

2. Marianne P. Byrn, The Role of Chlorophyll as a Chemical Intermediate in Photosynthesis, UCRL-16946, June 1966.

3. Charles Prevost, Catabolite Repression in the Synthesis of Inducible Enzymes in Escherichia coli, UCRL-16953, June 1966.

4. Robert T. Ross, I. The Quantum Conversion of Photosynthesis. II. Paramagnetic Resonance of Transition Metal Complexes Having Biological Interest, UCRL-16970, June 1966.

5. James M. Thorne, I. The Faraday Effect in Organic Molecules and Complexes. II. Conformations of Cellulose Triacetate, UCRL-17100, August 1966.

6. Edward A. Dratz, The Geometry and Electronic Structure of Biologically Significant Molecules as Observed by Natural and Magnetic Optical Activity: I. Protein Conformation and Plasticity. II. Chlorophyll-Chlorophyll Interactions. III. Electronic Structure of Metal Porphyrins, UCRL-17200, October 1966.

7. Terry L. Trosper, Chlorphyll a Interactions in Lipid Monolayers, UCRL-17321, December 1966.

SCIENTIFIC LECTURES BY THE SENIOR STAFF, 1966

James A. Bassham

1. Metabolic Regulation of Photosynthesis and Glycolysis. Biology Department, Brandeis University, Waltham, Mass., June 1966.
2. Photosynthesis. Gordon Conference on "Biochemistry and Agriculture," Tilton, N. H., June 1966.
3. Metabolic Regulation of Photosynthesis and Glycolysis. American Society of Plant Physiologists Symposium on "Carbon Metabolism in Photosynthesis," AIBS Meeting, University of Maryland, College Park, Md., August 1966.
4. Photosynthesis of Carbon Compounds. International Minerals and Chemicals Corp. Symposium on "Photosynthesis," Chicago, Illinois, October 1966.

Edward L. Bennett

1. Interanimal Transfer of Trained Responses. Symposium on "Memory Transfer," 5th International Congress of Neuropsychopharmacology, Washington, D. C., March 1966.
2. Tracer Studies of the Uptake of Organic Compounds by Planarians. Symposium on "Learning: Evaluation of Research on Planarians and Other Invertebrates," Michigan State University, East Lansing, Mich., September 1966.
3. Brain Chemistry and Anatomy: Implications for Theories of Learning and Memory. Lankenau Hospital Symposium on "Mind as a Tissue," Philadelphia, Pa., November 1966.

Melvin Calvin

1. Wanted: A Star. Wooster College Centennial Celebration, Wooster, Ohio, February 1966.
2. Chemical Evolution. Department of Chemistry, Wooster College, Wooster, Ohio, February 1966.
3. Chemical Evolution. California Section, American Chemical Society, Berkeley, California, April 1966.
4. Chemical Evolution of Life and Sensibility. Neurosciences Research Program, Intensive Study Program, University of Colorado, Boulder, Colo., July 1966.

Melvin P. Klein

1. Correlation Between Electron Spin Resonance and Mössbauer Spectra in Ferrichrome a. Second International Conference on "Magnetic Resonance in Biological Systems," Stockholm, Sweden, June 1966.
2. Derivation of Magnetic Resonance Information from Magentic Circular Dischroism. Second International Conference on "Magnetic Resonance in Biological Systems," Stockholm, Sweden, June 1966.

Richard M. Lemmon

1. Chemical Evolution. NSF Summer Institute in Molecular Biology, Berkeley, Calif., July 1966.

Vivian Moses

1. The Nature of Catabolite Repression of the Lactose Operon in Escherichia coli. LXth International Congress for Microbiology, Moscow, USSR, July 1966.

Roderic B. Park

1. Hill Reaction by Chloroplasts from Glutaraldehyde-Fixed Leaves. Biology Department, Harvard University, Cambridge, Mass., March 1966.

2. Hill Reaction by Chloroplasts from Glutaraldehyde-Fixed Leaves. Johnson Foundation, University of Pennsylvania, Philadelphia, Pa., March 1966.

3. Hill Reaction by Glutaraldehyde-Fixed Chloroplasts. Biology Department, University of California, San Diego, May 1966.

4. Freeze Etching of Chloroplasts. Brookhaven National Laboratory Symposium on "Energy Conversion by the Photosynthetic Apparatus," Brookhaven, N. Y., June 1966.

5. Freeze Etching of Chloroplasts. Department of Bacteriology, University of California, Berkeley, June 1966.

6. Molecular Cytology. Summer Institute in Electron Microscopy, University of California, Berkeley, August 1966.

7. Micellar Nature of Chloroplast Membranes. University of California, Davis, October 1966.

Kenneth H. Sauer

1. Applications of Lasers in Biology. Sigma Xi Symposium on "The Laser as a Tool for Scientific Research," University of California, Berkeley, March 1966.

2. Chlorphyll-Chlorophyll Interactions. Brookhaven National Laboratory Symposium on "Energy Conversion by the Photosynthetic Apparatus," Brookhaven, N. Y., June 1966.

3. Photosynthetic Light Reactions. Plant Physiology Division, University of California, Davis, November 1966.

4. Circular Dichroism of Quantasomes and Chromatophores. Plant Physiology Division, University of California, Davis, November 1966.

I. Tinoco, Jr.

1. Structure and Optical Properties of Polynucleotides. Chemistry Department, Stanford University, Stanford, Calif., April 1966.

2. Optical Properties of Ribonucleic Acids. Pacific Slope Biochemical Conference, Eugene, Oregon, August 1966.

3. Structure and Optical Properties of Polynucleotides. Ames Research Laboratory (NASA), Mountain View, Calif., December 1966.

Others

1. Fluorescence Polarization of Monolayers Containing Chlorphyll a. Terry L. Trosper. Biophysical Society Meeting, Boston, Mass., February 1966.

2. Principles and Applications of Magnetic Circular Dichroism to Problems in Chemistry and Biology (5 lectures). E. A. Dratz, Division of Biophysics, University of Michigan, Ann Arbor, Mich., October 1966.

3. Photosynthesis by Isolated Chloroplasts. Richard G. Jensen. American Society of Plant Physiologists Symposium on "Carbon Metabolism in Photosynthesis," AIBS Meeting, University of Maryland, College Park, Md., August 1966.

PERSONNEL LIST

Senior Staff

Melvin Calvin, Director
James A. Bassham
Edward L. Bennett
Paul M. Hayes
John E. Hearst
Melvin P. Klein
Richard M. Lemmon
Vivian Moses
Roderic B. Park
Henry Rapoport
Kenneth H. Sauer
Ignacio Tinoco, Jr.

Research Staff

Byrdie D. Ayres
Patricia J. Chu
Lelia M. Coyne
Wallace R. Erwin
Marie S. Hebert
Ann M. Hughes
Martha R. Kirk
Julia J. Ku
Chantal Lafont
Hiromi Morimoto
Ann Orme
Donald E. Phelps
Dell H. Roadman
Stephanie L. Rosenbaum
Pamela Sharp
Margaret A. Smith

Postdoctoral Fellows

David B. Boylan
Marianne B. Caple
Henry W.-S. Chan
Goran Claeson
Thomas R. Dehner
Edward A. Dratz
Urs Eppenberger
Catherine Fenselau
Eugene F. Friedman
Barrie S. Hesp
Richard G. Jensen
Benjamin Kirson
(visiting faculty)
Didier Lafont
Claude Lussan
(visiting faculty)
Ian Morris
(visiting faculty)
Bradford P. Mundy
Robert T. Ross
(faculty)
Hugo Sephton
Janet Splitter
John H. M. Thornley
(visiting faculty)

Laboratory Assistants

Mark Dickison
Peter Falk
Mark Lau
Ethel M. Lefall
Arthur Levit
Troy Wilcox

Graduate Students

Algis Alkaitis
Loring K. Bjornson
Mary E. Brewer
Gerald A. Corker
David E. Downie
Gerald Entine
Mark S. Fischer
Donald R. Gentner
Jerry Han
Stanley Jaskunas
Jeffrey J. Kelly
Hugh R. Matthews
Eugene D. McCarthy
Kam-sik Ng
Howard Ono
Jon C. Palmer
Linda K. Phillips
Helmut Pohlit
George C. Ruben
Alfred J. Schultz
Jean Thiery
Terry Trosper

Graduate Students (cont.)

Tz-hong Lin
Robert M. Macnab
Robert Mann
Harry G. Ungar
William Van Hoeven
Paul F. Wegfahrt, Jr.

Undergraduate Students (Research)

Robert Bazell
Franklin Collins

Shops

Electronics

Robert Acker
Robert Creedy
John Despotakis

Carpenter

Richard O'Brien

Glass

Bill Hart

Office

Diane Hinds
Evelyn Litton
Johanna Onffroy
Marilyn Taylor

PERMUTED INDEX

PERMUTED INDEX

PERMUTED INDEX

PERMUTED INDEX

PERMUTED INDEX

PERMUTED INDEX